NUMERICAL MODEL OF FLOW IN A STREAM-AQUIFER SYSTEM

by

Catherine E. Kraeger Rovey

August 1975

HYDROLOGY PAPERS
COLORADO STATE UNIVERSITY
Fort Collins, Colorado

74

NUMERICAL MODEL OF FLOW IN A STREAM-AQUIFER SYSTEM

by
Catherine E. Kraeger Rovey

HYDROLOGY PAPERS
COLORADO STATE UNIVERSITY
FORT COLLINS, COLORADO 80523

August 1975

No. 74

TABLE OF CONTENTS

LIST OF SYMBOLS

Symbol	Definition	Dimensions
A	area	L^2
A	coefficient as defined by Eq. 3-14 or Eq. 3-29	$L^2\ T^{-1}$
B	coefficient as defined by Eq. 3-15 or Eq. 3-30	$L^2\ T^{-1}$
C	coefficient as defined by Eq. 3-16 or Eq. 3-31	$L^2\ T^{-1}$
C_F	fluid compressibility	$M^{-1}\ LT^2$
D	coefficient as defined by Eq. 3-17 or Eq. 3-32	$L^2\ T^{-1}$
D	canal diversion	$L^3\ T^{-1}$
D_n	monthly diversion to a specified canal	$L^3\ T^{-1}$
d	river stage	L
E	coefficient as defined by Eq. 3-18	$L^2\ T^{-1}$
E_t	evapotranspiration	$L\ T^{-1}$
F	coefficient as defined by Eq. 3-19	$L^2\ T^{-1}$
G	coefficient as defined by Eq. 3-20 or Eq. 3-33	$L^2\ T^{-1}$
g	acceleration of gravity	$L\ T^{-2}$
H	head	L
h	elevation	L
h_{pb}	bubbling pressure head	L
i	subscript indicating direction along corrdinate axis	---
j	subscript indicating direction along coordinate axis	---
K_x, K_y, K_z	hydraulic conductivities in the three orthogonal coordinate directions	$L\ T^{-1}$
K_s	hydraulic conductivity of the silt layer	$L\ T^{-1}$
k	subscript indicating direction along coordinate axis	---
k_r	relative permeability	---
k_t, k_c	coefficients used in computation of evapotranspiration	---
k_x, k_y, k_z	absolute permeabilities in the three orthogonal coordinate directions	L^2
L	distance in some arbitrary direction	L
m	subscript denoting monthly value	---
m	aquifer saturated thickness	L
n	summation limit	---
n	Manning's roughness coefficient	$L^{-1/3}T$
P	pressure	$ML^{-1}\ T^{-2}$
P	precipitation	LT^{-1}
P_n	percentage of canal distribution region inside study area	---
p	percentage of daylight hours	---
Q	discharge	$L^3\ T^{-1}$

LIST OF SYMBOLS (Cont.)

Symbol	Definition	Dimensions
q	discharge per unit width	$L^2 T^{-1}$
R	net seepage discharge from river	$L^3 T^{-1}$
S	saturation	---
S_y	specific yield	---
S_e	effective saturation	---
s	energy gradient	---
T	transmissibility	$L^2 T^{-1}$
t	time	T
t	temperature	---
t_s	silt layer thickness	L
u	consumptive use	LT^{-1}
v	velocity	LT^{-1}
w	channel width	L
x	distance along coordinate axis	L
y	distance along coordinate axis	L
z	distance along coordinate axis	L
β	reciprocal of bulk modulus of elasticity of water	$M^{-1} LT^{-2}$
μ	fluid dynamic viscosity	$ML^{-1} T^{-1}$
ρ	fluid density	ML^{-3}
ϕ	porosity	---

ACKNOWLEDGEMENTS

The Ph.D. dissertation work is the subject matter of this paper. The writer wishes to express her appreciation to Dr. E. V. Richardson, advisor, for his guidance and encouragement throughout the course of the study, leading to this paper. Special thanks are given to Dr. J. W. N. Fead, who was a source of inspiration and encouragement during the writer's undergraduate and graduate schooling. Thanks are also extended to Dr. D. K. Sunada, who spent a great deal of time and effort reviewing the material, to Dr. N. S. Grigg, who contributed many helpful suggestions, and to Dr. D. B. McWhorter, whose expertise in the subject area was an invaluable asset.

The financial supports for this study given by the National Defense Graduate Fellowship Program of the Department of Health, Education, and Welfare, the Colorado State University Experiment Station, and by the United States Agency for International Development under contract No. AID/csd-2460, "Optimum Utilization of Water Resources for Agriculture with Special Emphasis on Water Removal and Delivery Systems and Relevant Institutional Development" are gratefully acknowledged.

ABSTRACT

A three-dimensional, finite difference model was developed for simulating steady and unsteady, saturated and unsaturated flow in a stream-aquifer system. The basis of the model is the finite difference form of Richard's equation for unsaturated and saturated subsurface flow. Effects of streamflow on groundwater movement are treated by applying the appropriate boundary conditions to Richard's equation. Contributions of groundwater to river flow are quantified by including seepage rates in the computation of river discharge. The three-dimensional model was developed for use in this study to interact with two-dimensional model segments, which were interfaced with the three-dimensional model on its upstream and downstream ends.

The model produced results which match observed data for the study area, which consisted of a 40 mile reach of the Arkansas Valley of Southeastern Colorado. Computed estimates of river discharge at each end of the study area and water table elevations throughout the region agreed reasonably well with observed data. An analysis of the sensitivity of results produced by the model to variation in the values of several input parameters was included as part of the study.

CHAPTER 1
INTRODUCTION

The rapid expansion of population, industry, and agriculture in arid regions of the world has brought about a substantial increase in usage of groundwater resources to supplement surface water supplies. Groundwater and surface water are not separate and independent units, as is often assumed, but are closely interrelated. Withdrawal of groundwater from the alluvial deposits near a river produces a time-delayed decrease in river flow. The water table, in turn, responds to fluctuations in streamflow. The interdependence of surface water and groundwater is not limited to the aquifer. Interactions with groundwater are also evident in the flow phenomena of canals, drainage ditches, recharge pits, lakes, and reservoirs.

Because of its profound effect on the behavior of surface water, groundwater development should be undertaken only after careful planning which includes an analysis of the probable influence of the development on the surrounding area. This analysis should be based on a thorough understanding of groundwater movement, surface water flow, and the relationships between them. Carefully planned groundwater development can result in more efficient and beneficial utilization of available water resources. Poorly planned groundwater development can be detrimental to the environment, to users of surface water, and to the overall efficiency of water resource utilization.

The purpose of this study is to develop a tool for analyzing the movement of groundwater, the flow of surface water, and the interaction between them, which can be used by water regulatory agencies to ensure maximum benefits from proposed and existing groundwater resource developments. This tool is a groundwater-surface water flow simulation model. Although this model can be adapted for simulating flows in a variety of groundwater-surface water systems, this discussion is concerned primarily with the use of the model for describing flow in a natural stream and the surrounding alluvial aquifer.

The equations describing the movement of water in a stream-aquifer system are fairly simple. However, these equations are difficult to solve using known classical, analytic techniques for most field situations because of complex boundary conditions. For this reason numerical techniques, with their capability for handling most types of boundary conditions, have become important as tools for analysis of water management problems. Results obtained using numerical models can be used to make decisions for settling water rights disputes, managing water resources in the manner most beneficial to water users and the environment, and perhaps most important, to predict the effects of proposed water resource development projects prior to their construction.

Because of their conceptual and operational simplicity, two-dimensional, horizontal models are often used in the analysis of flow problems in stream-aquifer systems. These models may be either of the finite difference or the finite element type. The applicability of these models is dependent on the validity of the following assumptions in any given field situation:

(1) If hydraulically connected to the groundwater aquifer, the stream extends to the underlying bedrock, and acts as a boundary of known head.

(2) If not hydraulically connected to the groundwater aquifer, the stream does not extend down to the unconfined aquifer, and acts as a boundary of known recharge.

(3) Flow is horizontal and uniform everywhere in a vertical section.

(4) The slope of the water table is mild, so that the velocity may be assumed proportional to the tangent of the angle of slope of the water table instead of the sine.

Assumptions (3) and (4) are the Dupuit-Forchheimer assumptions.

Unfortunately, field conditions often exist for which some or all of the above assumptions are not valid. For such conditions, conventional, two-dimensional models are inappropriate. A type of stream-aquifer system frequently found in the Western United States consists of a wide, shallow river traversing deep alluvial deposits. The river fails to extend to bedrock in most locations and its depth of penetration into the unconfined aquifer varies from place to place. At a given cross section of the river, a portion of the channel may be hydraulically connected with the unconfined aquifer while the rest is not. Rapid fluctuations of head, either in the river or in the aquifer, may induce gradients steep enough to invalidate the Dupuit-Forchheimer assumptions. Steep gradients may also result from heavy pumping or irregularities in the aquifer configuration. Seepage from a stream carrying silt-laden water may result in the formation of a thin silt layer on the channel bed and banks. The effect of this silt layer is to partially seal the channel boundary and limit the rate of seepage which can pass from the river to the aquifer. Groundwater withdrawal can produce a situation where the water table elevation drops below the elevation of the channel bed, and the hydraulic connection between the stream and the unconfined aquifer may be broken.

For the situation described above, none of the four assumptions necessary for the use of a simple, two-dimensional model is valid. It is evident that a need exists for a numerical model which can correctly simulate this type of stream-aquifer system. This model should have the capability of simulating three-dimensional flow in the unconfined aquifer and accounting for the influence of a thin silt layer on the rate of seepage from the river.

The objectives of this study are twofold: (1) Develop a numerical model for simulating three-dimensional, saturated and unsaturated, steady and unsteady flow in a stream-aquifer system in which the stream is partially penetrating and may or may not be hydraulically connected to the aquifer. The stream may act as a boundary of known head or known discharge, depending on the influence of a silt layer on the seepage rate across the river boundary. (2) Verify the model. This is to be accomplished in two stages:

(a) The model will be applied to several hypothetical stream-aquifer systems. Results of runs made

using synthetic data from these systems will be analyzed qualitatively to determine whether the model is operating correctly and producing reasonable.

(b) The model will be applied to an actual stream-aquifer system located in Southeastern Colorado. Runs will be made using field measurements taken from the study area as input data. Results of these runs will include a predicted water table elevation map for the area at the end of the time period being considered, and predicted values of streamflow at the upstream and downstream ends of the area at intervals throughout the study period. These results will be compared to field measurements of water table elevation and river discharge to determine the accuracy of the model in matching observed data.

It is desirable that this model have the capability of being interfaced with more simplified models for the purpose of conserving computer time and storage. By interfacing this model with a simpler, two-dimensional model a detailed three-dimensional analysis of a short reach of a stream-aquifer system can be included as part of a less detailed analysis of a much longer reach of the system, to even the entire river basin. The finite difference scheme has been chosen for use in this study. The combined model consists of a three-dimensional model segment interfaced on either end with a two-dimensional model segment.

The theory on which this model is based is developed in Chapter II. A description of the computer simulator is presented in Chapter III. The study area used in the final phase of model verification is described in Chapter IV, which also includes a discussion of the source and availability of data for each parameter used in the model, and assumptions made on various parameters in preparation as input to the model. Results of model runs and discussion of these results are contained in Chapter V, which also includes an analysis of the sensitivity of the model to variation of parameters. Conclusion and recommendations for further study and recommended uses of the model are presented in Chapter VI.

CHAPTER II
THEORETICAL DEVELOPMENT

The equations necessary for the development of the mathematical model of flow in a stream-aquifer system include: (1) equations for discharge and stage in a natural stream, (2) a groundwater flow equation, and (3) a set of equations describing flow for various conditions that may occur at the interface between the stream and aquifer. The Manning formula is widely accepted as a reliable and convenient means of relating stage to discharge for uniform flow in a natural stream. For a large-scale approximation model of the type used in this study, estimates of river stage obtained by Manning's formula applied to short reaches of the river in the study area are considered to be sufficiently accurate for evaluating the interaction between the river and the aquifer. The form of Manning's equation used in the computer simulator is written for a wide channel and solved for stage, d, and is given by

$$d = \left[\frac{Qn}{1.49ws^{1/2}}\right]^{3/5} \qquad (2\text{-}1)$$

where

Q = discharge

n = Manning's roughness coefficient

w = channel width

s = energy gradient, approximated by bed slope

The parameters on the right-hand side of Eq. 2-1 are input to the model as data.

The remainder of this chapter consists of a detailed development of the groundwater flow equations used in the computer simulator and the flow equations for various conditions at the stream-aquifer interface.

Derivation of the Three-Dimensional Groundwater Flow Equation

In order to correctly simulate the fluctuations of the water table in a fixed, three-dimensional grid system, it is necessary that the three-dimensional segment of the finite difference model developed in this study have the capability of describing transient flow in both the saturated and unsaturated zones of an unconfined aquifer. For this reason it is necessary to develop an equation for use in this model which describes the behavior of the two immiscible fluid phases, water and air, that are present in the unsaturated zone, as well as the single-phase flow of water in the saturated zone. The nonlinear, partial differential equation for transient, saturated-unsaturated, three-dimensional flow through porous media is obtained by combining the continuity principle, a force equation describing fluid motion in porous media, and equations characterizing saturation and hydraulic conductivity as functions of pressure.

The force equation describing flow through porous media is Darcy's law. For flow situations in which velocities are relatively small, and acceleration of the flow is negligible, Darcy's law yields an adequate representation of flow through porous media. These conditions of low velocities and negligible accelerations are prevalent in the flow situations with which this study is concerned, and Darcy's law is considered appropriate for describing them.

A derivation of an equation for multi-phase flow in porous media from Darcy's law and the continuity principle has been presented in detail by Reddell and Sunada (1970). This equation was written in differential form for a volume element similar to the one shown in Fig. 2-1.

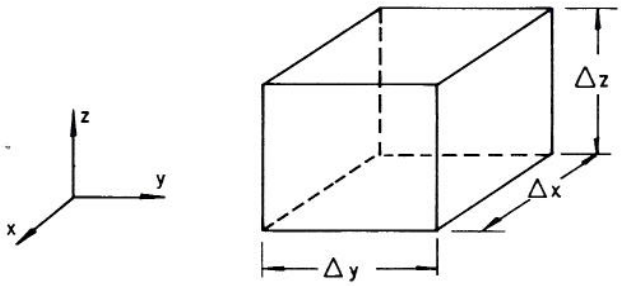

Fig. 2-1 Differential Volume Element for Three-Dimensional Flow Equation.

Assuming the principal directions of permeability coincide with the coordinate directions the flow equation for the volume element is:

$$\frac{\partial}{\partial x}\left[\frac{\rho k_x k_r}{\mu}\left(\frac{\partial P}{\partial x} + \rho g \frac{\partial h}{\partial x}\right)\Delta y \Delta z\right]\Delta x +$$

$$\frac{\partial}{\partial y}\left[\frac{\rho k_y k_r}{\mu}\left(\frac{\partial P}{\partial y} + \rho g \frac{\partial h}{\partial y}\right)\Delta x \Delta z\right]\Delta y +$$

$$\frac{\partial}{\partial z}\left[\frac{\rho k_z k_r}{\mu}\left(\frac{\partial P}{\partial z} + \rho g \frac{\partial h}{\partial z}\right)\Delta x \Delta y\right]\Delta z$$

$$= \frac{\partial}{\partial t}(\rho \phi S \, \Delta x \Delta y \Delta z) + \rho_p Q \, , \qquad (2\text{-}2)$$

where the terms on the left hand side of the equation represent the divergence of mass flux across the faces of the control volume; the first term on the right hand side represents the change of mass storage within the control volume with respect to time; and the second term on the right hand side is a mass source or sink term. The symbols used in Eq. 2-2 are defined as follows:

k_x, k_y, k_z are absolute permeabilities of the medium in the x, y, z directions, respectively,

k_r is the permeability relative to the fluid,

ρ is the mass density of the fluid,

μ is the dynamic viscosity of the fluid,

P is the fluid pressure,

g is the acceleration of gravity,

h is the elevation of the control volume with respect to an arbitrary datum perpendicular to the direction of gravity,

ϕ is the porosity of the medium,

S is the fluid saturation,

ρ_p is the density of the fluid passed in the source or sink,

Q is the volume flow rate of the source or sink which is positive in the case of a sink and negative for a source.

To accurately describe many cases of multi-phase flow, a relationship similar to Eq. 2-2 is required for each fluid phase. Breitenbach, et al. (1968) have developed such equations for the three phase system of oil, gas, and water. However, in the case of the two phase, air-water systems being considered in this study, an assumption can be made which greatly simplifies the mathematical description of the flow phenomenon. This assumption is that the resistance to air flow through the porous medium is negligible, and therefore the pressure of the air throughout the system is nearly constant and can be assumed atmospheric. This assumption is generally valid for flow in unconfined aquifer systems because velocities are very small, and for this reason it is considered permissible in this development to neglect the flow of air in the system. As a result, the only flow equation to be considered in the treatment of the unsaturated zone is Eq. 2-2 for the water phase. It will be demonstrated later in this section that Eq. 2-2 is applicable to flow in the saturated zone as well.

Equation 2-2 may be simplified by assuming the density of the water, ρ, is constant and uniform throughout the system, and assuming the porosity, ϕ, is not a function of time. The density of water varies with pressure according to the following relationship:

$$d\rho = \beta \rho dP \quad , \tag{2-3}$$

where β is the reciprocal of the bulk modulus of elasticity of water, and is approximately 3.3×10^{-6} in^2/lb. The maximum pressure variations within the systems being considered in this study are not expected to exceed 130 lb/in^2. Substitution of these values into Eq. 2-3 results in a maximum expected variation in density of less than 0.05 percent of ρ. The assumption of constant density was therefore considered valid.

Porosity is a function of the compressibility of the aquifer, and is related to the hydraulic pressure by the equation

$$\phi = \phi_o \left[1 + C_F \left(P - P_o\right)\right] \quad , \tag{2-4}$$

where

ϕ_o is the porosity at some arbitrary reference pressure,

P_o is the reference pressure,

C_F is the aquifer compressibility.

In most cases, C_F is of the order of magnitude of 10^{-6} in^2/lb, and thus variations in porosity are of the same order of magnitude as density variations. Therefore, the assumption that ϕ is constant at a given location is considered valid.

The assumption of constant density, along with the consideration of only the water phase, allows the pressures and elevation heads for all points in the system to be expressed in terms of the total head, H, which is defined as:

$$H = P/\rho g + h \tag{2-5}$$

Using this relationship, the following substitution may be made into the partial derivatives of pressure and elevation with respect to x in the left hand side of Eq. 2-2.

$$g \frac{\partial H}{\partial x} = \left(\frac{\partial P}{\partial x} + \rho g \frac{\partial h}{\partial x}\right) \quad , \tag{2-6}$$

with similar substitutions in the partial derivatives of pressure and elevation with respect to y and z. To implement the use of the three-dimensional groundwater flow equation in the finite difference model, the assumption is made that the material inside the control volume shown in Fig. 2-1 is homogeneous. Using this assumption, the porosity term may be placed outside the time derivative in the right-hand side of Eq. 2-2. A constant density term may also be eliminated from each side of the equation. The result is:

$$\begin{aligned} &\frac{\partial}{\partial x}\left[\frac{k_x k_r}{\mu}\left(\rho g \frac{\partial H}{\partial x}\right)\Delta y \Delta z\right]\Delta x + \\ &\frac{\partial}{\partial y}\left[\frac{k_y k_r}{\mu}\left(\rho g \frac{\partial H}{\partial y}\right)\Delta x \Delta z\right]\Delta y + \\ &\frac{\partial}{\partial z}\left[\frac{k_z k_r}{\mu}\left(\rho g \frac{\partial H}{\partial z}\right)\Delta x \Delta y\right]\Delta z \\ &= \phi \frac{\partial}{\partial t}\left(S \Delta x \Delta y \Delta z\right) + Q \quad . \end{aligned} \tag{2-7}$$

The permeability relative to the fluid, k_r, and the saturation, S, are constants for hydraulic pressures greater than or equal to zero gage pressure, and functions of pressure where pressures are negative. These relationships may be expressed as:

$$\begin{aligned} k_r &= k_r(p) \quad , \quad p < 0 \quad , \\ k_r &\equiv 1.0 \quad , \quad p \geq 0 \quad , \end{aligned} \tag{2-8}$$

$$\begin{aligned} S &= S(p) \quad , \quad p < 0 \quad , \\ S &\equiv 1.0 \quad , \quad p \geq 0 \quad . \end{aligned} \tag{2-9}$$

For a given, fixed point in space the parameters ρ, g, and h, relating total head to pressure are constants. Given the elevation of this point, h, the relative permeability, k_r, and the saturation, S, may be expressed directly as functions of total head, or as constants, within the following ranges of H values.

$$\begin{aligned} k_r &= k_r(H) \quad , \quad H < h \\ k_r &\equiv 1.0 \quad , \quad H \geq h \end{aligned} \tag{2-10}$$

$$\begin{aligned} S &= S(H) \quad , \quad H < h \\ S &\equiv 1.0 \quad , \quad H \geq h \end{aligned} \tag{2-11}$$

The hydraulic conductivity, K, is defined by combining terms from the left-hand side of Eq. 2-7, for

flow in each of the three coordinate directions. Hydraulic conductivities for flow in the x, y, and z directions respectively, are:

$$K_x = \frac{k_x k_r}{\mu} g , \qquad (2\text{-}12)$$

$$K_y = \frac{k_y k_r}{\mu} g , \qquad (2\text{-}13)$$

$$K_z = \frac{k_z k_r}{\mu} g . \qquad (2\text{-}14)$$

Having expressed k_r as a function of total head for some fixed point in space, K_x, K_y, and K_z at that point may also be related to H.

For K_x this relationship is

$$\begin{aligned} K_x &= K_{xo} k_r , \quad H < h \\ K_x &= K_{xo} , \quad H \geq h , \end{aligned} \qquad (2\text{-}15)$$

where K_{xo} is the hydraulic conductivity in the x direction under fully saturated conditions. Similar relationships exist for hydraulic conductivities in the y and z directions. Substitution of the hydraulic conductivities defined in Eqs. 2-12, 2-13, and 2-14 into Eq. 2-7 result in

$$\frac{\partial}{\partial x}\left[K_x \frac{\partial H}{\partial x} \Delta y \Delta z\right]\Delta x + \frac{\partial}{\partial y}\left[K_y \frac{\partial H}{\partial y} \Delta x \Delta z\right]\Delta y + \frac{\partial}{\partial z}\left[K_z \frac{\partial H}{\partial z} \Delta x \Delta y\right]\Delta z = \phi \frac{\partial}{\partial t}(S \Delta x \Delta y \Delta z) + Q . \qquad (2\text{-}16)$$

The right-hand side of Eq. 2-16 may be simplified by assuming that the dimensions of the volume element, Δx, Δy, and Δz do not vary with time. This assumption is valid for the development of this equation for use in the finite difference model because volume elements, or grids are sized arbitrarily and remain constant throughout time during any single use of the model. The result is that only the saturation, S remains inside the time derivative in the first term on the right-hand side of Eq. 2-16. Applying the chain rule for partial derivatives, the following substitution can be made to express S for a fixed point having known elevation as a function of H instead of t:

$$\frac{\partial S}{\partial t} = \frac{dS}{dH} \frac{\partial H}{\partial t} \qquad (2\text{-}17)$$

The derivative of S with respect to H is shown as a total derivative rather than a partial derivative because S can be expressed as a function of H alone. Substitution of Eq. 2-17 into Eq. 2-16 results in:

$$\frac{\partial}{\partial x}\left[K_x \frac{\partial H}{\partial x} \Delta y \Delta z\right]\Delta x + \frac{\partial}{\partial y}\left[K_y \frac{\partial H}{\partial y} \Delta x \Delta z\right]\Delta y + \frac{\partial}{\partial z}\left[K_z \frac{\partial H}{\partial z} \Delta x \Delta y\right]\Delta z = \phi \Delta x \Delta y \Delta z \frac{\alpha S}{\alpha H} \frac{\partial H}{\partial t} + Q , \qquad (2\text{-}18)$$

which is the general form of the three-dimensional flow equation on which the development of the three-dimensional segment of the finite difference model is based. Equation 2-18 is nonlinear because S and K_x, K_y and K_z are nonlinear functions of H. For saturated flow conditions within a given grid dS/dH is equal to zero, and K_x, K_y, and K_z are assigned constant values K_{xo}, K_{yo}, and K_{zo}, respectively, in which case Eq. 2-18 is linear. Although the differential lengths Δx, Δy, and Δz are constants which could have been eliminated from Eq. 2-18, they have been retained for comparison with the finite difference form of Eq. 2-18 developed for use in the computer model in Chapter III.

Development of the Two-Dimensional Groundwater Flow Equation

The development of the two-dimensional segment of the finite difference model is based on a groundwater flow equation which has been simplified by neglecting flow in the vertical direction and assuming (1) flow velocity is proportional to the slope of the water table, and (2) flow is horizontal and uniform everywhere in a vertical section. These assumptions are the Dupuit-Forchheimer assumptions as stated by Corey (1969). It is evident that these assumptions are contradictory in physical reality because any slope of the water table in the unconfined aquifer indicates a vertical component of velocity. However, in cases where the water table slope is mild and water table fluctuations are small compared to the saturated thickness of the aquifer, errors introduced by using the Dupuit-Forchheimer assumptions are generally negligible.

The use of the two-dimensional flow equation requires that streams traversing the area be either hydraulically connected with the underlying aquifer at all points on the boundary of a given cross section, or not hydraulically connected with the aquifer at any point on the cross section. Streams considered to be hydraulically connected with the aquifer are generally treated as boundaries of known or constant head. Flow into the aquifer from a reach of stream considered not to be hydraulically connected with the aquifer is treated as a source term, and the river itself is not considered as part of the aquifer for purposes of writing the groundwater flow equation. The river traversing the area being treated by the two-dimensional flow equation in this study is considered to act as a known-head boundary.

The development of the two-dimensional flow equation is based on the continuity principle and Darcy's law, as is the three-dimensional flow equation. The important difference between the development of these two equations lies in the manner in which vertical movements of the water table and volume fluxes in the vertical direction are treated mathematically.

The location and dimensions of the volume elements for which the three-dimensional flow equation is written are arbitrarily set, as shown in Fig. 2-1, and are independent of the location of the water table or the bedrock surface. Volume flux in the vertical direction is described by the third term in the left-hand side of Eq. 2-18. It is necessary to consider changes in saturation which may occur in each three-dimensional grid because the location of the water table can change with respect to the fixed elevation of these grids.

By contrast, only the horizontal dimensions of the volume elements treated by the two-dimensional flow equation can be set arbitrarily. The upper and

lower boundary elevations of these grids are determined by the location of the water table and the bedrock surface, respectively, as illustrated in Fig. 2-2. Because the upper grid boundary is located at the water table at all times, saturated flow conditions always exist within the grid. Volume flux in the vertical direction is accounted for by a source or sink term. The effects of saturation and movement of the water table on the volume of storage in the grid are accounted for by the specific yield, S_y, which is defined as the volume of water released from or taken into storage by an aquifer per unit surface area due to a unit change in water table elevation. Specific yield is considered to be constant at any given location.

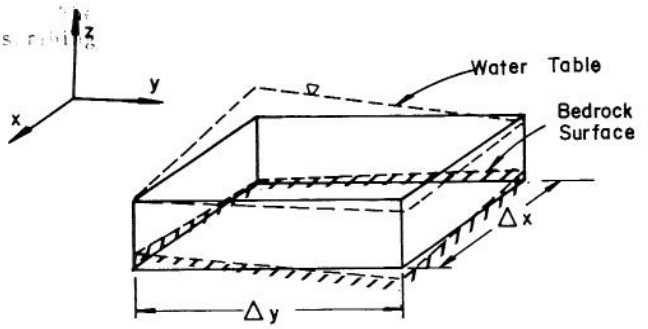

Fig. 2-2. Differential Volume Element for Two-Dimensional Flow Equation.

The nonlinear, partial differential equation describing saturated, two-dimensional, transient flow through porous media may be expressed in differential form as:

$$\frac{\partial}{\partial x}\left(K_x \frac{\partial H}{\partial x} m\Delta y\right)\Delta x + \frac{\partial}{\partial y}\left(K_y \frac{\partial H}{\partial y} m\Delta x\right)\Delta y = S_y \Delta x \Delta y \frac{\partial H}{\partial t} + Q \ , \qquad (2\text{-}19)$$

in which m is the saturated thickness, defined by the relationship:

$$m = H - h_b \ , \qquad (2\text{-}20)$$

where h_b is the elevation of the bedrock surface. Other symbols used in Eq. 2-19 have been defined previously. Because flow is assumed saturated, K_x and K_y take on the constant values for saturated hydraulic conductivity , K_{xo} and K_{yo}.

The development of a finite difference form of the two-dimensional flow equation is based on Eq. 2-19. Differentials Δx and Δy have been retained in the equation for comparison with the finite difference equation developed in Chapter III for use in the simulation model.

Equations Describing Flow Across the River Boundary

The primary purpose of this study is to develop a model capable of duplicating an actual, physical process with reasonable accuracy. For this reason, an understanding of the various conditions under which flow may occur across the boundary between a natural stream and the adjacent aquifer is of paramount importance. This study is limited to the treatment of three conditions believed to be most prevalent in the stream-aquifer system under consideration in this study. These are discussed in this section. These conditions are: (1) seepage from the aquifer into the stream and (2) seepage from the stream into the aquifer, both taking place with the stream and aquifer hydraulically connected and with the seepage rate controlled by the pressure gradient across the boundary between the stream and aquifer, and (3) seepage from the stream into the aquifer in which hydraulic connection between the two has been broken. Seepage rate in this case is determined by the depth of water in the stream alone, and is not dependent on the water table elevation in the aquifer so long as the hydraulic connection remains broken.

Equations for unsteady flow for each of these conditions should provide accurate representation of actual flow conditions. However, unsteady flow across the river boundary is caused primarily by fluctuations in the depth of water in the river, and these fluctuations ordinarily occur over durations of time that are very short compared to the time increments used in the finite difference model. Because of the usual short duration of these fluctuations, and the tendency over an increment of model time for the effects of many positive and negative fluctuations to cancel, it is assumed that seepage rate at a given location on the boundary between the stream and aquifer can be represented by an average value during each model time increment without introducing appreciable error. For this reason seepage rates across the stream-aquifer boundary are computed at each time increment using steady state flow equations and an estimated mean river depth.

The condition of seepage from the aquifer into the stream is illustrated in Fig. 2-3. Flow is considered from point A, some distance parallel to the direction of flow from the river boundary, to the river. The relationship for seepage velocity into the river from point A can be expressed by Darcy's law as:

$$v = K_{Lo} \frac{\Delta H}{\Delta L} \ , \qquad (2\text{-}21)$$

where

K_{Lo} is the hydraulic conductivity for saturated conditions in the direction of flow between point A and the river

ΔH is the difference in total head between point A and the river.

ΔL is the distance from point A to the river boundary in the direction of flow.

Forms of Eq. 2-21 written for flow in the x, y, and z directions are used to describe the boundary condition of seepage into the river from the aquifer in the three-dimensional portion of the finite difference model.

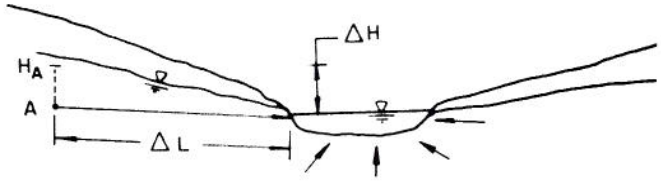

Fig. 2-3. Seepage from Aquifer into River.

The conditions of flow from stream to aquifer, with or without hydraulic connection, are both affected by the presence of a silt layer on the banks and bed of the river. This silt layer is formed by the deposition of particles of fine sediment on the stream banks and bed. The silt layer generally has a much lower hydraulic conductivity than the surrounding aquifer material, and can dramatically restrict the rate of seepage from the river.

A detailed discussion of the behavior of silt layers in natural channels has been presented by Matlock (1965), who conducted both field observations of natural streams and experiments in a laboratory flume to determine the effects of silt on infiltration rates. Following are some of Matlock's observations which have been considered in the development of the equations describing seepage from a stream to the adjacent shallow aquifer through a silt layer:

(1) Laboratory experiments showed that the silt layer forms and remains stable under a broad range of conditions commonly found in natural streams.

(2) Bedform movement does not generally disturb the silt layer because it is formed below the level of the bedforms.

(3) A break in the silt layer caused by some local disturbance results in an increased seepage rate, but only for a very short period of time in most instances. The high local seepage rate brings about the rapid accumulation of fine sediment in the break, and the silt layer re-forms almost immediately.

(4) A silt layer only one or two millimeters thick may reduce the seepage rate to as little as one one-hundredth of the seepage rate prior to the formation of the silt layer.

The inference of these observations is that, in general, seepage from a stream carrying silt-laden water is restricted by a silt layer on the bed and banks of the channel. This inference was substantiated by its use in a finite element model of a stream-aquifer system by Hurr (1972). In an area where seepage from the river was taking place both with and without a hydraulic connection between the river and aquifer, the response of the water table was simulated with good accuracy using Hurr's model.

The condition of seepage from the river with the stream and aquifer hydraulically connected is illustrated in Fig. 2-4. Flow is considered from the river through the silt layer to point B in the aquifer. The cross-sectional area of flow between the river and point B is assumed to be constant. This assumption holds true in the application of the finite difference model, and its use here simplifies the development of the equation for seepage velocity. Because steady state conditions are assumed to exist, seepage velocity may be expressed by Darcy's law in terms of the hydraulic gradient and conductivity, either in the silt layer or in the aquifer, as

$$v = K_s \frac{\Delta H_s}{t_s} = K_B \frac{\Delta H_B}{\Delta L} \quad , \qquad (2\text{-}22)$$

where

ΔH_s is the head loss through the silt layer,

ΔH_B is the head loss between the silt layer and point B,

K_s is the hydraulic conductivity of the silt layer,

K_B is the hydraulic conductivity of the aquifer material between the river and point B,

t_s is the thickness of the silt layer,

ΔL is the distance parallel to the direction of flow from the river to point B.

For use in the finite difference model, an equation for v in terms of the total head loss between the river and point B is necessary. For this purpose, Eq. 2-22 is rearranged and written as

$$\Delta H_s = \frac{v t_s}{K_s} \quad , \qquad (2\text{-}23)$$

$$\Delta H_B = \frac{v \Delta L}{K_B} \quad , \qquad (2\text{-}24)$$

By summing Eqs. 2-23 and 2-24, an expression is obtained which defines total head loss, ΔH_T and relates it to seepage velocity, v .

$$\Delta H_T = \Delta H_s + \Delta H_B = v \left(\frac{t_s}{K_s} + \frac{\Delta L}{K_B}\right) \qquad (2\text{-}25)$$

Rearranging Eq. 2-25 and solving for v results in

$$v = \left(\frac{K_B K_s}{t K_B + \Delta L K_s}\right) \Delta H_T \quad . \qquad (2\text{-}26)$$

Equation 2-26, written for flow in the x , y, and z directions, is used in the finite difference model to describe the boundary condition of seepage from the river when hydraulically connected with the adjacent aquifer.

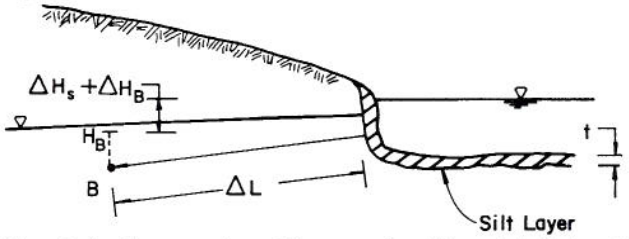

Fig. 2-4. Seepage from River to Aquifer with Hydraulic Connection.

The condition of seepage from the river, with no hydraulic connection to the adjacent aquifer is illustrated in Fig. 2-5.

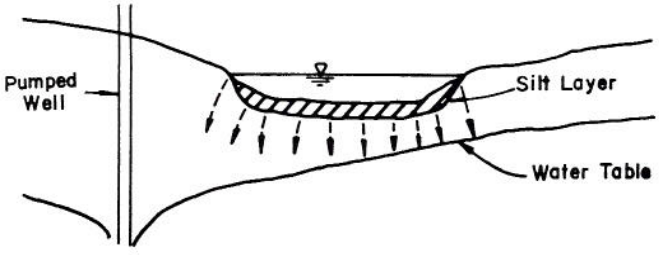

Fig. 2-5. Seepage from River to Aquifer without Hydraulic Connection.

This condition exists where a silt layer is present in the river bed and banks to retard the seepage rate from the stream. The maximum possible steady state seepage velocity which can pass through the silt layer is determined by the hydraulic conductivity of the silt layer, the positive pressure head at the upper surface of the silt layer, and an additional amount of negative pressure head which can be sustained at the lower surface of the silt layer with saturated flow conditions still prevailing. This negative pressure head is the bubbling, or air entry pressure head of the material composing the silt layer. This bubbling pressure head defines the lowest value of pressure head that can exist in the system for steady, saturated flow. Reducing the pressure head at the lower surface of the silt layer below this value would not increase the flow rate of water through the silt layer, but instead would initiate air flow. The expression for the maximum seepage velocity from the stream downward through the silt layer is obtained by writing Darcy's law for flow under steady state conditions through the silt layer. This expression is

$$v_{max} = K_s \left(\frac{d + t_s - h_{pb}}{t_s}\right) , \qquad (2\text{-}27)$$

where

d is the depth of flow in the river,

t_s is the silt layer thickness,

h_{pb} is the bubbling pressure head of the silt layer,

K_s is the hydraulic conductivity of the silt layer.

According to the sign convention used in this development, the value of h_{pb} is negative.

When the water table near the river recedes to such an extent that the difference in total head between the river and the underlying aquifer exceeds the maximum possible head loss as defined by Eq. 2-27, the hydraulic connection between the river and the aquifer ceases to exist. Further drawdown of the water table does not affect the seepage velocity from the stream, which remains constant at v_{max} as long as the depth of streamflow does not change.

Flow downward through the pervious material below the silt layer takes place under unsaturated conditions. Pressure and saturation at any point in this unsaturated zone depend on the physical properties of the aquifer material at that point. Pressure returns to atmospheric and saturation approaches 1.0 as flow reaches the water table. The pressure distribution for flow from the river to the water table in the underlying aquifer through a silt layer is shown in Fig. 2-6 for steady flow and homogeneous aquifer material. Equation 2-27 is used in the simulation model to describe seepage through the streambed to the underlying aquifer when the stream and aquifer are not hydraulically connected.

An equation similar to Eq. 2-27, but with no gradient of elevation head, describes lateral seepage out

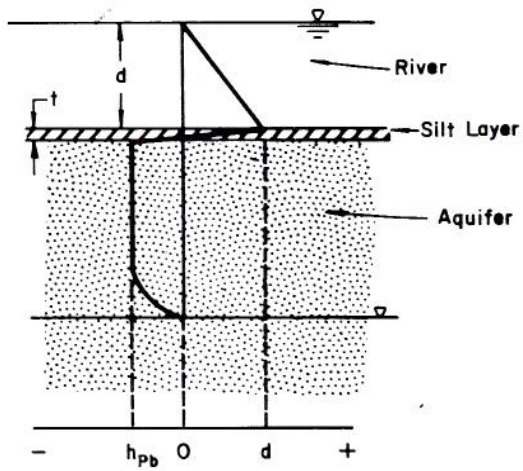

Fig. 2-6. Pressure Head Distribution for Seepage from River to Underlying Water Table.

through the stream banks. In order to determine an average seepage velocity through the bank, a hydrostatic pressure head distribution is assumed to exist in the river, as shown in Fig. 2-7. The pressure head in the adjacent section of the aquifer is assumed to be uniform, as it is in the finite difference representation of this flow situation used in the simulation model. The maximum discharge through a unit width of this stream bank for a given depth of streamflow is

$$q_{max} = \frac{K_s}{t_s} \int_0^d (h - h_{pb})\, dh = \frac{K_s d(d/2 - h_{pb})}{t_s} . \qquad (2\text{-}28)$$

The average seepage velocity for this maximum discharge is

$$v_{ave} = \frac{K_s d(d/2 - h_{pb})}{t_s} . \qquad (2\text{-}29)$$

In the finite difference representaiton of this flow situation, seepage rate out through the stream bank is assumed to be uniform and equal to v_{ave} at all points between the water surface in the river and the streambed. The seepage velocity above the water surface is zero. Equation 2-29 is used in the simulation model to describe seepage outward through the bank at a given cross section of the river when no hydraulic connection exists between the stream and aquifer at that point.

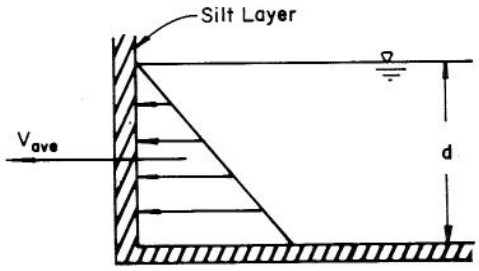

Fig. 2-7. Pressure Head Distribution for Unsaturated Seepage through the River Bank.

CHAPTER III
DEVELOPMENT OF THE SIMULATION MODEL

The basis of the model for simulating flow in a stream-aquifer system is the finite difference form of the groundwater flow equation, presented in Chapter II for both two-dimensional and three-dimensional flow. The application of the model consists of representing the study area by a grid system and writing the flow equation for each grid. The interactions between the river and aquifer are accomodated by imposing various boundary conditions on the grids through which the river flows. The nature of these boundary conditions was discussed in Chapter II. Inflows and outflows through the upper surface of the model include precipitation, evapotranspiration, irrigation, and pumping. Values of net surface flux for all two-dimensional grids and those three-dimensional grids adjacent to the upper surface are obtained by summing values of the various surface inflows and outflows in each grid. The values thus obtained are input to the model as production terms in the flow equation for each grid. The perimeter grids of the model may be treated as boundaries of known or constant head, known, constant, or zero discharge, or known or constant hydraulic gradient. Because data were readily available for values of head throughout the region considered in this study, the perimeter grids were treated as boundaries of known or constant head. Computations of discharge and stage in the river are external to the portion of the model dealing with the groundwater flow equations. Discharge is computed for each river grid by applying the continuity principle, including consideration of the contributions of seepage and canal diversions. The stage in each grid is then computed using the Manning formula. The remainder of this chapter consists of a description of each of the major components of the computer model developed in this study and an account of the operation of the computer program through one time cycle. Brief descriptions of each of the model subroutines and a listing of the computer program appear in Appendix A.

Development of Finite Difference Model for Groundwater Movement

Finite difference techniques are based on the substitution of ratios of discrete changes in the values of appropriate variables over small space and time intervals in place of derivatives. To facilitate the use of a finite difference technique, the study area is divided into a system of grids. The sizing and placement of the grids depends on the physiography of the region and the detail desired. Large grids are used where the physiography is fairly uniform and detail is not too important. Smaller grids are required to obtain more detailed information, or to accurately describe flow in regions having irregular bedrock contours, steep water table gradients, discontinuities in the subsurface geology, or other irregularities in the physiography that might influence the local flow pattern. Each grid in the three-dimensional model segment is assigned a value of hydraulic conductivity, a grid center elevation, and an initial head. Similarly, each grid in both two-dimensional model segments is assigned a value of hydraulic conductivity, a bedrock elevation, and an initial water table elevation. These parameter values are obtained by averaging data values for each individual parameter over the space within every grid. The flow equation for each grid is written in terms of the parameter values of that grid and of the adjacent grids, the distance intervals between the adjacent grid centers, and an arbitrary time interval. An implicit centered-in-space, finite difference scheme is used in this model to approximate the time and space derivatives in the groundwater flow equations.

An important limitation of the finite difference technique used in this model is its restricted applicability to linear equations only. Groundwater flow Eqs. 2-18 and 2-19 are both nonlinear. The hydraulic conductivity, K, which appears in vector notation in the terms on the left-hand side of Eq. 2-18 is a function of head, H, as is the saturation, S, which appears in a derivative with respect to H on the right-hand side of Eq. 2-18. The saturated thickness, m, which is included as a coefficient in the left-hand side terms of Eq. 2-19, is also a function of H. It appears that the finite difference scheme presented for use in this study is not appropriate for describing the flow situations described in Eqs. 2-18 and 2-19. However, these equations can be linearized by holding the values of the functions of H constant during each time increment, so that H is the only unknown in each equation. At the beginning of each time increment new values of K and dS/dH are computed for each three-dimensional grid as functions of head at the present time level. Similarly, new m values are computed as functions of head at the present time level in each two-dimensional grid. Errors resulting from the use of these approximations are negligible if care is taken to select a sufficiently small time increment so that the variation of H values throughout the model is small from one time level to the next. A suitable size of time increment for use in simulating flow in a given stream-aquifer system is determined by making trial runs of the model on data from that system with several different time increments. The largest time increment for which stable results are obtained, and for which changes in head from one time step to the next are below some arbitrary tolerance limit, is selected for use in making production runs. The tolerance limit used in this study was one foot. Analysis of trial runs of the model on field data used in this study resulted in the selection of a time increment of 30 days.

Three-Dimensional Flow Model

Development of the Finite Difference Equation. A typical grid used in the three-dimensional portion of the groundwater model is shown in Fig. 3-1, with the locations of the centers of the six adjacent grids indicated. The terms on the left hand side of Eq. 2-18

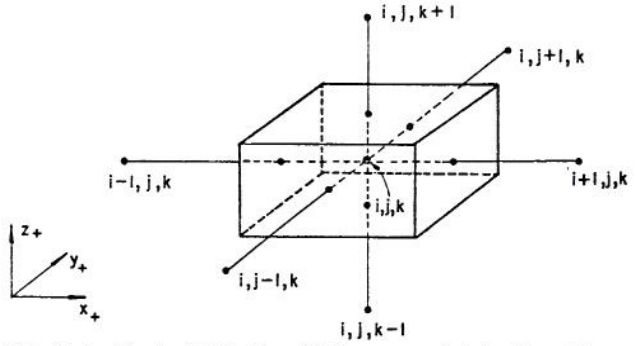

Fig. 3-1 Typical Finite Difference Grid for Three-Dimensional Flow

represent flow across the six grid faces. The flow across a given face can be expressed in terms of the dimensions of the two adjoining grids and the flow parameters at the grid centers. Two adjacent grids are shown in Fig. 3-2, with flow in the x direction across the connecting face being considered. According to Darcy's law, discharge from grid i into grid i+1 may be expressed as

$$Q_o = K_{xo} A_o \frac{H_i - H_{i+1}}{0.5(\Delta x_i + \Delta x_{i+1})} , \qquad (3\text{-}1)$$

where

k_{xo} is the hydraulic conductivity at the grid interface for flow in the x direction,

A_o is the cross-sectional area perpendicular to the direction of flow,

H_i is the head at the center of grid i,

H_{i+1} is the head at the center of grid i+1,

$0.5(\Delta x_i + \Delta x_{i+1})$ is the distance between the grid centers.

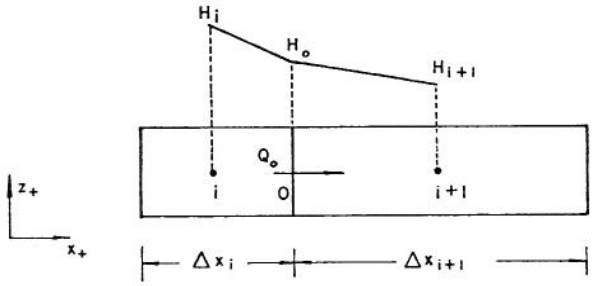

Fig. 3-2 Flow between Adjacent Grids of the Three-Dimensional Model

The finite difference approximation of steady flow during each time increment between adjacent grid centers is used to obtain an expression for Q_o in terms of adjacent grid dimensions and grid center parameters. Discharge between the center of grid i and the interface, and between the interface and the center of grid i+1 are both equal to Q_o, and may be expressed according to Darcy's law in terms of the respective grid parameters and dimension as:

$$Q_{i-o} = Q_o = K_i A_i \frac{H_i - H_o}{\Delta x_i / 2} , \qquad (3\text{-}2)$$

$$Q_{o-i+1} = Q_o = K_{i+1} A_{i+1} \frac{H_o - H_{i+1}}{\Delta x_{i+1} / 2} . \qquad (3\text{-}3)$$

The cross-sectional areas at all points between i and i+1 are uniform and may be expressed in terms of grid dimensions as

$$A = A_i = A_{i+1} = \Delta y \cdot \Delta z , \qquad (3\text{-}4)$$

where Δy and Δz are the grid dimensions perpendicular to the direction of flow. Substituting Eq. 3-4 into Eqs. 3-2 and 3-3 and rearranging results in

$$H_i - H_o = \frac{Q_o}{2\Delta y \Delta z} \frac{\Delta x_i}{K_i} , \qquad (3\text{-}5)$$

$$H_o - H_{i+1} = \frac{Q_o}{2\Delta y \Delta z} \frac{\Delta x_{i+1}}{K_{i+1}} . \qquad (3\text{-}6)$$

Equations 3-5 and 3-6 are added tobether to eliminate H_o. The resulting expression, after combining terms, is

$$H_i - H_{i+1} = \frac{Q_o}{2\Delta y \Delta z} \left(\frac{\Delta x_i K_{i+1} + \Delta x_{i+1} K_i}{K_i K_{i+1}} \right) . \qquad (3\text{-}7)$$

Solving Eq. 3-7 for Q_o yields the following expression for flow across the grid interface shown in Fig. 3-2.

$$Q_o = \frac{2 K_i K_{i+1} \Delta y \Delta z}{\Delta x_i K_{i+1} + \Delta x_{i+1} K_i} (H_i - H_{i+1}) . \qquad (3\text{-}8)$$

Comparison of Eqs. 3-1 and 3-8 indicates the following substitution has been made:

$$\frac{K_{xo}}{\Delta x_i + \Delta x_{i+1}} = \frac{K_i K_{i+1}}{\Delta x_i K_{i+1} + \Delta x_{i+1} K_i} , \qquad (3\text{-}9)$$

which shows that K_{xo}, the x component of the hydraulic conductivity at the interface, has been replaced by a combination of K_i and K_{i+1} at the adjacent grid centers. In the finite difference form of Eq. 2-18, K_x, K_y, and K_z are represented as combintions of the discrete, grid center K values in the appropriate directions. Expressions similar to Eq. 3-8, written for each of the six faces of every interior grid, constitute the finite difference form of the left-hand side of Eq. 2-18 used in the computer model. For grids located on the bottom layer of the grid network, flow across the lower surface is assumed to be equal to zero. Flow across the upper face of each surface grid of the network is assumed to be equal to the surface flux, which is computed separately from the matrix of groundwater flow equations.

The right-hand side of Eq. 2-18 contains a time derivative of H, which is approximated by the finite difference form:

$$\frac{\partial H}{\partial t} \approx \frac{H^{t+\Delta t} - H^t}{\Delta t} . \qquad (3\text{-}10)$$

where

superscripts t and t+Δt indicate time levels before and after an incremental time change, respectively,

Δt is the time increment,

H is the head in a given grid.

At each time level the derivative of saturation with respect to head and the hydraulic conductivity used in Eq. 2-18 for every grid in the three-dimensional model segment are assigned values that remain constant during the operation of the model through one time increment. These values are computed at the beginning of each time increment as functions of head in every three-dimensional grid. The approximations used in the

model for obtaining values of K and dS/DH in a given grid are:

$$K \sim K_{sat}\overline{k}_r \ , \tag{3-11}$$

$$\frac{dS}{dH} \sim \frac{\overline{\Delta S}}{\Delta H} \ , \tag{3-12}$$

where

K_{sat} is the hydraulic conductivity in the grid under saturated conditions,

$\overline{k}_r$ is the average relative permeability in the grid,

$\overline{\Delta S}$ is the average change in saturation over some small increment of head in the grid,

ΔH is the increment of head.

For grids entirely below the water table, $\overline{k}_r$ is equal to one and $\overline{\Delta S}$ is equal to zero. In order to obtain values of $\overline{k}_r$ and $\overline{\Delta S}$ for grids located partially or entirely above the water table, relationships for k_r and S as functions of pressure head, h_p, are needed. The plots of k_r and S versus h_p obtained for use in this study are described in Chapter IV. To compute $\overline{k}_r$ and $\overline{\Delta S}$ for a given grid, the vertical dimension of the grid is first divided into small, equal increments. An approximate value of the pressure head in each increment is then obtained by subtracting the elevation at that point from the head in the grid. If the pressure head thus obtained is nonnegative, the values k_r=1.0 and ΔS=0 are assigned to the increment directly. If the pressure head is negative, values of k_r and ΔS corresponding to the pressure head in the increment are obtained from the plots of k_r and S versus h_p. Values of k_r and ΔS are thus obtained for every vertical increment of the grid. The average of all k_r values in the grid is the value of $\overline{k}_r$ used in Eq. 3-10 to obtain a value of K at the grid center. The average of the incremental ΔS values in the grid is the value of $\overline{\Delta S}$ used in Eq. 3-11 to obtain an approximate value of dS/dH at the grid center.

The finite difference equation for three-dimensional flow is obtained by substituting Eq. 3-10 into the right-hand side of Eq. 2-18, writing expressions in the form of Eq. 3-8 for the left-hand side of Eq. 2-18, and assigning K and dS/dH constant values obtained by the procedure described in preceding paragraphs. The equation thus obtained is rearranged so that all unknown values of head, H, at time level t+Δt, appear on the left-hand side of the equation, with the known value of H, at time level t, on the right-hand side. The result, written for a typical grid as shown in Fig. 3-1 is

$$AH^{t+\Delta t}_{i-1,j,k} + BH^{t+\Delta t}_{i+1,j,k} + CH^{t+\Delta t}_{i,j-1,k} + DH^{t+\Delta t}_{i,j+1,k} + EH^{t+\Delta t}_{i,j,k-1} + FH^{t+\Delta t}_{i,j,k+1} - (A+B+C+D+E+F+G)H^{t+\Delta t}_{i,j,k} = Q - GH^{t}_{i,j,k} \ . \tag{3-13}$$

where

$$A = \frac{2K_{i-1,j,k}K_{i,j,k}\Delta y_j \Delta z_k}{\Delta x_{i-1}K_{i,j,k} + \Delta x_i K_{i-1,j,k}} \ , \tag{3-14}$$

$$B = \frac{2K_{i+1,j,k}K_{i,j,k}\Delta y_j \Delta z_k}{\Delta x_{i+1}K_{i,j,k} + \Delta x_i K_{i+1,j,k}} \ , \tag{3-15}$$

$$C = \frac{2K_{i,j-1.k}K_{i,j,k}\Delta x_i \Delta z_k}{\Delta y_{j-1}K_{i,j,k} + \Delta y_j K_{i,j-1,k}} \ , \tag{3-16}$$

$$D = \frac{2K_{i,j+1,k}K_{i,j,k}\Delta x_i \Delta z_k}{\Delta y_{j+1}K_{i,j,k} + \Delta y_j K_{i,j+1,k}} \ , \tag{3-17}$$

$$E = \frac{2K_{i,j,k-1}K_{i,j,k}\Delta x_i \Delta y_j}{\Delta z_{k-1}K_{i,j,k} + \Delta z_k K_{i,j,k-1}} \ , \tag{3-18}$$

$$F = \frac{2K_{i,j,k+1}K_{i,j,k}\Delta x_i \Delta y_j}{\Delta z_{k+1}K_{i,j,k} + \Delta z_k K_{i,j,k+1}} \ , \tag{3-19}$$

$$G = \frac{\phi \Delta x_i \Delta y_j \Delta z_k (dS/dH)_{i,j,k}}{\Delta t} \ , \tag{3-20}$$

Coefficients A, B, C, D, E, F, and G are held constant at values computed at the beginning of each time increment. The average value of the source or sink term, Q, over the time increment, is the value at which Q is held constant during the operation of the model through the time step.

Application of the Three-Dimensional Model. The three-dimensional grid system is placed so as to encompass all points in the stream-aquifer system where flow of water is likely to occur. For the study area used in the verification of this model, the grid system encloses the river and both the saturated and unsaturated subsurface flow zones. Because the climate of the study area is semiarid and most precipitation either percolates directly into the ground or evaporates where it falls, overland flow due to rainfall excess is assumed negligible and is not considered in the model. Flow in canals is not considered to enter the system until it is applied as irrigation water, a portion of which is assumed to leave the system as evapotranspiration, while the remainder percolates into the subsurface flow system.

A typical cross section of the river valley in the study area is shown in Fig. 3-3, with the three-dimensional grid system superimposed. The grid system has been distorted slightly for the purpose of locating the river in the uppermost grid of one column in each cross section, while keeping the water table below the surface of the model. Except at the side boundaries where the ground surface rises a considerable distance above the water table, the upper surface of the model is at or near the ground surface. The maximum angle of tilt produced by distorting the model for this purpose is less than one degree, and errors due to this small grid distortion are considered negligible.

The river is treated in the three-dimensional model by assigning it a grid in each cross section through which it passes. The grid is sized and located so as to approximate the true channel geometry of the river, as illustrated in Fig. 3-4. Width of the grid is set approximately equal to the average river width. The lower boundary elevation of the river grid is

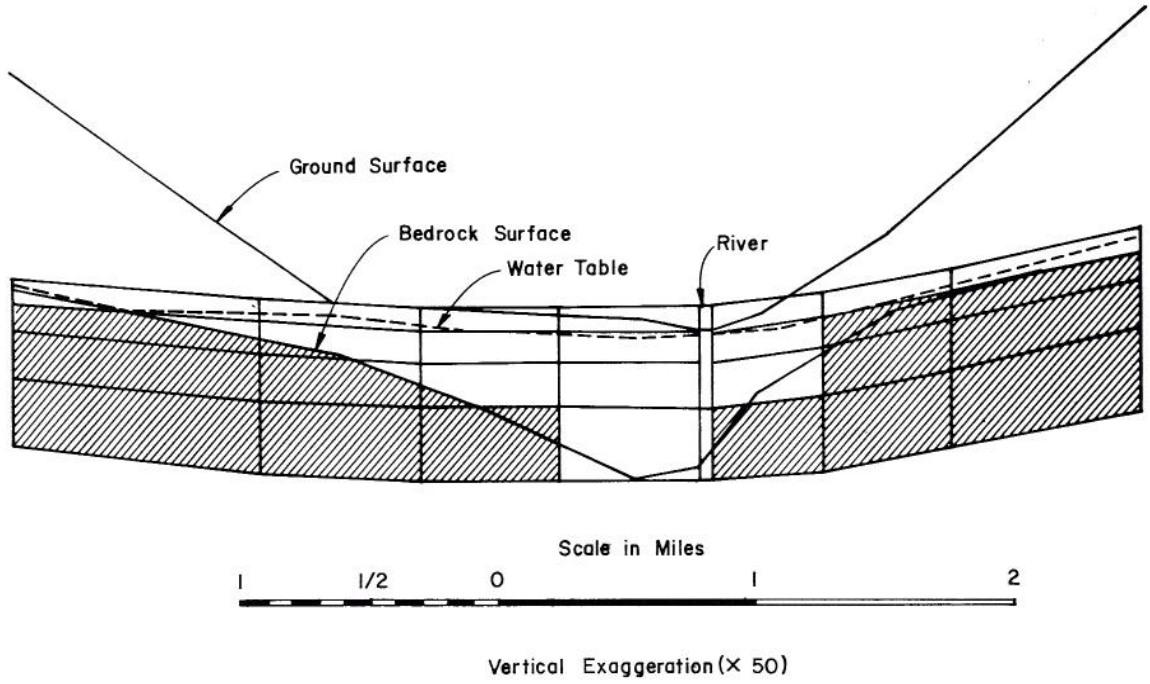

Fig. 3-3 Three-Dimensional Grid System Superimposed on a Cross Section of River Valley

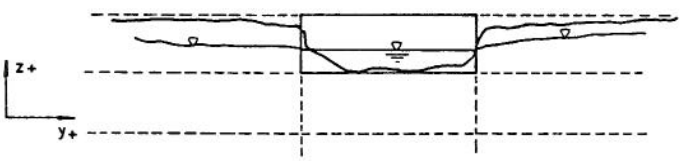

Fig. 3-4 Cross Section of River Grid in the Three-Dimensional Model Segment

approximately equal to the bed elevation. Because the channel of the river in the study area is generally wide and shallow, the rectangular approximation of the river cross section in the model is considered to be reasonable.

Grids lying below the bedrock surface in the three-dimensional model are assigned hydraulic conductivity values of zero, and are inactive in the computation of heads at each time step. Grids lying entirely above the bedrock surface are assigned conductivity values obtained from data. The conductivity values assigned to grids lying partially below and partially above the bedrock surface are reduced to compensate for the impermeable portion of the grid below bedrock, and the entire grid is then treated as part of the permeable alluvium above the level of bedrock.

Two-Dimensional Flow Model

Development of the Finite Difference Equation. The development of the finite difference equation for two-dimensional flow of groundwater is very similar to the development of the equation for three-dimensional flow, presented in a previous section of this chapter. A typical grid used in the two-dimensional portion of the groundwater model is shown with its four adjacent grids in Fig. 3-5. The terms on the left-hand side of Eq. 2-19 represent flow across the four lateral grid faces, and can be expressed in terms of dimensions of the center grid and the four adjacent grids, and the respective grid center parameters. Two adjacent grids

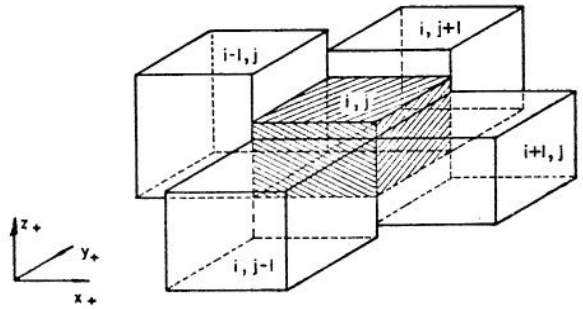

Fig. 3-5 Typical Finite Difference Grid for Two-Dimensional Flow

of the two-dimensional model are shown in Fig. 3-6. Flow in the x direction across the adjoining interface is considered. Discharge across the interface

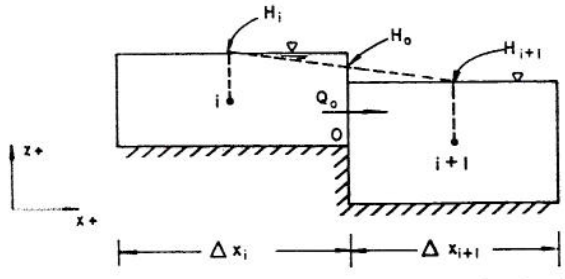

Fig. 3-6 Flow between Adjacent Grids of the Two-Dimensional Model

from grid i to grid i+1 may be expressed by Darcy's law in the form of Eq. 3-1, as was discharge between adjacent grids of the three-dimensional model. Assuming steady flow during each time increment, Eqs. 3-2 and 3-3 are used to represent flow in grids i and i+1 of Fig. 3-6, respectively. The cross-sectional areas of grids i and i+1 are not equal, as was the case in the three-dimensional model grids, but are variables whose value at a given location for a particular time are defined by

$$A = m\Delta y \ , \tag{3-21}$$

where

m is the average saturated thickness of the grid, and is a variable,

Δy is the fixed lateral grid dimension perpendicular to the direction of flow.

Equation 3-21 is substituted into Eqs. 3-2 and 3-3 to obtain the expression for flow in each grid. The result is:

$$Q_{i-o} = Q_o = K_i m_i \Delta y \frac{H_i - H_o}{\Delta x_i/2} \ , \tag{3-22}$$

$$Q_{0-i+1} = Q_o = K_{i+1} m_{i+1} \Delta y \frac{H_o - H_{i+1}}{\Delta x_{i+1}/2} \tag{3-23}$$

Equations 3-22 and 3-23 are rearranged and added together for the purpose of eliminating H_o, resulting in

$$H_i - H_{i+1} = \frac{Q_o}{2\Delta y}\left[\frac{K_i m_i \Delta x + K_{i+1} m_{i+1} \Delta x_i}{K_i K_{i+1} m_i m_{i+1}}\right] . \tag{3-24}$$

Solving Eq. 3-24 for Q_o yields the following expression for flow across a grid interface of the two-dimensional model:

$$Q_o = \frac{2K_i K_{i+1} m_i m_{i+1} \Delta y}{K_i m_i \Delta x_{i+1} + K_{i+1} m_{i+1} \Delta x_i}(H_i - H_{i+1}) . \tag{3-25}$$

A comparison of Eq. 3-25 to 3-1 indicates the following substitution has been made of scalar quantities for hydraulic conductivity in the x-direction at the interface:

$$\frac{K_{xo} A_o}{\Delta x_i + \Delta x_{i+1}} = \frac{K_i K_{i+1} m_i m_{i+1} \Delta y}{K_i m_i \Delta x_{i+1} + K_{i+1} m_{i+1} \Delta x_i} . \tag{3-26}$$

The saturated thickness, m, is a function of head, H, defined as:

$$m = H - h_b \ . \tag{3-27}$$

where h_b is the bedrock elevation in the grid. However, in order to linearize Eq. 3-24 so that it can be solved using finite difference techniques, m is held constant during each time increment. A value of m is obtained at the beginning of each time step for every grid in the two-dimensional model, as explained in a previous section of this chapter. Saturated thickness is therefore considered a constant, and the only unknown quantities in Eq. 3-24 are H_i and H_{i+1}.

The time derivative of H which appears on the right-hand side of Eq. 2-19 is approximated by the finite difference form given in Eq. 3-10, which is also used in the finite difference form of the three-dimensional flow equation.

The finite difference equation for two-dimensional groundwater movement is obtained by substituting expressions in the form of Eq. 3-25 for each of the four lateral grid faces into the left-hand side of Eq. 2-19, and by substituting Eq. 3-10 into the right-hand side of Eq. 2-19. The resulting equation is then rearranged so that all unknown values of H, at time level $t+\Delta t$, appear on the left-hand side of the equation, with the known H value, at time level t, on the right hand side. The result, written for the central grid shown in Fig. 3-5 is

$$AH_{i-1,j}^{t+\Delta t} + BH_{i+1,j}^{t+\Delta t} + CH_{i,j-1}^{t+\Delta t} + DH_{i,j+1}^{t+\Delta t} - (A+B+C+D+G)H_{i,j}^{t+\Delta t} = Q - GH_{i,j}^{t} \ . \tag{3-28}$$

where

$$A = \frac{2K_{i-1,j} K_{i,j} m_{i-1,j} m_{i,j} \Delta y_i}{K_{i-1,j} m_{i-1,j} \Delta x_i + K_{i,j} m_{i,j} \Delta x_{i-1}} \ , \tag{3-29}$$

$$B = \frac{2K_{i+1,j} K_{i,j} m_{i+1,j} m_{i,j} \Delta y_i}{K_{i+1,j} m_{i+1,j} \Delta x_i + K_{i,j} m_{i,j} \Delta x_{i+1}} \ , \tag{3-30}$$

$$C = \frac{2K_{i,j-1} K_{i,j} m_{i,j-1} m_{i,j} \Delta x_i}{K_{i,j-1} m_{i,j-1} \Delta y_i + K_{i,j} m_{i,j} \Delta y_{j-1}} \ , \tag{3-31}$$

$$D = \frac{2K_{i,j+1} K_{i,j} m_{i,j+1} m_{i,j} \Delta x_i}{K_{i,j+1} m_{i,j+1} \Delta y_j + K_{i,j} m_{i,j} \Delta y_{j+1}} \ , \tag{3-32}$$

$$G = \frac{S_y \Delta x \Delta y}{\Delta t} \ . \tag{3-33}$$

Coefficients A, B, C, D, and G are held constant at values computed at the beginning of each time increment. Q is held constant at its average value during the operation of the model through the time increment.

Application of the Two-Dimensional Model. The two-dimensional model is designed to consider only those flows in the stream-aquifer system that take place under saturated conditions. Grid placement in the two-dimensional model presents no problem because the upper and lower grid boundaries are defined by water table and bedrock elevations, respectively. The two-dimensional model utilizes the Dupuit-Forchheimer assumptions, of uniform conditions everywhere in a vertical section and horizontal flows throughout the model. The river does not occupy an entire grid, but is incorporated in a grid which includes the surrounding and underlying aquifer. In the model developed in this study the head in the river is assigned to the entire grid on the basis that (1) the stream and aquifer are always hydraulically connected; and (2) response to fluctuations of either the river or aquifer in the other component is fairly rapid, so that the head in the surrounding aquifer is always approximately equal to the head in the river, for a given grid. A typical cross section of the study area used in the verification of the computer model is shown in Fig. 3-7 with the two-dimensional, finite difference grid system superimposed.

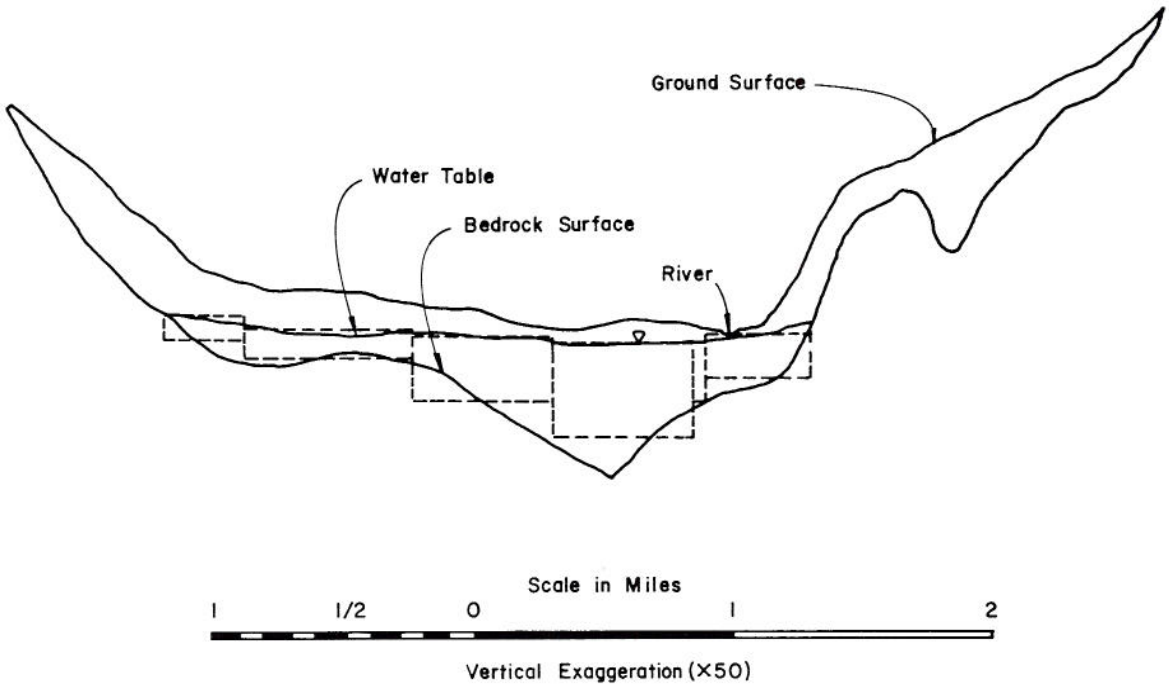

Fig. 3-7 Two-Dimensional Grid System Superimposed on a Cross Section of River Valley

Mathematical Treatment of the Interfaces between Two-Dimensional and Three-Dimensional Model Segment

The three-dimensional segment of the groundwater model developed in this study may be used alone or in conjunction with two-dimensional model segments positioned along any number of its sides. In this study, the three-dimensional model segments. The positioning the model on the study area is discussed further and illustrated in Chapter IV.

A cross section of the interface between a two-dimensional grid and a column of three-dimensional grids is shown in Fig. 3-8. The flow equation for

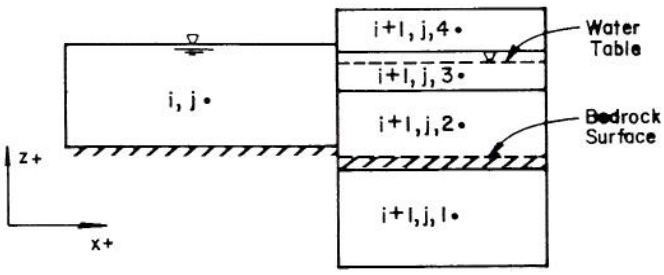

Fig. 3-8 Cross Section of an Interface between Two-Dimensional and Three-Dimensional Model Grids

grid i,j is obtained by writing Eq. 3-28, with a modification of the term describing flow across the face adjacent to the three-dimensional grid column. In this particular case, the term $BH_{i,j+1}^{t+\Delta t}$ is replaced with a set of terms describing flow into each individual grid of column i+1,j. This set of terms is obtained by writing the coefficient B as usual, according to Eq. 3-30, as if an ordinary two-dimensional grid existed in place of the column of three-dimensional grids. The value of B is then divided among the grids in column i,j+1 according to the fraction in each grid of the total saturated thickness in column i,j+1. The expression for the flow coefficient in the kth grid of column i,j+1 is

$$B_k = \frac{\Delta m_k}{m} B \ , \qquad (3\text{-}34)$$

where

Δm_k is the saturated thickness in grid k of column i,j+1

m is the total saturated thickness in column i+1,j.

The value of m in the three-dimensional grid column is obtained by subtracting the top elevation of the uppermost impermeable grid from the head in the top grid. The flow equation for grid i,j is obtained by substituting Eq. 3-34 for each grid in column i+1,j into Eq. 3-28, resulting in

$$AH_{i,j-1}^{t+\Delta t} + \sum_{k=1}^{n} B_k H_{i,j+1,k}^{t+\Delta t} + CH_{i=1,j}^{t+\Delta t} + DH_{i+1,j}^{t+\Delta t}$$

$$-(A+\sum_{k=1}^{n} B_k + C+D+E)H_{i,j}^{t+\Delta t} = Q - EH_{i,j}^{t} \ , \qquad (3\text{-}35)$$

where n is the number of grids in column i+1,j. For the particular case illustrated in Fig. 3-8, coefficients B_k for grids i+1,j,1 and i+1,j,4 are zero, grid i+1,j,1 because it lies below the bedrock surface and is considered impermeable, and grid i+1,j,4 because it lies entirely above the water table and therefore contains no portion of the saturated thickness in column i+1,j.

The flow equation in a given grid of the three-dimensional model segment adjacent to a two-dimensional grid is obtained by writing Eq. 3-13 just as if another column of three-dimensional grids existed in place of the two-dimensional grid. In order to do this, the two-dimensional grid must be divided into a set of subgrids whose vertical dimensions match those of the adjacent three-dimensional column. The boundaries of this set of subgrids may, and usually do, extend above and below the boundaries of the two-dimensional grid itself. For subgrids lying below the two-dimensional grid boundary, which is the bedrock surface, the hydraulic conductivity is assigned a value of zero. For subgrids located partially above and partially below the bedrock level, the conductivity value assigned is that of the two-dimensional grid reduced in proportion to the amount of subgrid space occupied by impermeable material. To obtain hydraulic conductivity values for subgrids lying partially or totally above the two-dimensional grid boundary, the relative permeability of the subgrid is obtained, as it is for grids in the three-dimensional model segment. The pressure head datum for this calculation is the water table in the two-dimensional grid. The hydraulic conductivity is then obtained using Eq. 3-11, with the relative permeability of the subgrid and the conductivity of the two-dimensional grid. No change of parameters is necessary for subgrids lying entirely inside the boundaries of the two-dimensional grid. Using the subgrids of grid i in Fig. 3-8, Eq. 3-13 is written for each of the grids in column i+1,j with no changes in the form of the equation.

Method of Solution for the Groundwater Model

At the end of each model time increment, the flow equation is written in its appropriate form for every model grid for which the head at the next time step is unknown. Boundary conditions are required in all exterior grids of the model in order to obtain a solution. The boundary conditions used in this model are: (1) known heads in all perimeter grids, (2) known flow into the top of all surface grids of the three-dimensional model segment. At a few locations along the perimeter of the model, where data indicates a steady increase in the water table elevation over the study period, values of head in the perimeter grids are periodically increased by a small amount. The remainder of the heads in perimeter grids remain constant. Boundary conditions at the river are not essential to the solution of the flow equations, but are necessary for the correct representation of the actual flow situation. In the two-dimensional segments of this model the river is treated as a boundary of known head, while the portion of the river in the three-dimensional segment may act either as a boundary of known head or of known discharge. The flow equations are entered into a matrix and solved simultaneously for new values of head in each grid. Subroutine BSOLVE employs the Gauss Elimination technique of matrix solution. BSOLVE was adapted for use in digital groundwater models at CSU from the BANDSOLVE algorithm developed by Thurnau (1963).

Development of Equations for River Discharge and Stage

A value of the head in each river grid of the model is needed at every time increment to compute boundary conditions used in the solution of the groundwater flow equations. The head values are obtained by adding the river stage to the river bed elevation in each grid. The river stage is computed by the Manning formula, for which a value of discharge in each grid is needed. Calculation of the discharge in each grid is based on the continuity principle and the assumption that spatial variation in river flow at a given time is due to seepage to and from the adjacent aquifer, canal diversions and tributary inflows.

Continuity Equation for River Discharge

Discharge calculations are begun at a grid superimposed over a reach of river where a gaging station is located, and the flow at each time increment is known. Three river gaging stations are located in the study area used in the verification of this model, two of which are located at opposite ends of the region, with the third located near the center of the study area. Calculations of discharge are initiated at the center gaging station and moved upstream and downstream from that grid. The reasons for starting at the center and moving both directions, rather than beginning at one end and progressing through the entire length of the model is to assure that values of discharge in the three-dimensional model segment are reasonably close to the correct values, and to shorten the distance over which a given error can be propagated. Discharge in a given grid is computed as a function of the known discharge in the adjacent grid, and the seepage rates and canal diversions between the centers of the two grids. River grids are numbered consecutively from upstream to downstream. Moving upstream from the center gaging station, and assuming known discharge in the L+1th grid, the discharge in the Lth grid is computed as

$$Q_L = Q_{L+1} + D_{L+1} + 0.5(R_L + R_{L+1}) , \quad (3\text{-}36)$$

where

Q is river discharge in cubic feet per second

D is the sum of the discharges diverted to canals in cubic feet per second,

R is the net seepage from the river in each grid in cubic feet per second.

Moving downstream from the gaging station and assuming known discharge in the L-1th grid, the discharge in the Lth grid is computed as

$$Q_L = Q_{L-1} - D_L - 0.5(R_{L-1} + R_L) . \quad (3\text{-}37)$$

Canal diversions between two adjacent grid centers are assigned to the downstream grid for convenience. The seepage in each three-dimensional river grid is obtained by summing the components of seepage through each bank and the bed of the river. These components are obtained by multiplying the seepage velocity through each face of the river grid by the area of that face. Seepage in the two-dimensional river grids includes only the components of flow through the river banks. These seepage components are computed during the previous model time increment for all faces of each river grid which are adjacent to the aquifer grids. Calculations of Q by Eqs. 3-36 or 3-37 are repeated until a value of Q is obtained in every river grid of the model. Computed values of discharge in the end grids of the model are then compared to values measured at the two gaging stations located at the upper and lower ends of the study area, as a test of the accuracy of results obtained using the model.

Computation of River Stage by the Manning Formula

The computation of depth of flow in each river grid of the model is based on the assumptions (1) that flow in each grid is steady and uniform and (2) that the channel is generally wide, shallow and has an approximately rectangular section throughout the study area. Flow is assumed uniform in each section because channel geometry throughout the area does not vary significantly from place to place, and, except at the diversion points of canals the changes in discharge with respect to distance along the channel are small. In addition, sufficient information is not available for calculating depths of nonuniform flow. Flow is considered steady because the model time increment is much larger than the duration of most river fluctuations and the passage of these fluctuations through the study area. The effects of numerous positive and negative fluctuations in river discharge over a model time increment tend to cancel, thus minimizing the errors incurred by assuming steady flow.

The Manning formula, written for a wide channel and solved for stage, d, is given by Eq. 2-1. Values of channel width, w, bed slope, s, and Manning's n are input to the model as data for each river grid. The value of discharge, Q, is obtained by Eqs. 3-36 or 3-37. A value of d is obtained for each river grid at each time increment, using Eq. 2-1. This value is then added to the average river bed elevation of the grid, which has been read in as data, resulting in a value of head which is used to compute the appropriate boundary condition for use in the solution of the groundwater flow equations.

Boundary Conditions at the Stream-Aquifer Interface

Equations for the seepage velocity across the stream-aquifer interface were discussed in Chapter II for the three prevailing flow configurations. The finite difference forms of these equations are used in the three-dimensional model segment to obtain boundary conditions for groundwater flow equations. A typical three-dimensional model grid is illustrated in Fig. 3-9, with a river grid located adjacent to its upper face. The finite difference equation for seepage from

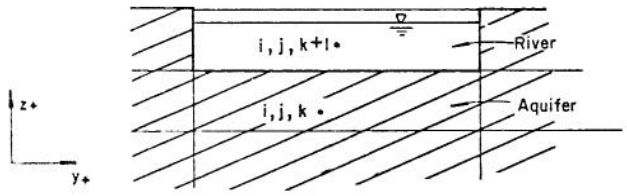

Fig. 3-9 Aquifer Grid Adjacent to River Grid

the aquifer into the river is obtained for grid i,j,k by multiplying the expression for seepage velocity given in Eq. 2-21 by the area of the interface between grids i,j,k and i,j,k+1. The result is

$$Q = K_{i,j,k} \frac{\Delta x_i \Delta y_j}{\Delta z_k/2} (H_{i,j,k+1} - H_{i,j,k}) . \quad (3\text{-}38)$$

where $\Delta z_k/2$ is the distance from the center of grid i,j,k to the river boundary. The coefficient in the right hand side of Eq. 3-38 is used as the coefficient E in the groundwater flow Eq. 3-13, with $H_{i,j,k+1}$ as a known head boundary condition. The equation for seepage into the river from a laterally adjacent aquifer grid is identical in form to Eq. 3-38, with grid dimensions and subscripts changed accordingly. The coefficient of this equation is used in Eq. 3-13 as the coefficient A, B, C, or D, depending on the location of the aquifer grid with respect to the river.

The equation for seepage from the river into the aquifer with the stream and aquifer hydraulically connected is obtained for grid i,j,k by multiplying the area of the interface by the expression for seepage velocity given in Eq. 2-26. Assuming seepage takes place from the river boundary, through the silt layer to the center of grid i,j,k, the result is

$$Q = \frac{K_{i,j,k} K_s \Delta x_i \Delta y_j}{t_s K_{i,j,k} + (\Delta z_k/2) K_s} (H_{i,j,k+1} - H_{i,j,k}) . \quad (3\text{-}39)$$

The coefficient in the right hand side of Eq. 3-39 is used as the coefficient F in Eq. 3-13, with $H_{i,j,k+1}$ as a known head boundary condition. The equation for seepage into the aquifer from a laterally adjacent river grid with the stream and aquifer hydraulically connected is identical in form to Eq. 3-39, with grid dimensions and subscripts changed accordingly.

The equation for seepage from the river to the aquifer with no hydraulic connection between the river and aquifer is obtained by multiplying the area of the interface between grids i,j,k and i,j,k+1 by the expression for the seepage velocity given in Eq. 2-27. Assuming seepage takes place from the river boundary, through the silt layer to the center of grid i,j,k, the result is

$$Q = K_s \frac{\Delta x_i \Delta y_j}{t_s} (d - h_{pb} + t_s) . \quad (3\text{-}40)$$

Because all the values on the right-hand side of Eq. 3-40 are known prior to the solution of the groundwater flow equations, the value of Q can be obtained directly and input as the production term on the right-hand side of Eq. 3-13. Because $H_{i,j,k}$ does not appear in Eq. 3-40, the coefficient F in Eq. 3-13 is set equal to zero. This constitutes a known discharge boundary condition. The equation for seepage from the river to a laterally adjacent aquifer grid with no hydraulic connection between the river and aquifer is obtained by multiplying the interface area between the grids by the expression for the seepage velocity given in Eq. 2-29. For adjacent grids in the x-direction the result is

$$Q = K_s \frac{\Delta y_j \Delta z_k}{t_s} (d/2 - h_{pb}) . \quad (3\text{-}41)$$

At every time increment, for each grid interface between the river and the aquifer, a decision must be made as to which among Eqs. 3-38, 3-39, and 3-40 is appropriate for describing the type of seepage taking place. This decision is based on the difference between the head in the river and the head in the aquifer. The decision process executed in the model to determine the appropriate equation for flow across the stream-aquifer interface is diagrammed in Fig. 3-10 for the grid shown in Fig. 3-9.

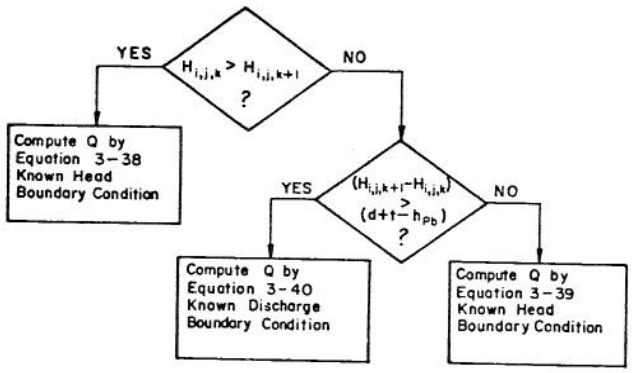

Fig. 3-10 Diagram of Decision Process for Selecting the Appropriate Boundary Condition at the Stream-Aquifer Interface

Boundary Conditions at the Model Surface

At the beginning of each time increment a value of the net inflow through the top of each grid adjacent to the ground surface is computed and input as a known discharge boundary condition to the groundwater flow equation for that grid. Contributions to the net surface inflow to each grid include precipitation, evapotranspiration, irrigation, and pumping. The method of calculating a value for each of these contributions is discussed in this section.

Precipitation. Monthly precipitation data are available for one centrally located station is the study area. The assumption is made that the amount of precipitation over the entire region is uniformly distributed, and is equal to the value measured at the gaging station. The input to a given grid, in cubic feet per day is

$$Q_R = \frac{P}{360} \Delta x \Delta y \ , \qquad (3\text{-}42)$$

where

P is the measured precipitation in inches month, assumed in this study to be 30 days,

Δx and Δy are the dimensions of the grid surface,

360 is the factor for converting units from inches per month to feet per day.

Evapotranspiration. The Modified Blaney-Criddle Method is used to obtain estimated values of monthly evapotranspiration, which are applied uniformly over the entire study area. Because these computations are made external to the model and input as data, they are discussed in detail in Chapter IV rather than in this section. The outflow in cubic feet per day from the surface of a given grid due to evapotranspiration is

$$Q_E = \frac{E_t}{30} \Delta x \Delta y \qquad (3\text{-}43)$$

where

E_t is the monthly evapotranspiration in feet,

30 is the factor for converting units from feet per month to feet per day.

Irrigation. The computation of an estimated value of the inflow to each grid due to irrigation is based on the assumption of uniform distribution of water within the region served by each canal in the study area. A detailed description of the delineation of the distribution regions of the canals is presented in Chapter IV. Each surface grid of the model is located in no more than one canal distribution region. Grids not included in any canal distribution region are assumed to receive no surface inflow from irrigation. The inflow due to irrigation in cubic feet per day for a grid lying inside a canal distribution region is obtained by the equation.

$$Q_I = 1452 \frac{\Delta x \Delta y}{A_n} P_n D_n \ , \qquad (3\text{-}44)$$

where

$\Delta x \Delta y$ is the grid surface area,

P_n is the percentage of the canal distribution region inside the study area,

D_n is the monthly canal diversion in acre feet.

1452 is the factor for converting units from acre feet per month to cubic feet per day.

Pumping. A large percentage of the groundwater withdrawn from the alluvial aquifer in the study area is eventually returned to the ground in the same vicinity where it was pumped. With the time lag between pumping and the return of the pumped water to the aquifer assumed to be less than the thirty day model time increment, and with evapotranspiration losses considered separately, the contribution of pumping to surface inflow and outflow in any grid is expressed as

$$Q_p = Q_w - Q_r = 0 \ , \qquad (3\text{-}45)$$

where

Q_w is the amount of water withdrawn from a particular grid in cubic feet per day,

Q_r is the amount of pumped water returned to the aquifer in that grid in cubic feet per day, assumed to be equal to Q_w.

At one location in the study area, large quantities of water are pumped for use as cooling water in a power plant. The power plant wells are distributed over the area of two grid columns in the three-dimensional model segment. Power plant waste water is discharged into a canal and is carried out of the area and distributed for irrigation along with the water diverted from the river. Very little of the water pumped in this location is returned to the aquifer in the same vicinity, and the surface flux due to pumping, Q_p, is not zero, as computed in Eq. 3-44, but instead is considered equal to Q_w, the withdrawal. The water returned to the ground, Q_r, is treated in the model by adding it to the amount of water diverted from the river into the canal, and applying the total amount to the canal distribution region, as described in the previous section of this chapter. The water withdrawn from the power plant wells is not taken just from the surface grids of the two columns affected, but is withdrawn from all the grids in the columns, according to the amount of saturated thickness in each grid.

Equation for Surface Flux. The equation for the surface flux into a given grid of the model, for both the two-dimensional and three-dimensional segments, is obtained by summing the contributions of precipitation, evapotranspiration, irrigation and pumping. For all grids except those containing the power plant wells, the equation for surface inflow to a grid is

$$Q_S = Q_R - Q_E + Q_I \ . \qquad (3\text{-}46)$$

Because the pumping contribution, Q_p, is equal to zero for these grids, it is not included in Eq. 3-46. For the surface grids of the two grid columns containing the power plant wells the surface inflow is

$$Q_S = Q_R - Q_E + Q_I - Q_P \ , \qquad (3\text{-}47)$$

where

Q_P is computed in a separate part of the program according to the saturated thickness in the grid at each time step.

For the lower grids of these two columns, a value of Qp is similarly obtained. The values of Q_S for each surface grid and Qp for each grid affected by the power plant wells are input to the appropriate flow equation for each grid as production terms.

Operation of the Computer Model

The operation of the computer program for simulating flow in a stream-aquifer system consists of setting up initial conditions at some specified time then running the model through a predetermined number of time increments until a solution is reached at the desired later time. The solution consists of a map of water table elevations for the two-dimensional model segments, a map of heads in the three-dimensional segment, and a tabulation of the discharge in each river grid. Intermediate solutions may be printed out at the end of every time increment if desired. The program operation through a single time increment consists of reading or computing the appropriate boundary conditions, setting up the matrix of groundwater flow equations, then solving these equations for new values of head in each grid. A simplified flowchart of the program is shown in Fig. 3-11.

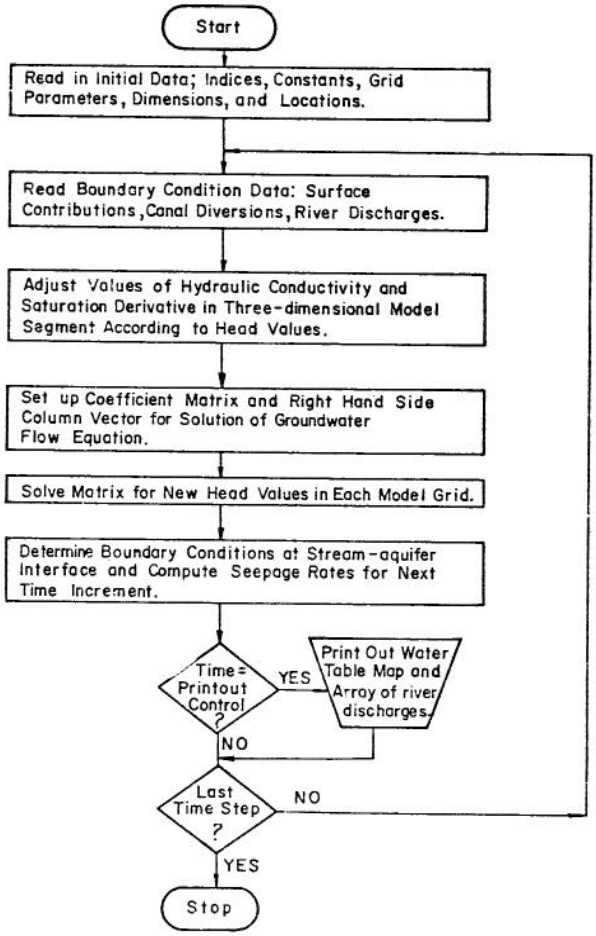

Fig. 3-11 Flowchart of Computer Program

CHAPTER IV
DATA USED FOR VERIFICATION OF MODEL

The study area selected for simulation by the computer model is located in the Arkansas Valley of Southeastern Colorado and Western Kansas. The boundaries of the model encompass a four mile wide strip of land extending from John Martin Dam in Bent County, across the width of Prowers County, to Coolidge, Kansas as shown in Fig. 4-1. Most of the area is occupied by irrigated farmland where sugar beets, alfalfa, corn and sorghums are the principle crops grown. The only industry in the area using a significant amount of water is the thermal power plant owned and operated by the city of Lamar, which has a population of about 7500. The entire area lies within the Great Plains physiographic province and the climate is semiarid. The mean annual precipitation is about 14 inches. Most of the water used in this region is presently derived from surface flows in the Arkansas River and groundwater from the unconfined alluvial aquifer which underlies the river valley through the length of the study area.

The Arkansas River traverses the study area lengthwise and is the principal source of water supply for the region. Flows into the upstream end of the area are controlled by releases from John Martin Dam. The average quantity of water released annually is about 235,000 acre-feet. The average annual discharge in the river at Coolidge is roughly 150,000 acre-feet. The diversion points of nine major irrigation canals lie within the study area. The total of the average yearly diversions of each of these canals is about 160,000 acre-feet. Of several tributaries flowing into the Arkansas River within the boundaries of the study area, only Big Sandy Creek consistently contributes significant quantities of flow to the river. An estimated 14,500 acre-feet enters the Arkansas River annually at the mouth of Big Sandy Creek, located about seven miles east of Lamar. Additional gains and losses in river flow due to seepage between the river and the underlying alluvial aquifer may be substantial. Results of an investigation by Voegeli and Hershey (1965) indicate that losses in river flow due to seepage generally exceed gains in this region.

The valley-fill aquifer underlying the study area rest in a U-shaped trough cut in relatively impermeable limestone and shale. The estimated storage capacity of the aquifer is over 1,000,000 acre-feet. This aquifer is recharged by underflow from adjacent areas, seepage from canals, the river, and other streams, precipitation, and spreading of irrigation water. Contributions to discharge from the aquifer include underflow to adjacent areas, evapotranspiration, seepage into canals, streams, and the river, and pumping. Of the 160,000 acre-feet of water per year diverted from the river for irrigation, an estimated 100,000 acre-feet are distributed to land lying within the study area boundaries. The average annual evapotranspiration loss in the study area is estimated to be about 2.5 feet. It is estimated that 50,000 to 55,000 acre-feet of water enters the area each year as groundwater underflow. Total groundwater withdrawal in the area is roughly 35,000 to 45,000 acre-feet per year, of which approximately 75 percent is used for irrigation. Combined uses of groundwater for public supply and domestic and livestock consumption account for about 5,000 acre-feet per year, and withdrawals for cooling water at the Lamar power plant constitute an additional 7,500 acre-feet annually. During the eight year period considered in this study, the annual increase in aquifer storage was estimated to be between 5,000 and 10,000 acre-feet, as indicated by the mass balance diagram for the study area shown in Fig. 4-2. Values of hydraulic conductivity throughout the aquifer tend to be rather high, causing the aquifer to respond rapidly to the effects of these various inflows and outflows.

Investigation by Voegeli and Hershey (1965) and by Hurr and Moore (1972) indicate that the Arkansas River does not extend down to bedrock at most locations along its course through the study area. A typical

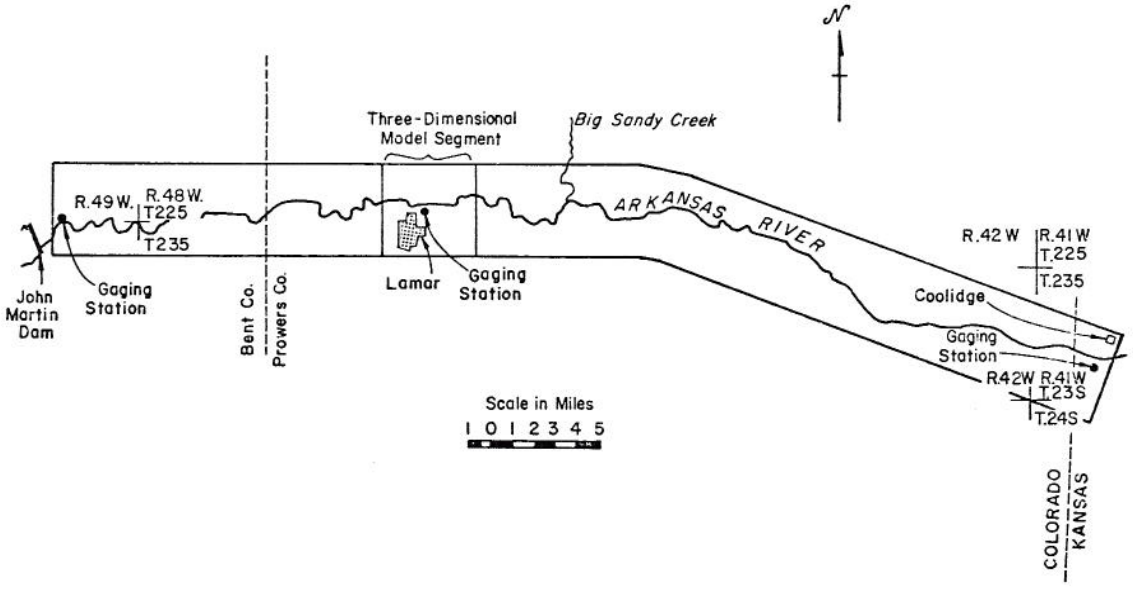

Fig. 4-1 Location of Study Area

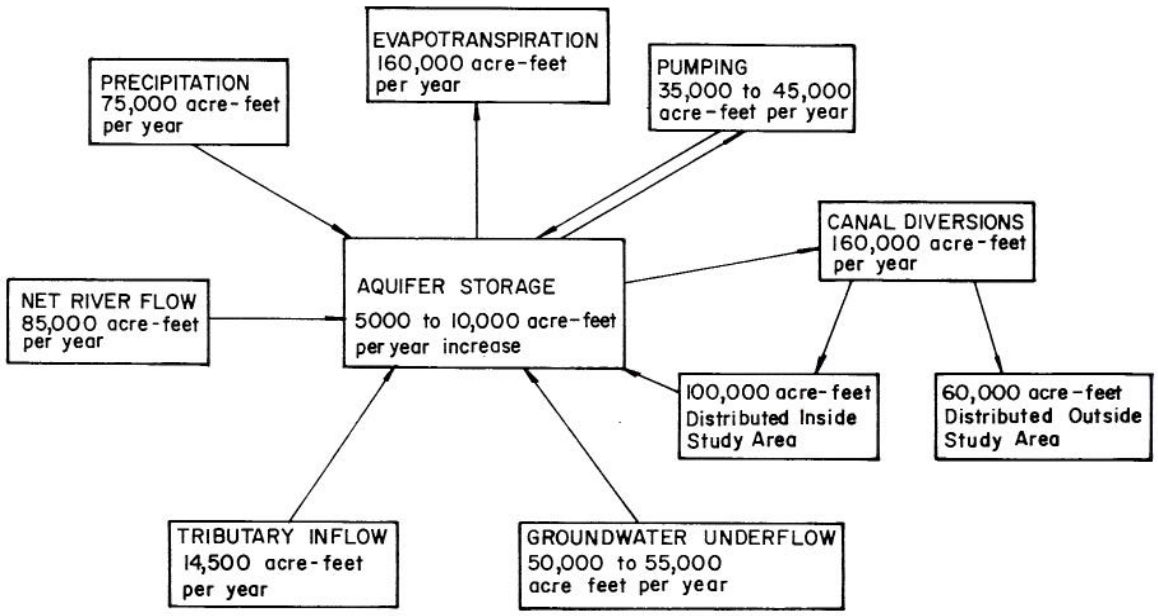

Fig. 4-2 Mass Balance Diagram for Arkansas Valley Study Area

geologic section of the Arkansas Valley, shown in Fig. 4-3 illustrates this type of configuration. This section is one of several mapped by Voegeli and Hershey (1965) and is located about two miles west of Lamar. Throughout much of the study area, water table elevations indicated that the river and aquifer remain hydraulically connected most of the time. The notable exception exists at Lamar, where the withdrawal of large quantities of cooling water for the Lamar municipal power plant has produced a large drawdown cone which extends beneath the riverbed nearby. The location of the Lamar power plant wells is indicated in Fig. 4-4. A detailed study of the interaction between the river and the alluvial aquifer in the Lamar area was conducted by Moore and Jenkins (1966). Their measurements indicated that continuous pumping at an average rate of about ten cubic feet per second has maintained water table elevations near the river at levels ranging from two to eleven feet below the level of the streambed over a two mile reach in the vicinity of the Lamar power plant wells. Further observations revealed that, although the river was losing water in this two mile reach, the rate of leakage was much less than the flow rate toward the wells indicated by steep water table gradients near the river. Furthermore, fluctuations in the water table appeared to have no measurable effect on the leakage rate. Moore and Jenkins suggested that these observations indicated a silt layer was present in the streambed which controlled the leakage rate, and that no hydraulic connection existed between the river and aquifer in the two mile reach affected by the Lamar power plant wells.

The boundaries of the model have been located so as to roughly coincide with physical boundaries of the study area for the purpose of eliminating, as much as possible, the problem of dealing with unknown boundary conditions in the operation of the model. The side boundaries encompass most of the alluvial aquifer adjacent to the river. The end boundaries of the model

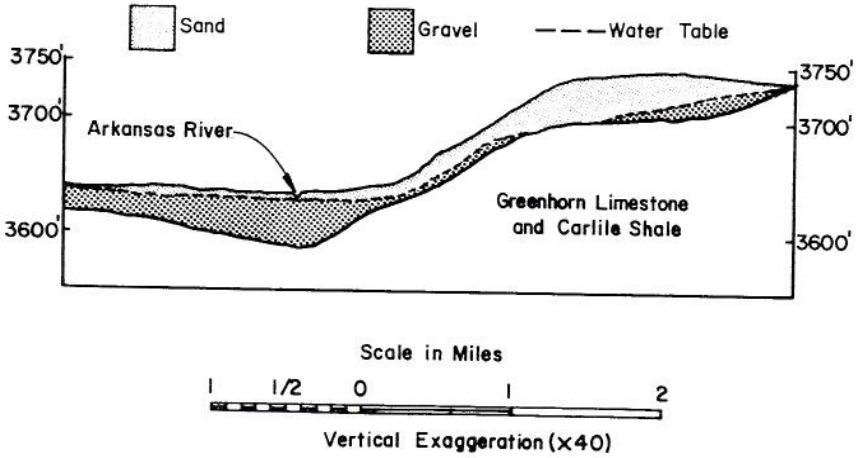

Fig. 4-3 Geologic Section of Arkansas River Valley

have been located at river gaging stations near John Martin Dam and Coolidge which are operated by the U.S. Geological Survey. A third U.S.G.S. gaging station is located at Lamar, a short distance from the power plant well field. The location of this gaging station proved extremely advantageous for the purposes of this study. The three-dimensional portion of the model was applied to the Lamar area in order to simulate the unusual behavior of the system under the influence of the high pumping rates at the power plant wells. River flow data at this location provided known boundary conditions that were essential in calibrating this portion of the model.

The remainder of this chapter is devoted to a discussion of the data taken from the Arkansas Valley study area and adapted for use with the computer model. The availability and sources of data, adaptations made for use with this model, and estimated data are discussed for each input parameter.

Groundwater Flow Parameters

Water Table Elevations. Maps of water table contours constructed by Voegeli and Hershey (1965) from measurements taken in Prowers County, Colorado in 1957-58 were used as initial conditions in the computer model. Water table elevation data for the portion of the study area lying in Bent County was not available for that time. However, a comparison of water table contours in Prowers County near the Bent County line in 1957-58 with contours in 1971 indicated little change, suggesting that water table elevations upstream of this location in Bent County could be assumed not to have changed significantly between 1957 and 1971. This assumption is further supported by the physiography of the region. The alluvial aquifer in Bent County is less than a mile wide at most locations and flux into and out of the aquifer is minimal except at the river. The water table at the upstream end of the region is controlled by seepage from John Martin Dam, and is considered to be fairly stable from year to year. Based on the assumption that water table elevations in the Bent County portion of the study area do not change appreciably on an annual basis, it was considered permissible to use measurements taken in 1971 as initial data for model runs beginning in 1958. Measurements of water table elevations in Bent County in 1971 were obtained and mapped by Hurr and Moore (1972). Water table contour maps for Prowers County in 1966 and 1971 were constructed by Hurr and Moore (1974). The 1966 map is used for comparison with water table contours produced by the computer model after runs of several years of model time. Maps of water table contours in the vicinity of Lamar were constructed by Moore and Jenkins (1966) for October 1964, and by Hurr (1971) for March 1966. These maps were valuable in the verification of the three-dimensional portion of the model. To obtain the initial water table elevation for each grid, a transparent diagram of the grid system was superimposed on the water table contour map. An average value over the area of each grid was then obtained by visual inspection. Because three-dimensional pressure distributions in the saturated zone were not available as data, pressure heads in the three-dimensional zone were assumed to be equal to the average water table elevation over the projected area of each vertical column of grids. The initial water table elevation maps for the three-dimensional segment, the upstream two-dimensional segment, and the downstream two-dimensional segment of the model are shown in Figs. 4-4, 4-5, and 4-6, respectively, with the appropriate grid systems superimposed. The values of water table elevation for each grid used as initial conditions for the model are tabulated in Appendix B.

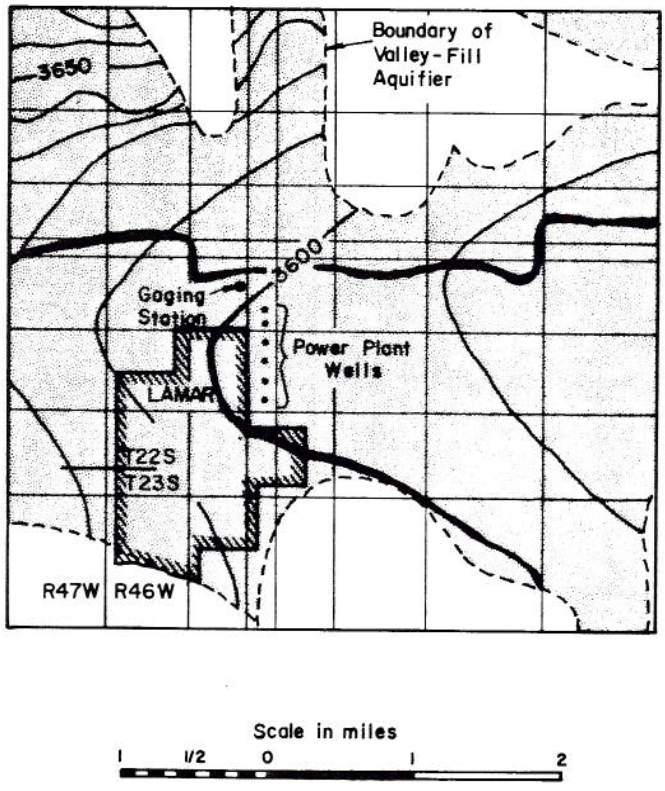

Fig. 4-4 Initial Water Table Elevations in Dimensional Model Segment

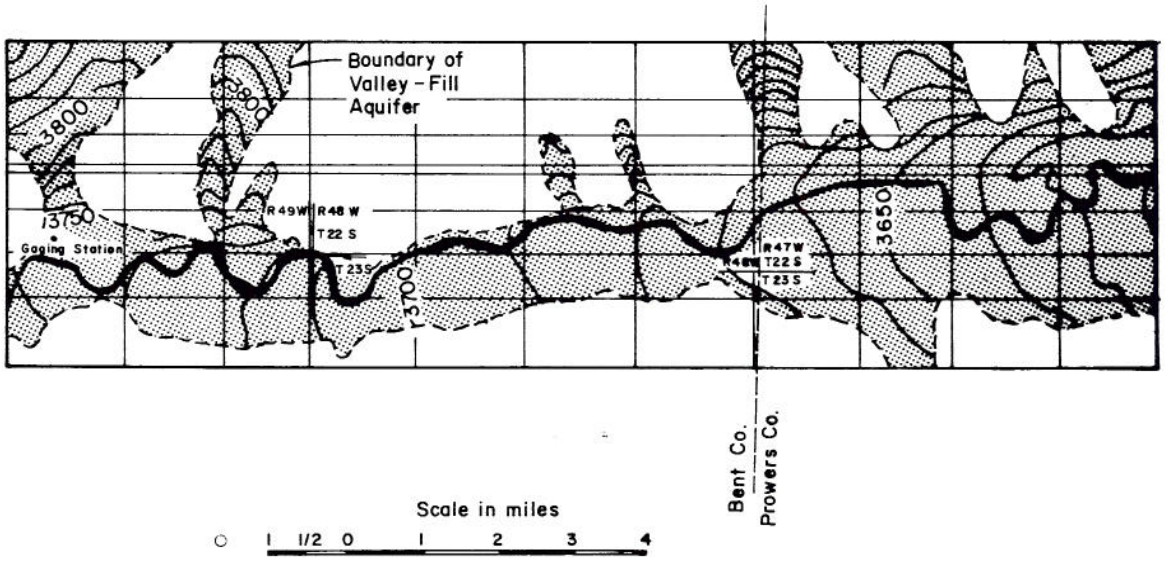

Fig. 4-5 Initial Water Table Elevations in Upstream, Two-Dimensional Model Segment

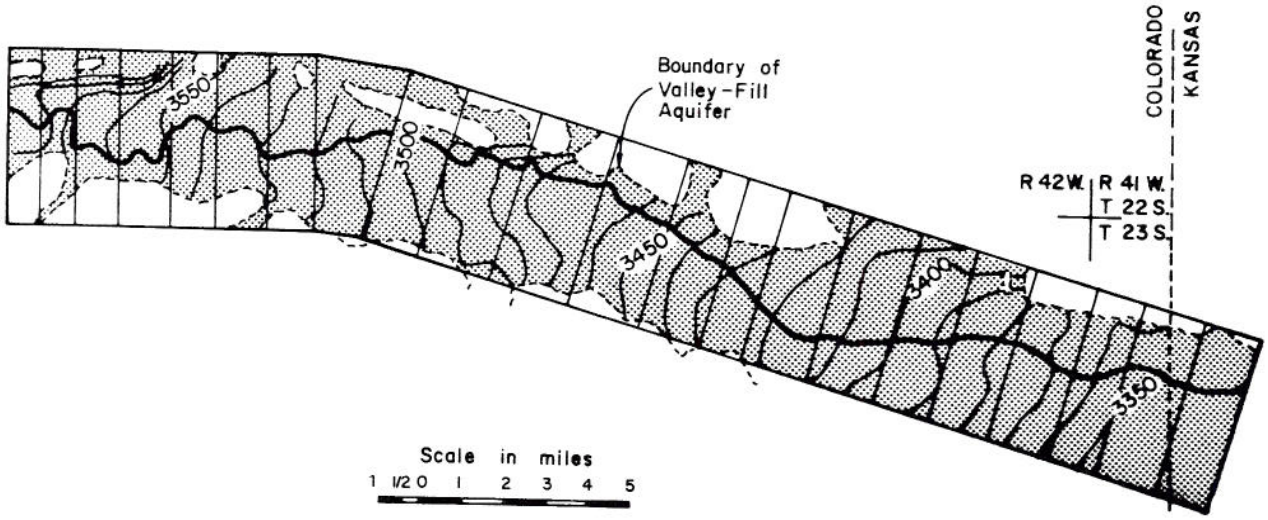

Fig. 4-6 Initial Water Table Elevations in Downstream, Two-Dimensional Model Segment

Bedrock Elevations. Elevations on the bedrock surface in the study area were measured and mapped by Voegeli and Hershey (1965) and by Hurr and Moore (1974) for Prowers County, and by Hurr and Moore (1972) for Bent County. Single values of bedrock elevation for each grid were obtained in the same manner as single grid values of water table elevation, by superimposing the grid system over a bedrock elevation map and obtaining an average value for each grid by visual inspection. Bedrock elevations were not used directly in the three-dimensional segment of the model, but were plotted on cross sections at the center of each row of grid center elevations, as was explained in Chapter III. The values of bedrock elevation assigned to each grid in the two-dimensional model segments as initial data are tabulated in Appendix B, along with the grid center elevations used in the three-dimensional model segment.

Hydraulic Conductivity. Hydraulic conductivities throughout the study area were not measured directly, but were computed using values of transmissibility and saturated thickness of the alluvial aquifer which were measured and mapped for Prowers County by Hurr and Moore (1974) and for Bent County by Hurr and Moore (1972). Single values of transmissiblity, T, and saturated thickness, m, were obtained for each grid by superimposing the grid system over the T and m maps and visually estimating average values. The hydraulic conductivity, K, for each grid was then obtained using the equation

$$K = \frac{T}{m} . \qquad (4\text{-}1)$$

In the three-dimensional segment of the model these conductivities were assigned only to the grids located above the bedrock surface. Grids below the bedrock surface were assigned hydraulic conductivities of zero. The single values of hydraulic conductivity assigned to each model grid as initial data are tabulated in Appendix B.

Parameters for Partially Saturated Flow. The two parameters, relative permeability, k_r, and saturation, S, are important in the analysis of partially saturated subsurface flow. No information concerning the nature of either of these parameters in the Arkansas Valley study area was available. Plots of k_r and S versus pressure head, h_p, were therefore estimated on the basis of the general description of the material in the alluvial aquifer given by Voegeli and Hershey (1965). For a well-graded sand and gravel mixture of the type found in the Arkansas Valley alluvium, the finer particles generally determine the range of pressure head values over which k_r and S vary. Shapes of the k_r and S versus h_p curves are determined by the particle size distribution. It was decided that plots of k_r and S versus h_p for a well-graded medium sand would be suitable substitutes for actual measured values of these parameters, although the measured values would have been preferable. Brooks and Corey (1964) conducted laboratory experiments to obtain plots of saturation and relative permeability as functions of capillary pressure head for five materials, including volcanic sand, fine sand, and a fragmented mixture. McWhorter (1971) obtained similar plots for Poudre Sand, and unconsolidated river sediment having a wide distribution of pore sizes. These experiments were conducted using Soltrol "C" core test fluid, a hydrocarbon manufactured by the Phillips Petroleum Company. According to Brooks and Corey (1964) the capillary pressure head of water is approximately twice that of Soltrol. For use in this study, plots of k_r and S were redrawn as functions of capillary pressure head of water using a scale factor of 2. Capillary pressure head may be converted to gage pressure head by simply changing the sign. This was done to make the plots of k_r and S compatible with the gage pressure heads computed at each grid center in the three-dimensional segment of the model. It is convenient for the purposes of this study to plot h_p as the abscissa, with k_r and S as ordinates. The resulting plots of relative permeability and saturation as functions of negative gage pressure head are shown in Figs. 4-7 and 4-8, respectively. For use with the computer simulator, plots of k_r versus h_p were discretized into step functions, and S versus h_p curves were approximated by series of straight line segments. The use of the adapted forms of these plots was discussed in Chapter III.

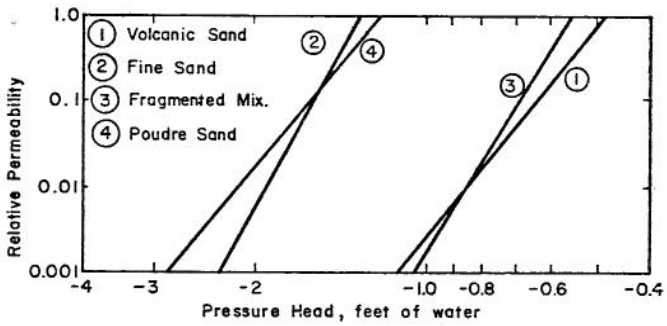

Fig. 4-7 Relative Permeability as a Function of Negative Pressure Head

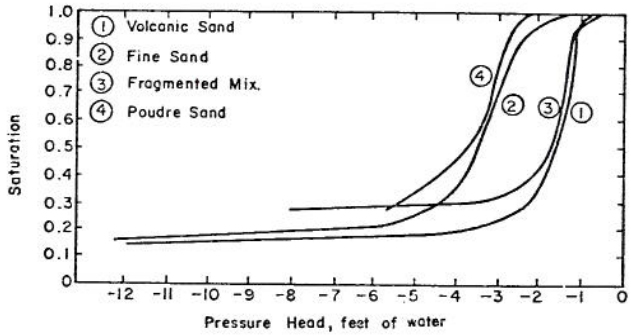

Fig. 4-8 Saturation as a Function of Negative Pressure Head

Specific Yield. Voegeli and Hershey (1965) calculated values of the specific yield for several wells located throughout the alluvial aquifer in the Arkansas Valley of Prowers County. They obtained values ranging from 10 to 20 percent. These values were obtained over fairly short durations of continuous pumping, and it was observed that longer durations of pumping resulted in higher values of specific yield up to about 10 days, at which point the specific yield values for

many of the wells were close to 20 percent. The time increment used in the computer model is 30 days, so that any increase or decrease in water table elevation is treated by the model as continuing for that length of time. For this reason it was considered appropriate to use the value of 20 percent in perference to lower values associated with smaller time increments. Because information concerning the location and results of specific well tests was insufficient for developing any sort of distribution of specific yield values over the area, the value of 20 percent was assigned to all grids in the two-dimensional portions of the model.

Porosity. The aquifer material in the study area was described by Voegeli and Hershey (1965) as well sorted, uniform textured sand and gravel. According to Walton (1970) the range of porosities for such materials is between 20 and 35 percent. The value of porosity, ϕ, used in this study was obtained using the relationship

$$S_y = \phi S_e \qquad (4\text{-}2)$$

where

S_y is the specific yield

S_e is the effective saturation

The effective saturation may be defined as the fraction of water contained in a given porous medium under fully saturated conditions that can be drained from the material by gravity. From the plots of saturation versus negative pressure head in Fig. 4-8 an average value for S_e of 0.80 was estimated. Using this value, and the specific yield of 20 percent, Eq. 4-2 was solved for ϕ, resulting in a value of 25 percent for the porosity in the study area.

River Parameters

Discharge. The average monthly flows in cubic feet per second were obtained for the four gaging stations in the study area, one of which is located on Big Sandy Creek, and the other three on the Arkansas River. The data for these gaging stations was collected and published by the U.S. Geological Survey in water supply papers (1958-1960), surface water supply data releases (1961-1964), and water resource data releases (1965-1966). Records for gaging stations located below John Martin Dam, Colorado, and at Coolidge, Kansas were continuous throughout the study period, which extended from January 1958 through December 1965. Records for the gaging station at Lamar, Colorado were continuous from April 1959 throughout the remainder of the study period, with no records for the period of January 1958 through March 1959. For the purpose of estimating these missing values, plots were drawn of measured flows at Lamar during the period from April 1959 to December 1965 versus flows past the John Martin Dam gaging station, flows at John Martin Dam minus canal diversion above Lamar, flows past the Coolidge gaging station, and canal diversions between John Martin Dam and Lamar. The plot of flows at Lamar versus flows at John Martin Dam appeared to have the best correlation. Therefore, discharge values at Lamar for the period from January 1958 through March 1959 were estimated by the following relationships derived from this plot.

$$Q_{LAM} = Q_{JMD}(15 - 3.6t) \quad \text{January - March,}$$

$$Q_{LAM} = 0.10\, Q_{JMD} \quad \text{April - December.} \qquad (4\text{-}3)$$

where

Q_{LAM} is estimated flow at Lamar for a given month,

Q_{JMD} is measured flow at John Martin Dam for the same month,

t is time in months.

Flows into the Arkansas River from Big Sandy Creek have been measured only since February 1968, when a U.S. Geological Survey gaging station was established at the mouth of the creek. Because no data are available for any time during the study period, all monthly discharge values for Big Sandy Creek had to be estimated. For the years for which records on Big Sandy Creek exist, discharge values were plotted against various other flows, as was done for Lamar flows. There appeared to be good correlation between annual discharges at John Martin Dam and annual discharges from Big Sandy Creek. This correlation is reasonable because quantities of water diverted for irrigation are dependent on releases from John Martin Dam, and return flow from irrigation is the main contribution to flow in Big Sandy Creek. Good correlation also appeared to exist between flows at Big Sandy Creek for the same months of different years. Therefore, the following relationship was used to obtain estimates of monthly discharge values from Big Sandy Creek.

$$(Q_{BSC})_m = (\bar{Q}_{BSC})_m \frac{(Q_{JMD})_y}{(\bar{Q}_{JMD})_y} \qquad (4\text{-}4)$$

where

$(Q_{BSC})_m$ is the estimated value of monthly discharge from Big Sandy Creek,

$(\bar{Q}_{BSC})_m$ is the average monthly discharge at Big Sandy Creek during the period of record,

$(Q_{JMD})_y$ is the annual discharge at John Martin Dam for the year in which $(Q_{BSC})_m$ is being estimated,

$(\bar{Q}_{JMD})_y$ is the average annual discharge at John Martin Dam for the period of record or flows at Big Sandy Creek.

Average monthly discharges in cubic feet per second are tabulated in Appendix B for the three gaging stations on the Arkansas River for each month throughout the study period. The values tabulated include those estimated as a substitute for missing data at Lamar as well as the measured values at all three gaging stations. Estimated values of monthly discharge from Big Sandy Creek are tabulated in Appendix B along with canal diversion data, and are given in units of acre-feet.

Canal Diversions. Monthly diversions in acre-feet were obtained for the nine major canals whose diversion points are located within the study area. Records for the period from January 1958 through October 1964 were published in a water utilization study of the Arkansas Valley Region in Colorado by Skinner (1965). Data for the period from November 1964 through December 1965 were obtained from irrigation company records filed in the office of the State Engineer in Denver. Monthly diversions of the nine canals in the study area are

tabulated in Appendix B for each month throughout the study period.

Channel Geometry. Estimated values of the channel width, bed elevation, and energy slope in each grid of the model through which the river passes were computed from measurements taken from U.S. Geological Survey 7.5 minute topographic maps. The value of river width for a given grid was taken as the mean of several measurements of width in the reach of river contained within that grid. To estimate the bed elevation for a given grid, the center of the reach of river contained within that grid was found by measuring river distance between the grid boundaries, then determining the midpoint of that distance. The approximate elevation of that point was then obtained by linear interpolation between contour lines. The value thus obtained was assigned as the river bed elevation for that grid. Energy slope was approximated by channel bed slope. The justification of the use of this approximation was presented in Chapter III. The channel bed slope was obtained by dividing the elevation difference between the ends of the reach contained in the grid by its length. Values of channel width, bed elevation and bed slope for each of the 42 river grids in the model are tabulated in Appendix B.

Manning's Roughness Coefficient. A single value of the Manning roughness coefficient, n, was used in the calculation of river stage values in all river grids of the model, although it is known that n varies with location along the river and with depth of flow. The reason for this simplification is that information from which values of n may be deduced is insufficient to warrant assigning a value or an array of stage-related values of n to each individual river grid. Such detail would require much more comprehensive channel geometry data than is available. The estimate of the single value of Manning's n was based on the three stage-discharge relationships at the three river gaging stations located on the Arkansas River within the study area. Values of river stage and associated discharge were obtained from surface water supply papers published by the U.S. Geological Survey (1962). For every pair of stage and discharge values at each of the three stations, a value of n was calculated using the Manning formula, so that an array of n values was obtained for each station. The n value associated with the mean discharge at each station was then obtained, and the average of these three values was computed. The single n value resulting from these calculations was 0.04, which was considered reasonable for this reach of the Arkansas River as a result of comparison with similar rivers having approximately the same n values. Channel width in the vicinity of each section was then adjusted so that the mean discharge would correspond to an n value of 0.04. By using a value of n corresponding to the mean discharge at each of the three gaging stations, the errors resulting from using a constant n value are expected to be somewhat diminished.

Silt Layer Characteristics. Information regarding the thickness, hydraulic conductivity, and bubbling pressure head of the silt layer which forms on the bed and banks of the river channel under the condition of seepage from the river were not available. A value of silt layer bubbling pressure head had to be estimated. A range of probable values for h_{pb} was estimated on the basis of known characteristics of the material. After trial runs of the model with several values in this range, a value for h_{pb} of -2.4 feet was selected because it produced what appeared to be the most reasonable values of river discharge.

Measurements of the seepage rate from the Arkansas River were taken by Moore and Jenkins (1965) at several locations in the vicinity of Lamar where the river and aquifer were not hydraulically connected. These measurements were helpful in estimating values of silt layer thickness and conductivity. The average seepage rate reported by Moore and Jenkins (1965) was about 16 gallons per day per square foot. Similar results were obtained in an independent study reported by Hurr (1970). This seepage rate was assumed to correspond roughly to mean discharge. It was necessary to obtain values of t_s and K_s for use in Eqs. 3-39, 3-40, and 3-41, so that seepage rate could be computed as a function of river stage, d. For this purpose, a value for K_s of 0.08 feet per day was assumed. Using this value, the measured seepage velocity of 16 gallons per day per square foot, the value of river stage corresponding to mean discharge at Lamar, a bubbling pressure head value of -2.4 feet, and a unit area of riverbed a value of silt layer thickness of 0.2 feet was obtained by solving Eq. 3-40 for t_s. It is important to note that none of the values of K_s, t_s or h_{pb} is necessarily representative of true values of these parameters found in the field. For their use in this model, however, this restriction is not serious, as long as the combination of the estimated values used in the mathematical expression for seepage velocity produces approximately correct results.

Surface Flux Parameters

Precipitation. Precipitation data for the study area were obtained from annual records published by the U.S. Department of Commerce Weather Bureau (1958-65). Monthly values measured at Lamar were considered to be fairly representative of the entire area, because of Lamar's approximately central location in the region, and were applied uniformly over the entire study area. Values of monthly precipitation at Lamar for each month throughout the study period are tabulated in Appendix B.

Evapotranspiration. The Modified Blaney-Criddle Method was used to estimate monthly values of evapotranspiration in the study area. This method is described in a technical release published by the United States Department of Agriculture Soil Conservation Service (1967). This method was selected in preference to others because (1) it was developed in Eastern Colorado for an area having climatic and physiographic characteristics that are very similar to the Arkansas Valley study area, and (2) the procedure is simple, yields results which are sufficiently accurate for the purposes of this study, and requires a minimal amount of data. The information necessary for carrying out the calculation of estimated monthly evapotranspiration includes mean monthly temperature and percent of daylight hours, and total acreages of the various crops grown in the area. Values of mean monthly temperature at Lamar were assumed to be fairly representative of the area. These values were obtained from U.S. Department of Commerce Weather Bureau records (1958-65), and were applied to the entire study area. Percentage of daylight hours in a given month is a function of latitude, which for Lamar is North 38°04'. The function was found tabulated in the Soil Conservation Service technical release (1967), from which daylight percentage values were obtained directly. Acreages of principal crops grown in Prowers County were given by Voegeli and Hershey (1965). Bittinger and Stringham (1963) conducted a study of phreatophyte growth in the Arkansas Valley from which the total acreage of phreatophytes between John Martin Dam and the Kansas state line, and the associated evapotranspiration rates were

obtained. For each cultivated crop, plots of crop growth stage coefficients throughout the growing season were obtained from the Soil Conservation Service technical release (1967). Monthly values for each crop were extracted from these plots. A single value of crop growth stage coefficient for each month for the entire area was then computed as the average of the coefficients for each crop, weighted according to the total acreage of the crop in the study area. Phreatophytes were included in this calculation, as well as estimated areas of water and non-evaporating surfaces, such as paved roads. An additional value needed for estimating evapotranspiration by the Modified Blaney-Criddle Formula is the climatic coefficient, which was obtained from the Soil Conservation Service technical release (1967), where values of this coefficient are tabulated as functions of mean monthly temperature. Using the climatic coefficient, the composite crop growth stage coefficient, and mean monthly temperature and percentage of daylight hours, an estimate of monthly evapotranspiration in inches was obtained for the study area using the formula

$$u = \frac{tp}{100} k_t k_c , \qquad (4\text{-}5)$$

where

u is consumptive use or evapotranspiration,

t is the mean monthly temperature,

p is the monthly percentage of daylight hours,

k_t is the climatic coefficient,

k_c is the crop growth stage coefficient.

This calculation was carried out for each month during the growing season throughout the study period. The growing season for the Arkansas Valley region in Colorado is considered to begin April 1 each year and end September 30. Evapotranspiration values for the months from October through March were considered negligible, due to frozen ground, little or no plant growth, cool temperatures, and low percentages of daylight hours. Monthly evapotranspiration values for the study area are tabulated for each month throughout the duration of the study period in Appendix B.

Groundwater Withdrawal. For reasons discussed in Chapter III, information concerning well locations and groundwater withdrawal rates were not needed as input data for the computer model for all wells in the study area except those operated by the Lamar municipal power plant. The effects of these wells had to be considered because water withdrawn from them is not returned to the ground in the same vicinity from which it is extracted, which results in the formation of a considerable drawdown cone in the water table surrounding the wells, and a contribution of this water to other areas. Moore and Jenkins (1966) reported that groundwater is withdrawn for cooling purposes by the power plant wells at the rate of about ten cubic feet per second. After its use, this cooling water is discharged into the Lamar Canal and distributed for irrigation along with water diverted from the Arkansas River. Moore and Jenkins (1965) observed that because the Lamar Canal is fairly well sealed with deposits of fine sediments, the leakage rates from the canal are small, and as a result very little of the water withdrawn by the power plant wells is returned to the aquifer until it is applied for irrigation in the farmland east of Lamar. The mathematical treatment of the Lamar power plant wells in the computer model was explained in Chapter III.

Irrigation. Because available data were found to be insufficient for directly evaluating the input to each model grid from irrigation at every time increment, values of irrigation input to each grid had to be estimated. These estimates were based on the assumption that water diverted into each canal at every time increment is applied uniformly over the entire distribution region of the canal. Data sources for monthly diversions of the nine major irrigation canals in the study area were discussed in a previous section of this chapter. The distribution region of each canal was delineated approximately on a topographic map. The percentage of each canal distribution region lying inside the study area was then determined by superimposing the model grid network over the topographic map and visually estimating the percentage of the region inside the grid network. The boundaries of the portion of each distribution region inside the study area were adjusted to coincide with individual grid boundaries, so that this portion of the region consisted of a set of whole grids. The area of the portion of each distribution region inside the study area was then computed by summing the areas of the constituent grids. The percentage of distribution region inside the study area, and the area of this percentage are tabulated in Appendix B for each of the nine major canals in the study area. The use of these values in the computer model was discussed in Chapter III.

CHAPTER V
RESULTS AND DISCUSSION

The verification of the finite difference model developed in this study was carried out in two stages: In the first stage the model was used to simulate flow in several hypothetical stream-aquifer systems. Runs were made using the synthesized data describing these systems to determine whether the model was operating correctly. In the second stage the model was used to simulate flow in an actual stream-aquifer system located in the Arkansas Valley of Southeastern Colorado. Runs were made using field measurements as input data. Results of these runs include a water table elevation map of the study area at the end of the time period being considered, and average monthly values of river discharge at the upstream and downstream ends of the area throughout the study period. These results were compared to field measurements to determine the ability of the model to accurately match observed data.

An analysis of the sensitivity of results obtained using this model to changes in the values of various input parameters was conducted as part of the study. The purpose of this sensitivity analysis was to determine the importance of the accuracy of each input parameter to the quality of results. This information is helpful in deciding how much time and effort should be devoted to obtaining accurate data values for each parameter. The sensitivity analysis was conducted using data from the Arkansas Valley study area.

The remainder of this chapter includes the presentation and discussion of results obtained using the model in the two stages of verification. The sensitivity of results to changes in the values of several parameters is also discussed.

Qualitative Analysis of Results Obtained Using Synthetic Data

The initial phase of model verification was carried out by simulating flows in several simplified, hypothetical stream-aquifer systems. The purpose of using simplified systems was to detect errors in the operation of the model that might have remained undiscovered amid the complexities of a real system. This stage of verification was intended for checking the operation of those subroutines concerned with computing seepage rates to and from the river and setting up and solving the groundwater flow equations.

The model was used to simulate flow in hypothetical stream-aquifer systems with the following configurations: (1) horizontal initial water table and uniform saturated thickness; (2) initial water table of uniform gradient in the direction parallel to the river, and aquifer of uniform saturated thickness; (3) initial water table of uniform gradient parallel to the river, nonuniform slope perpendicular to the river, and aquifer of nonuniform saturated thickness. The water table in the third configuration sloped toward the river from both sides in a U-shape, and the saturated thickness increased toward the river, with the maximum thickness occurring directly beneath the river.

The aquifer material in all three configurations was assumed to be everywhere homogeneous and isotropic. The river traversed each system from end to end in a straight path through the center of the model. Each river grid was assigned a value of head at the beginning of every run which remained constant throughout the run. A well was located about 0.5 miles from the river in the three-dimensional model segment of each configuration. The grid representation of the system having a horizontal water table is illustrated in Fig. 5-1.

Three runs were made with each hypothetical system: (1) with no pumping of the well; (2) with steady pumping of the well throughout the run; (3) with steady pumping of the well for the first half of the run and no pumping for the remainder of the run. Runs 1 and 2 were made over a period of 100 days, with 10 day time increments. Run 3 spanned 200 days, also with 10 day increments.

Results of run 1, with no pumping of the well, were similar for each of the three hypothetical stream-aquifer systems. A comparison of the water table configuration at the end of the run to the initial water table map for each case indicated little or no change, which was the expected result. Seepage rates between the river and the aquifer were zero for the system having a horizontal water table and the system having a uniformly sloping water table in the direction of the river and no slope perpendicular to the river. Substantial seepage rates from the aquifer into the river were computed for the system having a water table with nonuniform slope toward the river from both sides. Seepage rates into the river were higher in the region of the three-dimensional model segment than elsewhere. The reason for this is that contributions to seepage in the three-dimensional segment include flow up through the riverbed from the underlying grids, whereas only lateral inflows are included in seepage calculations in the two-dimensional model segments. This result implies that seepage calculations in the three-dimensional model segment are sensitive to errors in initial heads or surface fluxes, which might cause positive errors in head values in the grids located beneath the river. However, the seepage rates computed in the three-dimensional segment appeared to be reasonable and agreed well with hand-calculated estimates of seepage rate for this system. Favorable results obtained from run 1 for each system indicated that the portions of the model for computing groundwater movement and seepage between the stream and aquifer were operating correctly.

Results of run 2, with steady pumping of the well throughout, indicated the formation of a drawdown cone in each hypothetical system. The shape of this drawdown cone varied with the configuration of each system. This drawdown resulted in seepage from the river in the system with the horizontal initial water table and in the system with an initial water table having uniform slope parallel to the river and no slope perpendicular to the river. The result of the drawdown due to pumping in the system having an initial water table sloping toward the river from both sides was a reduction in the rate of seepage into the river from the aquifer. Near the end of the run the seepage rate in the river grid nearest the well approached zero, then changed sign, indicating that the river was losing flow in the vicinity of the well. Results of run 2 for each system indicated that the portions of the model for simulating groundwater movement and computing seepage to and from the river were apparently operating correctly.

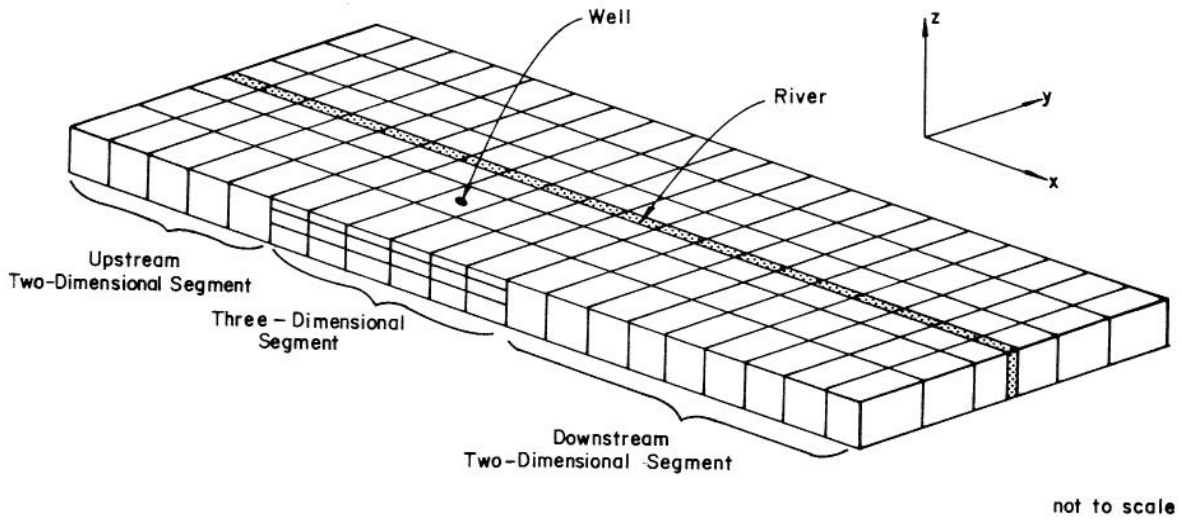

Fig. 5-1 Model Representation of Hypothetical Stream-Aquifer System with Horizontal Water Table

Results for the first half of run 3 were identical to results obtained in run 2 for each system. After pumping ceased, the water table in each system began to recover from the effects of drawdown. At the end of the run, water table elevations in each grid appeared to be approaching their initial values. The recovery of the water table was accompanied in each case by a reduction in the rate of seepage from the river. For the system in which the initial water table configuration sloped toward the river, seepage from the river ceased within a few time steps after pumping was discontinued, and flow from the aquifer into the river was reestablished at all locations along the river. Results of run 3 for each hypothetical stream-aquifer system indicated that the handling of partially saturated grids in the three-dimensional model segment permits the resaturation of these grids, so that the model is capable of simulating positive and negative water table fluctuations.

Analysis of Results Obtained Using Field Data

The ability of the computer model to correctly simulate flow in an actual stream-aquifer system was tested using data from a region of the Arkansas Valley in Southeastern Colorado. A detailed description of the Arkansas Valley study area was presented in Chapter IV, along with a discussion of the sources and preparation of data from the area for use with the model. The treatment of boundary conditions in the use of the model with field data was discussed in Chapter III.

A run was made with the model over a time period of 8 years, beginning in January 1958 and ending in December 1965, using a time increment of 30 days. Computed results included mean monthly discharge values below John Martin Dam and near Coolidge, Kansas, and maps of water table elevations in the two-dimensional model segment and heads in the three-dimensional model segment at three-month intervals throughout the run.

Computed River Discharges at John Martin Dam and Coolidge

The values of river discharge at John Martin Dam and at Coolidge computed for the year 1960 are considered typical of the results obtained at each location for the entire eight years. Computed values of mean monthly discharge below John Martin Dam are plotted along with observed values at the John Martin Dam gaging station in Fig. 5-2 for 1960. Computed and observed values of river discharge at Coolidge for 1960 are plotted in Fig. 5-3.

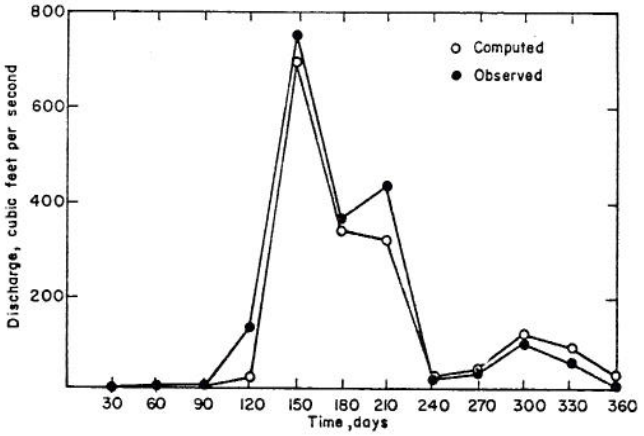

Fig. 5-2 Computed and Observed Mean Monthly Discharge below John Martin Dam, 1960

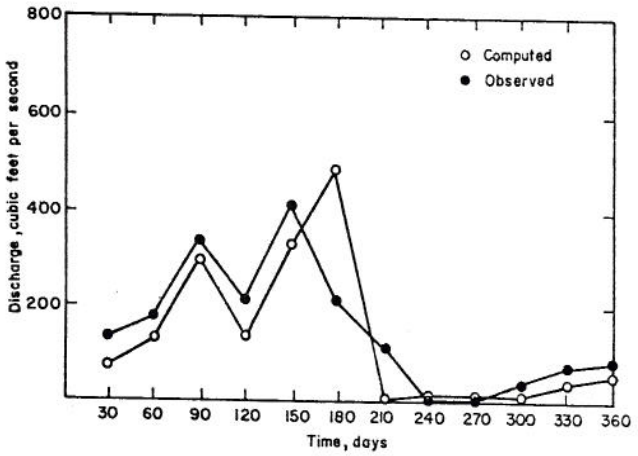

Fig. 5-3 Computed and Observed Mean Monthly Discharge at Coolidge, 1960

Computed values of monthly discharge below John Martin Dam agreed well with observed values. The observed mean discharge for 1960 at this location was 158 cubic feet per second, while the computed mean discharge was 139 cubic feet per second, resulting in a discrepancy of 12 percent of the observed value. The primary reason for this discrepancy is believed to be inaccuracy of estimated values of seepage between the river and aquifer in the reach of river between Lamar, where calculations of river flow are begun, and John Martin Dam. Seepage rates are dependent, either directly or indirectly, on nearly every parameter used in the computer model, so that inaccurate seepage rates may result from a large number of possible combinations of data errors. The sensitivity of computed discharge values to errors in the value of several parameters is discussed later in this chapter. Incorrect seepage rates may also result from inaccuracies in some of the assumptions made to facilitate the use of this model, particularly the assumption of idealized channel geometry and the set of assumptions made to simplify the calculation of surface flux values. The use of an average gradient between the river boundary and an adjacent aquifer grid for computing seepage rates instead of the gradient at the river boundary may be responsible for incorrect values of computed seepage rate. The average discrepancy between computed and observed values of mean annual discharge below John Martin Dam for the eight-year study period was 12 percent of the observed value.

Computed values of discharge at Coolidge appeared to follow the pattern of observed discharges fairly well. However, discrepancies between individual pairs of computed and observed values were often quite large, as was the case for June 1960, shown in Fig. 5-3. In spite of such large individual discrepancies, however, the observed mean annual discharge for 1960 at Coolidge was 145 cubic feet per second, the computed mean annual discharge was 128 cubic feet per second, and the difference between these values was only 12 percent of the observed value. The average discrepancy between observed and computed mean annual discharge values for the eight-year study period was 23 percent. A probable cause of these discrepancies is inaccurate computed estimates of seepage rates between the river and aquifer. Greater difficulty is expected in obtaining accurate discharge values at Coolidge than at John Martin Dam because the distance between Lamar and Coolidge is approximately twice the distance between Lamar and John Martin Dam. The difficulty in obtaining accurate computed estimates of discharge at Coolidge is compounded by several factors: (1) Inflows to the Arkansas River from Big Sandy Creek contribute a significant amount to the flows at Coolidge. These inflow values have been estimated for the study period according to the procedure described in Chapter IV, because discharge data were not available, and these estimates may be inaccurate. (2) Water diverted from the Arkansas River is used extensively in the region between Lamar and Coolidge for irrigation. The areal distribution of this diverted water over the study area by the computer model was carried out on the basis of several assumptions, which were discussed in Chapter III. If any or all of these assumptions are invalid at a given location in the study area, large errors in computed values of surface flux, hence errors in head values can occur. The effect of such errors can be transmitted to the value of river discharge at Coolidge through the computed rate of seepage across the stream-aquifer boundary. (3) Whereas the boundaries of the alluvial aquifer between Lamar and John Martin Dam are almost entirely contained within the boundaries of the study area, the aquifer widens between Lamar and Coolidge, and a significant portion of it extends beyond the study area boundaries. For this reason the assumption of known or constant head boundaries at the perimeter of the model may not be entirely valid in the Lamar-to-Coolidge reach, which may result in errors in head values. These errors affect the seepage rates, which in turn affect the computed discharge values at Coolidge.

The least accurate estimates of river discharge at both John Martin Dam and Coolidge were produced by the model for the year 1965. Plots of observed and computed monthly discharge values for this year are presented in Fig. 5-4 for John Martin Dam, and in Fig. 5-5 for Coolidge. The discrepancy between observed and computed values of mean annual discharge at John Martin Dam was 32 percent in 1965. For mean annual discharge at Coolidge, the discrepancy between the observed and computed values was 58 percent. A comparison of the plots of observed and computed discharge values presented in Figs. 5-4 and 5-5 indicates that both these discrepancies were caused primarily by an anomaly in the pattern of computed discharge values for the month of June. At John Martin Dam, the computed discharge was about 500 percent higher than the observed value for June; at Coolidge it was roughly 80 percent lower. Computed discharges at both stations for the remaining months of 1965 followed the pattern of observed flows fairly well. The cause of this anomaly is believed to be the failure of the model to account for inflow to the river from surface runoff or from tributaries other than Big Sandy Creek, and its lack of a dynamic equation for correctly describing the movement of a flood wave down the river. These contributions to river flow apparently became significant during the period from June 16 to June 20, 1965, when a flood passed through the study area. Large quantities of precipitation occurred in the area over a short period of time, which apparently resulted in considerable runoff. This runoff reached the river both directly, as overland flow, and indirectly, through several small tributaries in the area. The flows in these tributaries are generally insignificant, but at this time were apparently considerable and contributed significant amounts to river flow. The effects of surface runoff and tributary inflows on the volume of river flow is evidenced by the observed discharge at each of the three river gaging stations in the area on June 18. Discharge below John Martin Dam was 17 cubic feet per second, at Lamar the flow was 25,000 cubic feet per second, and at Coolidge

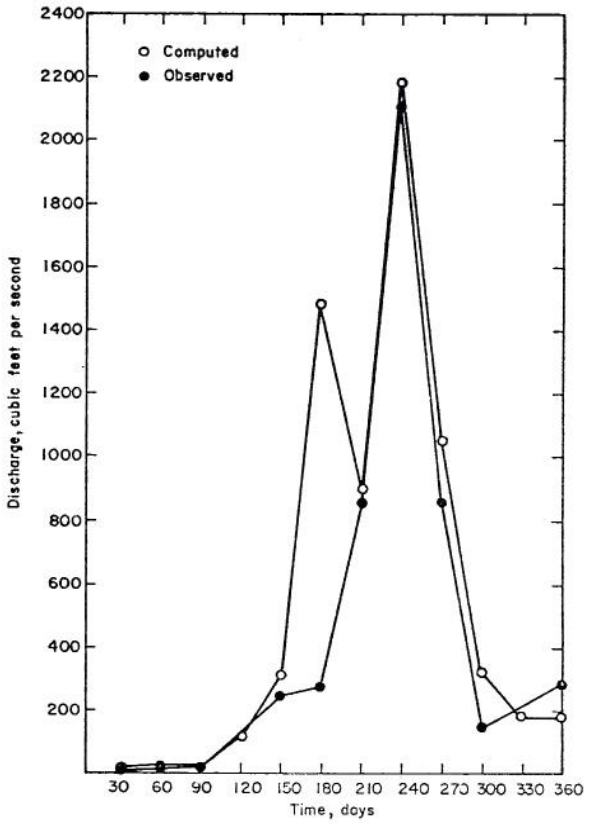

Fig. 5-4 Computed and Observed Mean Monthly Discharge below John Martin Dam, 1965

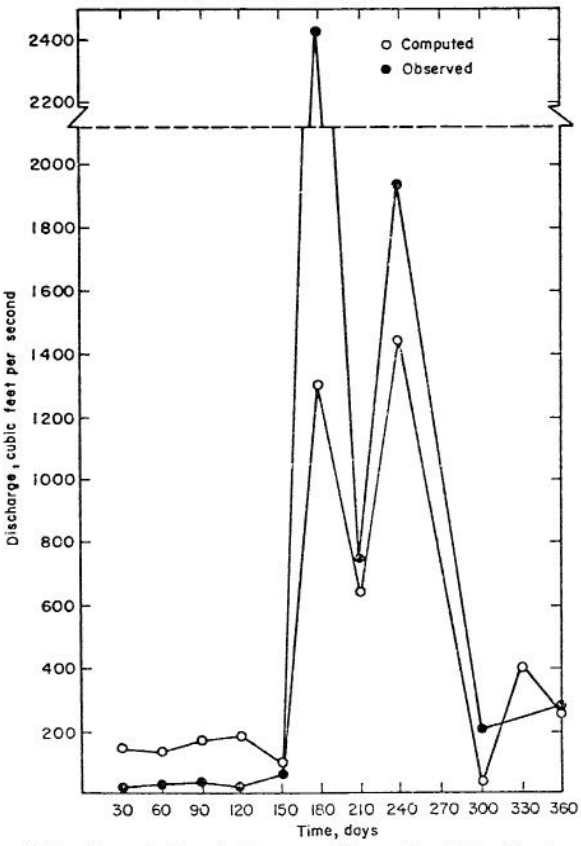

Fig. 5-5 Computed and Observed Mean Monthly Discharge at Coolidge, 1965

the discharge had increased to 101,000 cubic feet per second. Because discharge calculations are initiated at Lamar for each month, the underestimation of inflows to the river throughout the study area for June 1965 caused an overestimation of the discharge below John Martin Dam, and an underestimation of the discharge at Coolidge, as is apparent from the plots of observed and computed monthly discharge values shown in Figs. 5-4 and 5-5.

Computed Water Table Elevations and Heads

Computed values of water table elevation in each grid of the two-dimensional model segments, and head in each grid of the three-dimensional segment, were obtained at the end of every three months throughout the eight-year run of the model with field data. Data were not available for heads at each level of the area modeled by the three-dimensional segment. Therefore, in order to facilitate the comparison of model results with field data, values for water table elevation had to be obtained in each column of three-dimensional grids. This was done by assigning each grid column a water table elevation equal to the head in the uppermost grid of the column containing a portion of the saturated zone. These values were then used, along with water table elevation values from the two-dimensional segments, to construct a contour map. The contour map was then compared with a similar map constructed from measured water table elevations throughout the area. A map of water table contours constructed from values computed for December 1965 has been plotted along with a set of contours constructed from observed values which were obtained from measurements taken early in 1966. The portion of this map obtained by the upstream two-dimensional model segment is shown in Fig. 5-6. The center section of the map, obtained by the three-dimensional model segment is shown in Fig. 5-7, and the downstream portion of the map is shown in Fig. 5-8.

Comparison of computed with observed values of water table elevations mapped in Fig. 5-6 indicates good agreement at most locations. Where discrepancies do occur they are generally small and localized. Such discrepancies may result from a number of factors including (1) inaccurate surface flux values, (2) incorrect perimeter boundary heads, (3) response of the aquifer to inaccurate computed seepage rates, (4) effects of discretizing parameters and linearizing gradients to facilitate the use of the finite difference technique.

Comparison of computed with observed water table elevations mapped in Fig. 5-7 indicated reasonable agreement over a majority of the area. However the computed contours are generally shifted slightly to the right of the contours constructed from observed data, indicating a higher water table. This shift is also noticeable in the water table downstream of Lamar, as shown by the location of computed contours in Fig. 5-8. The primary cause of this shift was believed to be the incorrect representation by the model of the June 1965 flood. The effects on computed river discharge values of the model's inability to simulate surface runoff was discussed previsouly, and the effect on the water table was to raise it, because large quantities of water which should have been treated as surface runoff were instead added to the groundwater reservoir.

An additional factor which may have been partially responsible for the shift in the water table contours

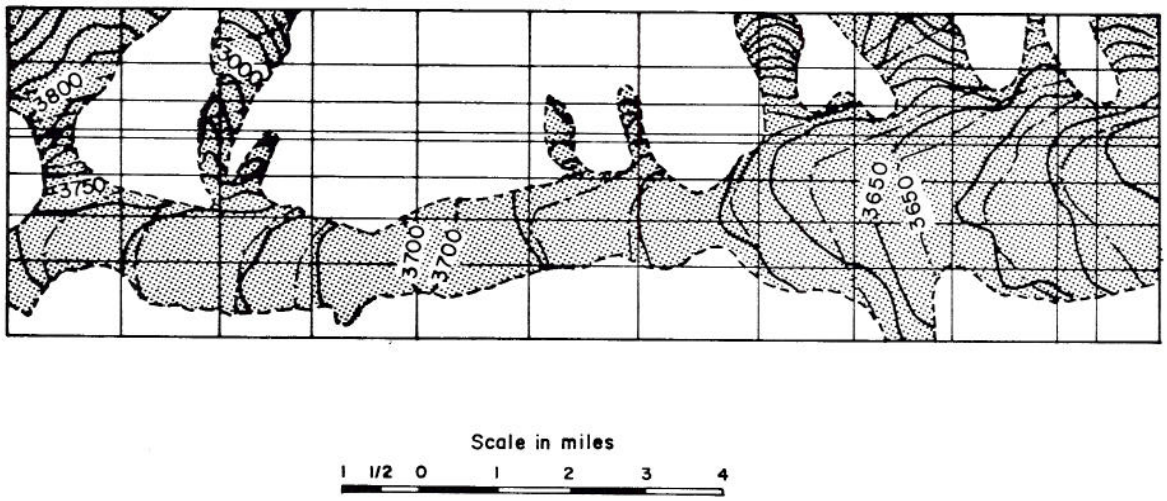

Fig. 5-6 Computed and Observed Water Table Elevation Contours in Upstream, Two-Dimensional Model Segment, December 1965

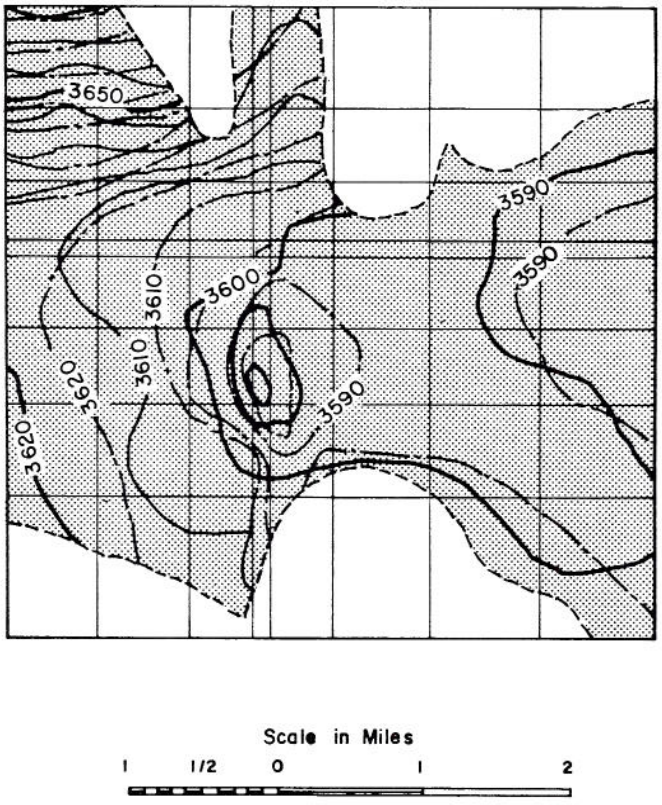

Fig. 5-7 Computed and Observed Water Table Elevation Contours in Three-Dimensional Model Segment, December 1965

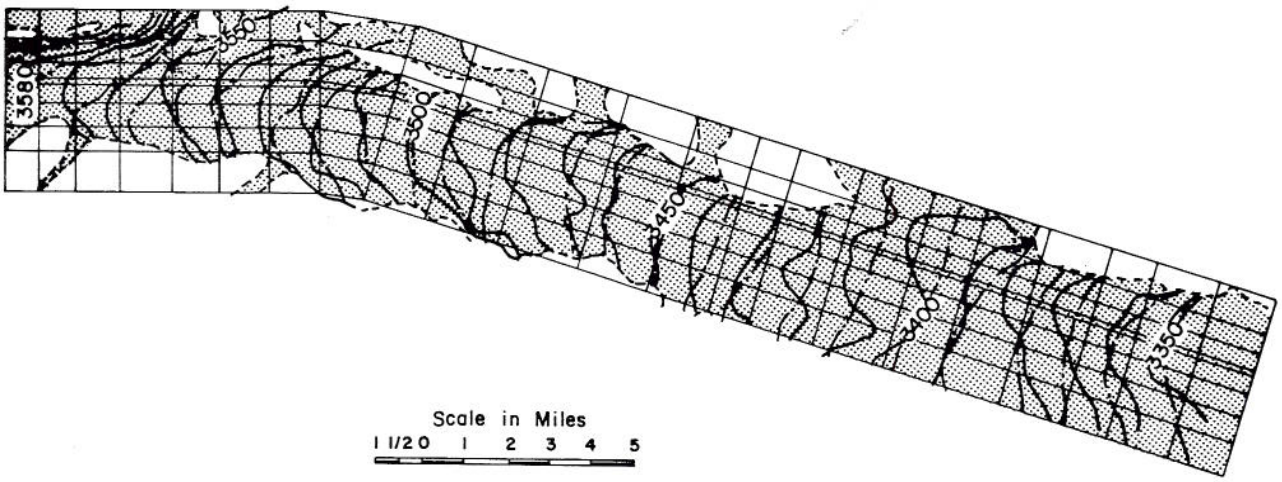

Fig. 5-8 Computed and Observed Water Table Elevation Contours in Downstream, Two-Dimensional Model Segment, December 1965

is the simplified treatment by the model of the application of irrigation water, and the limited capability of the model to treat the time lag from application at the surface to arrival at the water table. This simplified model representation of flow above the water table has the effect of overestimating water table fluctuations. The unsaturated zone in the actual case may be thought of as a damping member of the system, which reduces water table fluctuations by absorbing or releasing water in response to surface application and water table fluctuations, but with the response taking place after a time delay. The treatment of flow in the unsaturated zone by the model includes linarizing gradients and using average values of the unsaturated flow parameters of dS/dH and k_r over large model grids representing the unsaturated zone. While this simplification does not entirely negate the damping property of the unsaturated zone, it does significantly reduce its effectiveness. This shortcoming of the model could be reduced by using a larger number of grids in the three-dimensional segment having smaller thicknesses, on the order of one foot or less. This improvement was not undertaken as part of this study because such a large number of grids would exceed available computer storage.

The computed drawdown cone in the vicinity of the Lamar power plant wells, which is indicated by the contour lines in Fig. 5-7, is somewhat larger in areal extent than the observed drawdown cone. This may be due to several factors including (1) underestimated values of hydraulic conductivity in the well field, (2) underestimated value of porosity in the area, (3) overestimated water table fluctuations, (4) incorrect estimation of surface input in the vicinity of the well field, (5) and use of the finite difference approximation. The effect of this discrepancy is not apparent in the configuration of the computed water table more than about one mile from the well field, and for this reason is not considered to cause significant errors in results, either in the water table elevations in the remainder of the study area, or in the computed river discharges at John Martin Dam and Coolidge.

Computed head values in the three-dimensional model segment indicated that no hydraulic connection exists between the river and the aquifer over a reach approximately 2.5 miles in length in the vicinity of the Lamar power plant wells. This indication is based on the fact that computed water table elevations in this reach ranged from 2 to 12 feet lower than the elevations of the riverbed directly overhead. These results agreed well with water table elevations which were measured by Moore and Jenkins (1965). The most important aspect of this result is that it shows the model's capability to simulate a complex flow situation, in which the combined effects of high-volume pumping near a river, and a silt layer on the bed and banks of the channel have caused the hydraulic connection between the river and aquifer to be broken. Boundary condition indices printed out as intermediate results by the model indicated that seepage from the river in this 2.5 mile reach was being correctly represented as partially saturated flow, with seepage velocity determined entirely by silt layer characteristics and river stage.

Comparison of computed with observed values of water table elevations mapped in Fig. 5-8 indicates fairly good agreement throughout the area. Small, localized differences between computed and observed water table elevations may have been caused by several factors discussed in previous paragraphs of this section. In this region the accuracy of surface flux values and perimeter heads is more important for obtaining accurate water table elevations than it is in the areas treated by the other two segments of the model. The reasons for this are (1) extensive use of water diverted from the Arkansas River for irrigation, (2) the areal extent of the aquifer beyond the boundaries of the study area. The effects of these factors on the water table elevations were discussed in a previous section of this chapter along with a description of their influence on the accuracy of computed discharge values at Coolidge.

Analysis of Sensitivity of Results to Variation of Parameters

As part of this study, an analysis was conducted of the sensitivity of results obtained with the model to variations in the values of several parameters. Field data from the Arkansas Valley study area were used in this analysis, which was limited primarily to the consideration of those parameters for which comprehensive data were not available, and for which values used as input to the computer model had to be estimated or assumed.

The parameters considered in this analysis were (1) bubbling pressure head of the silt layer, h_{pb}, (2) silt layer hydraulic conductivity, K_s, (3) the array of relative permeability values, k_r, (4) the array of values of the derivative of saturation with respect to head, dS/dH, (5) the porosity, ϕ, (6) the array of values of surface flux, Q_s, (7) the array of initial values of head, H, and (8) the first three values of monthly discharge at Lamar, Q_L. The analysis of the sensitivity of results to each of the first six of these parameters was carried out by first making a short run of the model with the parameter set equal to the value or array of values used in the eight-year run. The short run was then repeated with nothing changed except the value of the parameter under consideration. Mean monthly discharges at John Martin Dam and Coolidge were obtained for each of the two parameter values and were plotted together and compared with each other, and also with observed discharge values, to determine the effect of varying the parameter value. As an example, values of monthly discharge below John Martin Dam, which were obtained using two different bubbling pressure head values, are plotted in Fig. 5-9, along with observed values. Water table elevation contour maps obtained using the two parameter values were also compared for the purpose of determining the effects of the parameter variation. Sensitivity runs for these six parameters spanned 180 days each, with 30 day time increments. Because the number of water table elevation maps and plots of monthly discharge values generated in this analysis was quite large, these maps and plots were not included in this discussion. Instead, the results of the sensitivity analysis for variations of h_{pb}, K_s, k_r, dS/dH_p, ϕ, and Q_s are summarized in Table 5-1. The original value or array of values of each parameter, the value or array to which it was changed and the resulting influence of this change on discharge below John Martin Dam, discharge at Coolidge, and water table throughout the study area are indicated in Table 5-1. Following is a brief discussion of these results for each of the six parameters included in Table 5-1, and also of the results of analyses of the sensitivity of model results to variations in initial heads and initial discharges at Lamar.

Silt Layer Bubbling Pressure Head. Increasing the value of h_{pb} from -2.40 feet to -0.25 feet produced the effect of decreasing the maximum possible rate of seepage from the river in the three-dimensional model segment. As a result, seepage from the river was underestimated both upstream and downstream of the Lamar gaging station. This produced underestimates of discharge values at John Martin Dam and initial overestimates of discharge at Coolidge, as indicated in Table 5-1. Reducing the rate of stream depletion, thereby reducing the rate of recharge to the aquifer, caused the water table to drop in the three-dimensional model segment. Eventually, this drop caused a lowering of the water table all the way to Coolidge. The result of the lower water table was lower rates of seepage into, or higher rates of seepage from the river. This effect caused an underestimation of seepage rates at Coolidge

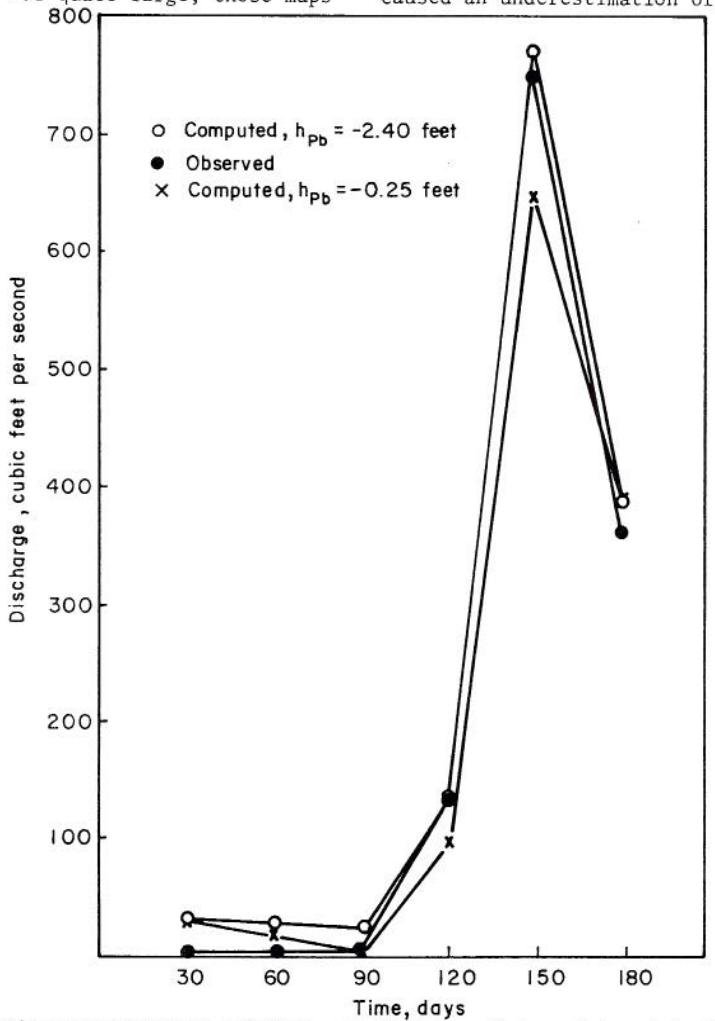

Fig. 5-9 Comparison of Computed and Observed Discharge Values below John Martin Dam for Sensitivity of Results to Bubbling Pressure Head Variation

Table 5-1 Summary of Sensitivity Analysis Results for Six Parameters

Parameter	Initial Value	Final Value	Effect of Changing Parameter Value on: Mean Monthly Discharge at John Martin Dam	Mean Monthly Discharge at Coolidge	Water Table Elevations
Silt Layer Bubbling Pressure Head, h_{pb}	-2.40 feet	-0.25 feet	Underestimated by 15 to 20 percent	Initially overestimated by less than 5 percent. Thereafter underestimated by 10 to 30 percent	As much as 3 feet lower near Lamar wells. Up to 1 foot lower downgradient from wells to Coolidge
Silt Layer Hydraulic Conductivity, K_s	0.08 ft/day	0.16 ft/day	Overestimates low flows by less than 5 percent. Underestimates high flows by 10 to 20 percent.	Irregular estimates. Oscillates from 200 percent overestimate to 100 percent underestimate	Approximately 1 foot higher from Lamar to Coolidge
Relative Permeability, k_r (array)	Array A Table 5-2	Array B Table 5-2	Overestimated by 10 to 30 percent	Oscillates from 50 percent overestimate to 50 percent underestimate	1 to 3 feet higher in immediate vicinity of Lamar wells.
Saturation Derivative, dS/dH (array)	Array C Table 5-2	Array D Table 5-2	Overestimated by 5 to 15 percent	Oscillates from 10 percent overestimate to 10 percent underestimate	1 to 3 feet lower near Lamar Up to 1 foot higher elsewhere
Porosity, ϕ	0.25	0.30	Less than ±5 percent error in estimates	Errors in estimates ranged from ±5 to ±10 percent	Up to 1 foot higher near Lamar wells.
		0.20	Less than ±5 percent error in estimates	Errors in estimates ranged from ±5 to ±10 percent	Up to 1 foot lower near Lamar wells.
Surface Flux, Q_s (array)	Read in at each time increment	0.0 everywhere	Overestimates high flows by 10 to 15 percent. Estimates of low flows satisfactory.	Underestimates high flows by 10 to 30 percent. Estimates of low flows satisfactory	As much as 2 feet higher or lower, depending on time and location

after the first few time increments, as indicated in Table 5-1.

Silt Layer Hydraulic Conductivity. Changing the value of K_S influences the rate of stream depletion in the three-dimensional model segment, as does changing the value of h_{pb}. It would therefore be expected that increasing the value of K_S from 0.08 feet per day to 0.16 feet per day would produce the opposite effects from those described in the previous paragraph. This is the case for low flows at John Martin Dam and for the elevation of the water table. Excessive seepage from the river in the three-dimensional segment of the model results from the high K_S value. During the winter, when the water table is low, excessive stream depletion values between Lamar and John Martin Dam result in computed discharge values at John Martin Dam which are higher than the observed discharges. However, this excessive stream depletion also provides excessive recharge to the aquifer, hence a higher water table. Later in the year, when surface irrigation and high river flows begin to provide even more recharge to the aquifer, the water table rises still higher. By late spring the water table generally rises above the level of the river in most places and the aquifer begins recharging the river. With the water table exceptionally high, the rate of seepage into the river is overestimated, resulting in an underestimation of the discharge at John Martin Dam. This result is recorded in Table 5-1.

An interesting effect resulting from raising the value of K_S is observed in the behavior of this model in predicting discharges at Coolidge. The high water table between Lamar and Coolidge, which results from high seepage rates in the three-dimensional model segment, initially causes overestimated seepage rates into the river between Lamar and Coolidge, which result in an overestimated discharge value at Coolidge. Near the lower end of the reach, the computed discharge, hence the head in the river, becomes so high that it may exceed the head in the surrounding aquifer. As a result, seepage rates into the river calculated for use in the next time step are drastically underestimated and may be negative, indicating seepage away from the river. The use of these seepage rates in the next time increment results in substantial underestimates of discharge at Coolidge and in the reach of river upstream of Coolidge for several miles. These underestimated discharges, accompanied by low heads in the river, result in overestimated seepage rates, as were observed in the same area two time steps before. The result of these events is the prediction of monthly discharge values at Coolidge which are alternately too high and too low. This result is recorded in Table 5-1. The reason for this fluctuation is the use at the present time level of seepage rates computed at the previous time level. The problem could be alleviated by using an iterative scheme to solve for seepage rates at the present time level using present head values, or by using smaller model time increments. Because of the excessive amount of computer time and storage such an iterative scheme would consume, this was not done as part of this study. However, as was reported in the previous section of this chapter, reasonably accurate estimates of discharge at Coolidge were obtained using a 30 day time increment and the existing procedure for computing seepage rates, when reasonably accurate parameter

values were used. For this reason, the procedure for estimating seepage rates and the 30 day time increment were left unchanged for further use of the model in this study.

Relative Permeabilities. The array of k_r values used in the eight-year run is given in Table 5-2 as Array A. The array of values used to analyze the sensitivity of results to variations in k_r values appears as Array B. Array B is a more realistic representation of the relative permeability of a naturally occurring sandy material than Array A. The values of Array B were obtained from the plot of relative permeability as a function of pressure head for fine sand given in Fig. 4-7. However, trial runs of the model using Array B resulted in the erroneous results summarized in Table 5-1, and Array A was used instead to obtain the more accurate results of the eight-year run. The apparent reason for the inaccurate results obtained using Array B is the overestimation by the model of lateral flow between partially unsaturated grids in the three-dimensional model segment. The overestimation of lateral flow contributes to an overestimation of flow in from the side boundaries of the model. Seepage to or from the river, depending on the direction of the gradient, may also be overestimated. These factors cause the elevated water table, overestimated discharge at John Martin Dam, and oscillating predictions of discharge at Coolidge, as indicated in Table 5-1. The cause of the overestimation of lateral flows in the partially saturated grids is the overprediction of lateral flow above the water table in these grids. Two possible reasons for this are: (1) The relative permeability function given by Array B may not be representative of the aquifer material in the Lamar area. If the actual material is coarser than that represented by Array B, a function whose values decrease more sharply with increasing capillary pressure head would be more appropriate. Array A is such a function. (2) If vertical flow exists above the water table, the average gradient between the saturated zones of two adjacent grids may not be equal to the gradient in the unsaturated zones of the grids. This problem could be alleviated greatly by using a larger number of much thinner grids to represent the portion of the aquifer in which unsaturated flow is likely to occur. This was not done in this study because the treatment of such a large number of grids would exceed available computer storage.

Table 5-2 Arrays of Relative Permeabilities and Saturation Derivatives Used in Sensitivity Analysis

Capillary Pressure Head, H_p, feet	Relative Permeability, k_r		Saturation Derivative, dS/dH	
	Array A	Array B	Array C	Array D
0.5	1.000	1.000	0.000	0.000
1.0	1.000	1.000	0.000	0.000
1.5	1.000	0.980	0.020	0.010
2.0	1.000	0.900	0.060	0.030
2.5	0.000	0.650	0.160	0.080
3.0	0.000	0.200	0.300	0.150
3.5	0.000	0.100	0.480	0.240
4.0	0.000	0.070	0.260	0.130
4.5	0.000	0.045	0.140	0.070
5.0	0.000	0.030	0.080	0.040
5.5	0.000	0.020	0.060	0.030
6.0	0.000	0.015	0.040	0.020
6.5	0.000	0.010	0.020	0.010
7.0	0.000	0.010	0.020	0.010
7.5	0.000	0.010	0.010	0.005
8.0	0.000	0.010	0.010	0.005
8.5	0.000	0.010	0.008	0.004
9.0	0.000	0.010	0.004	0.002
9.5	0.000	0.010	0.002	0.001
10.0	0.000	0.010	0.000	0.000

Saturation Derivatives. The array of values of dS/dH used in the expression for flow in the three-dimensional model segment for the eight-year run is given in Table 5-2 as Array C. The values of Array C were obtained from the plot of saturation as a function of pressure head for fine sand given in Fig. 4-8. The array of values used to analyze the sensitivity of results to variations in the values of dS/dH appears as Array D in Table 5-2. The values of this array were obtained by dividing each value of Array C by two. Although the resulting function is purely artificial and not representative of any particular material, its shape is similar to functions of dS/dH typical of silty soil. Using Array D in place of Array C as the function of dS/dH resulted in an effect similar to what would be expected as a result of decreasing the specific yield in the two-dimensional model segments. Greater changes in head resulted from increasing or decreasing the storage of grids located partially or totally within the unsaturated zone. Inflow to the grids of the three-dimensional model segment from surface flux, seepage from the river, and flow to the interior grids from the perimeter, resulted in head values which were generally overestimated, except in the immediate vicinity of the Lamar Power Plant wells. The effect of overestimated heads in the three-dimensional model segment on estimated discharges at John Martin Dam and Coolidge are summarized in Table 5-1, and were discussed previously.

Porosity. Increasing the value of ϕ from 0.25 to 0.30 produced the effect of increasing the available storage in the three-dimensional model segment, and decreasing the response of head values to changes in storage. As a result, heads near the river were more insensitive to inflows and outflows than before. Small errors in computed seepage rates occurred, which in turn produced minor errors in the estimates of mean monthly discharge at John Martin Dam and at Coolidge. The only differences produced in the water table by using a value for ϕ of .30 were slightly higher head values in the immediate vicinity of the well, which occurred as a result of the increased storage in the aquifer.

Because of effects produced by changing the value of ϕ from 0.25 to 0.30 were inconclusive a second sensitivity run was made with a ϕ value of 0.20, to determine whether the results were insensitive to changes in ϕ within a probable range of values, or whether the use of the value of ϕ of 0.30 coincicidently produced reasonable results. The results sensitivity runs using ϕ values of 0.30 and 0.20, which are summarized in Table 5-1, indicate that using a value of 0.20 for ϕ produces errors opposite in sign and approximately equal in magnitude to errors produced using a ϕ value of 0.30. It is therefore concluded that variations in the value of porosity within a probable range does not produce significant errors in the results obtained using the model developed in this study.

Surface Flux. The procedure for estimating a value of surface flux at each time increment for every surface grid of the model was discussed in Chapter III. Although seasonal variations in the magnitude and direction of flux, and the variations with location in the study area are considerable, the net annual flux for the entire study area is on the order of 0.2 feet. The sensitivity of results to variations with time and location of surface flux was tested to determine whether surface flux could have been neglected altogether in the analysis of flow in this particular stream-aquifer system, without decreasing the accuracy of results. This was accomplished by using surface flux values of zero for all surface grids of the model, in place of those calculated from data at the beginning of each time increment. Results are summarized in Table 5-1. While low flows, both at Coolidge and at John Martin Dam were estimated with reasonable accuracy, high flows were overestimated at John Martin Dam and underestimated at Coolidge. The errors in estimates of high discharge values are believed to result from the failure of the water table predicted by the model to rise, as it normally would in response to large inflows at the surface due to irrigation in the late spring and early summer months. The failure of the water table to rise at this time results in low estimates of seepage into the river, hence the errors in estimated mean monthly discharge values below John Martin Dam and at Coolidge. The water table exhibits a high degree of sensitivity to surface flux throughout the study area, as was determined by comparing water tables obtained with and without surface flux at various times.

Because seasonal and spatial variations in surface flux have a significant influence on the quality of results, it was concluded that consideration of surface flux should not be excluded in the analysis of flow in the stream-aquifer system considered in this study.

Initial Heads. Runs one year in length with 30 day time increments were made to determine the effect on results of variations in the array of values of initial head, H. This was accomplished by making two runs of the model with boundary condition data from 1960, run 1 with the correct initial head array from 1960, and run 2 with an array of initial head values from 1959. Resulting monthly discharge values were plotted along with observed values for both John Martin Dam and Coolidge.

The plot of computed and observed mean monthly discharges at Coolidge is shown in Fig. 5-10. Initially,

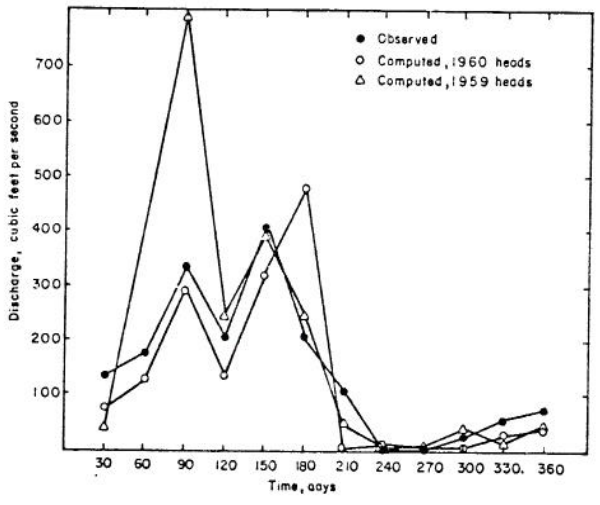

Fig. 5-10 Comparison of Computed and Observed Discharge Values at Coolidge for Sensitivity of Results to Variation of Initial Heads

the pattern of computed discharge values obtained in run 1, using 1959 initial heads, exhibits no similarity to the pattern of discharges computed in run 2, using 1960 heads, or to the pattern of observed discharge values. Beginning in July, however, the computed discharge values from the two runs appear to begin converging, with only October showing a significant discrepancy. The computed values of discharge for December are nearly equal. Results at John Martin Dam were similar, showing an even more definite pattern of convergence for the two sets of computed discharge values. Comparison of the water table elevation map obtained at the end of run 1 with the map obtained in run 2 indicated differences of less than 0.5 feet at most locations, whereas differences of as much as 4 feet existed between the initial water table maps used in the two runs.

The conclusion drawn from these observations is that the effect of initial head values on results for heads obtained by the model diminishes with time. This implies that small errors in the array of initial head values probably have little or no effect on results obtained after several years. A more detailed analysis would be required to determine the number of time steps needed for the effects of an error of given magnitude and at some given location in this model to become negligible.

Initial Discharges at Lamar. Runs two years in length with 30 day time increments were made to determine the effect on results of variations in the values of monthly discharge at Lamar for the first three months of the run. Values of monthly discharge at Lamar for January, February, and March of 1959 had to be estimated because data were not available. The procedure for estimating these values, which were used as input to the model for the eight-year run, was described in Chapter IV. Two runs were made using initial data from 1959 and boundary conditions from 1959 and 1960. Run 1 was made using the estimated mean monthly discharge values as Lamar for the first three months of 1959. These values were 120 cubic feet per second for January, 82 cubic feet per second for February, and 46 cubic feet per second for March. Run 2 was made using a value of 200 cubic feet per second as the mean monthly discharge for January, February, and March 1959. Resulting values of mean monthly discharge were plotted along with observed values for both John Martin Dam and Coolidge.

The plot of computed and observed mean monthly discharge values at John Martin Dam is shown in Fig. 5-11. After the first three months of the run, values of computed discharge at John Martin Dam appear to converge almost immediately. After October 1959 values computed by run 1 are indistinguishable from those computed by run 2. Results at Coolidge showed a slower convergence of computed discharge values. Discharge values computed by run 1 agreed closely with values computed by run 2 after June 1960. The greater susceptibility of computed values of discharge at Coolidge to inaccurate seepage rates computed in the Lamar area is believed to account for the slower convergence of computed discharge values. In run 2, the initially high values of discharge at Lamar apparently resulted in the overestimation of seepage rates from the river into the aquifer, which in turn raised the water table in the Lamar area. Downstream propagation of this slightly elevated water table was accompanied by higher than actual seepage rates into the river, or lower than actual seepage rates from the river. This resulted in overestimated discharge values at Coolidge for several months after the intentional overestimation of discharge at Lamar ceased. A comparison of the water table map obtained in run 2 with the map obtained in run 1 indicated that water table elevations from Lamar to Coolidge were as much as one foot higher than those obtained in run 1. This result serves as another indication of the overestimated seepage rates caused by the high values of initial discharge at Lamar.

It is concluded from the foregoing results that variations in values of monthly discharge at Lamar have virtually no residual effects on computed discharge values upstream at John Martin Dam. However, significant differences between computed discharge values at Coolidge from run 1 and from run 2 persisted for several months after March 1959. Similar residual effects were observed in the water table downgradient from Lamar. However, the tendency of discharges at Coolidge computed in run 2 to approach the values of discharge computed in run 1 after June 1960 indicates that the residual effects of variations in discharge at Lamar diminish with time. The implication of this conclusion is that erroneous values of the estimated discharge at Lamar would not adversely affect results obtained by the model after several years. A more detailed analysis would be required to determine the time lapse required before the effects of an error of given magnitude in the mean monthly discharge at Lamar would become negligible.

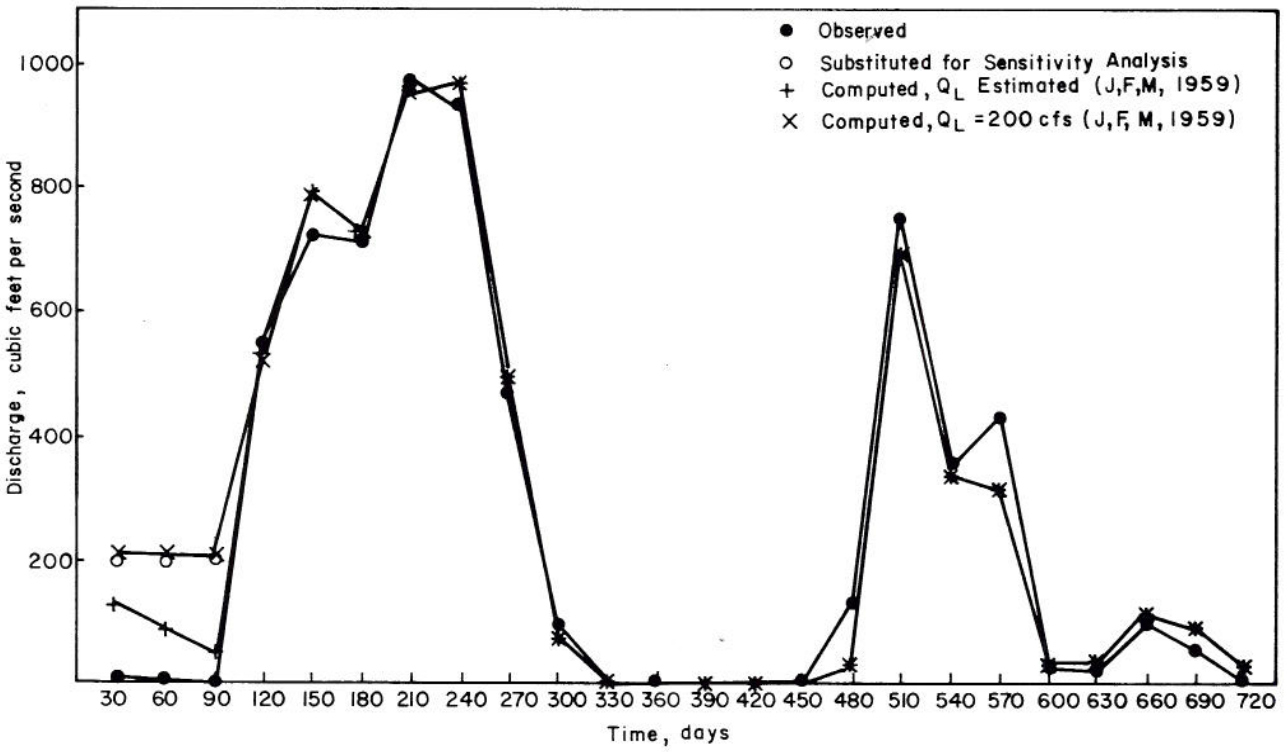

Fig. 5-11 Comparison of Computed and Observed Discharge Values below John Martin Dam for Sensitivity of Results to Variation of Discharge of Lamar

CHAPTER VI
CONCLUSIONS AND RECOMMENDATIONS

Conclusions

A finite difference model for simulating three-dimensional, saturated, and unsaturated, steady and unsteady flow in a stream-aquifer system was developed. This model was designed for use in this study to interact with a finite difference algorithm for simulating two-dimensional flow of groundwater under fully saturated conditions. The resulting combined model was then used to simulate flow in hypothetical and actual stream-aquifer systems, and its ability to produce accurate results was analyzed. As a result of this study the following conclusions were drawn.

1. The model was successful in simulating flow in several simplified, hypothetical systems, as was determined by a qualitative analysis of results produced by the model. The hypothetical stream-aquifer systems which were modeled had the following configurations: (1) horizontal initial water table and uniform saturated thickness; (2) initial water table of uniform gradient in the direction parallel to the river, and aquifer of uniform saturated thickness; (3) initial water table of uniform gradient parallel to the river, nonuniform slope perpendicular to the river, and aquifer of nonuniform saturated thickness. The water table in the third configuration sloped toward the river from both sides and the saturated thickness increased toward the river from either side. Results of runs made with and without the pumping of a well in each of the three systems indicated that the model was capable of producing a physically reasonable simulation of flow for each case.

2. The ability of the model to correctly simulate flow in an actual stream-aquifer system was demonstrated. This conclusion was based on the success of the model in reproducing, with reasonable accuracy, observed values of monthly discharge at two stream gaging stations in the Arkansas Valley study area, and matching observed water table elevations in the area within reasonable limits of error. The simulation included the consideration of the combined effects of a flow-retarding silt layer on the bed and banks of the river channel, and high volume pumping near the river in the vicinity of Lamar. The model correctly simulated the resulting break in the hydraulic connection between the river and the aquifer over a two mile reach influenced by the drawdown in the well field.

3. Water table elevations and river discharge values obtained by this model were shown to have varying degrees of sensitivity to changes in the values of several parameters. Significant effects on these results were obtained by changing values of the silt layer bubbling pressure head, h_{pb}, the silt layer hydraulic conductivity, K_s, the array of values of relative permeability, k_r, the array of values of saturation derivative, dS/dH, and the array of values of surface flux, Q_s. The effect on results obtained by changing the value of porosity, ϕ, was not considered significant. Varying the initial values of head, H, throughout the model and mean monthly discharge, Q, at Lamar produced significant effects on the character of results obtained. These effects, however diminished with time.

Recommendations for Further Study

The following recommendations are made for further investigation in connection with the finite difference model developed in this study.

1. The possiblity of more sophisticated and more detailed representation of flow above the water table should be explored. The use of a larger number of thinner model grids was previously suggested as a means of accomplishing part of this objective. Because of the large amount of computer time and storage this would require, however, it is suggested that alternate methods should be considered.

2. A subroutine for representing overland flow due to rainfall excess, flow in minor tributaries, and unsteady, nonuniform river flow should be added to the model if the intended application includes simulation of flood flows. This need is demonstrated by the failure of the model to correctly simulate the June 1965 flows in the Arkansas Valley study area.

3. Efforts should be made to obtain more comprehensive data for future applications of this model, so that the use of a number of assumptions and estimates which were made to obtain values for input parameters in this study could be eliminated. Because of the considerable effects of surface flux values on model results, special attention should be directed to obtaining information concerning type and areal distribution of crops grown in the area of interest, and distribution in time and space of water diverted from the river for irrigation.

Recommended Uses of the Model

The three-dimensional, finite difference model developed in this study for simulating complex flows in a stream-aquifer system may be used singly or in combination with two-dimensional finite difference models. The model interfaced on both ends with the two-dimensional model segments for its use in this study.

Used singly, the model provides an effective means of analyzing complex flows in small basins, on the order of 100 square miles or less. The following uses are proposed for this form of the model: (1) use by water regulatory agencies as an aid in settling water rights disputes among users of groundwater and surface water in a given basin, (2) use as an aid in making water resource management decisions which are most beneficial to the maximum number of users and to the environment, (3) use as an aid in determining the feasibility and probable benefits of proposed water resource development projects, by mathematically simulating the results of such projects prior to implementation.

Used in combination with a large two-dimensional model, the three-dimensional model provides a detailed analysis of a limited portion of a large stream-aquifer system. With this combination of models it is possible to obtain a localized detailed flow analysis where it is needed without consuming large amounts of computer time and storage in an unnecessarily detailed simulation of areas which are not of major concern, or in which the flow can be accurately simulated using less sophisticated methods.

The various components of this model have been set up as separate subroutines so that a given component can be easily modified, replaced, or in some cases deleted without disturbing any other part of the computer program. For this reason the model is readily adaptable for use in analyzing flow in several types of groundwater-surface water systems other than a stream-aquifer system. The following recommendations are made for the use of this model in analyzing flow in these systems.

1. With no modification necessary other than setting up the appropriate geometry for a given case the model may be used to simulate the interaction between earth canals and the adjacent aquifer. Because of its capability of simulating three-dimensional flow, the model is particularly useful in the analysis of seepage loss problems, in which vertical flows are important.

2. The model may be used to analyze flow in drainage channels, and is particularly useful as a design tool, in determining the most efficient channel geometry for obtaining optimal drainage conditions. No modification of the model is necessary for this application except setting up the appropriate geometry for the particular case.

3. The model may be used to analyze flows in recharge pits, and is especially useful as design tool for determining efficient geometry, as was the case for drainage channels. The capability of the model to simulate three-dimensional flow is advantageous in this application, because vertical flow downward from recharge pits is often important. A suggested adaptation of the model for this application is a replacement of the subroutine for computing surface water elevations by the Manning formula. This subroutine is used in the model in its present form to determine depth of flow in the river. No adaptation of the model is necessary for the correct representation of the recharge pit boundaries, in which no silt layer is present. By assigning the silt layer hydraulic conductivity a value equal to the hydraulic conductivity of the surrounding aquifer material, and the silt layer bubbling pressure head a value of zero, the flow retarding effects of the layer are neutralized. The model then simulates flow across the boundary as if no silt layer were present. For this application the use of the three-dimensional model segment alone is recommended.

4. With only an adaptation of the model subroutine for determining surface water elevation, the model can be used to simulate the interaction between a lake or reservoir and the surrounding aquifer. This model is especially useful in determining the change in storage of a reservoir-aquifer system due to a given change in water surface elevation in the reservoir. Such information is useful in determining optimal reservoir management policies. The three-dimensional model segment, used alone, should provide an adequate representation of flow in a reservoir-aquifer system.

BIBLIOGRAPHY

Bittinger, M.W. and Stringham, G.E., "A Study of Phreatophyte Growth in the Lower Arkansas River Valley of Colorado," Civil Engineering Section, Colorado State University, Fort Collins, Colorado, April 1963.

Breitenbach, E.A., Thurnau, D.H., and van Poollen, H.K., "The Fluid Flow Simulation Equations," Society of Petroleum Engineers of AIME, Preprint SPE 2020, Dallas Meeting, April 1968.

Brooks, R.H. and Corey, A.T., "Hydraulic Properties of Porous Media," Hydrology Paper No. 3, Colorado State University, March 1965.

Corey, A.T., "Flow in Porous Media," Class Notes for AE 728 and AE 730, Colorado State University Agricultural Engineering Department, Fort Collins, Colorado, 1969.

Hurr, T.R., Seminar on Seepage in the Lower Arkansas Valley of Colorado, Colorado School of Mines, 1970.

Hurr, T.R., "Modeling Steady-State and Transient Confined and Unconfined Groundwater Flow by the Finite Element Method," Engineering Report, Colorado School of Mines, May 1971.

Hurr, T.R. and Moore, J.E., "Hydrogeologic Characteristics of the Valley-Fill Aquifer in the Arkansas Valley, Bent County, Colorado," Hydrologic Investigations Atlas HA-461, United States Geological Survey, Washington, D.C., 1972.

Hurr, T.R. and Moore, J.E., "Hydrogeologic Characteristics of the Valley-Fill Aquifer in the Arkansas Valley, Prowers County, Colorado," Hydrologic Investigations Atlas (in preparation), United States Geological Survey, Washington, D.C.

Matlock, W.G., "The Effect of Silt-Laden Water on Infiltration in Alluvial Channels," Ph.D. Dissertation, University of Arizona, Department of Civil Engineering, 1965.

McWhorter, D.B., "Infiltration Affected by Flow of Air," Ph.D. Dissertation, Colorado State University, March 1971.

Moore, J.E. and Jenkins, C.T., "An Evaluation of the Effect of Groundwater Pumpage on the Infiltration Rate of a Semipervious Streambed," Water Resources Research, Vol. 2, No. 4, 1966.

Reddell, D.L. and Sunada, D.K., "Numerical Simulation of Dispersion in Groundwater Aquifers," Hydrology Paper No. 41, Colorado State University, 1970.

Skinner, M.M., "Water Utilization Study Project No. Colorado P-30/Arkansas Valley Region," Colorado State University, April 1965.

Thurnau, D.H., "Algorithm 195, Bandsolve," Communications of the Association for Computing Machinery, Vol. 6, No. 8, 1963.

United States Department of Agriculture, "Irrigation Water Requirements," Technical Release No. 21, April 1967 (Revised September 1970).

United States Department of Commerce, "Climatological Data, Colorado," Vols. 63-71, Weather Bureau, Asheville, 1958-1966.

United States Department of the Interior, "Surface Water Supply of the United States, 1958, Part 7. Lower Mississippi River Basin," Geological Survey Water-Supply Paper 1561, U.S. Government Printing Office, Washington, 1960.

United States Department of the Interior, "Surface Water Supply of the United States, 1959, Part 7. Lower Mississippi River Basin," Geological Survey Water-Supply Paper 1631, U.S. Government Printing Office, Washington, 1960.

United States Department of the Interior, "Surface Water Supply of the United States, 1960, Part 7. Lower Mississippi River Basin," Geological Survey Water-Supply Paper 1711, U.S. Government Printing Office, Washington, 1962.

United States Department of the Interior, "Surface Water Records of Colorado," U.S. Geological Survey, 1961-1964.

United States Department of the Interior, "Water Resources Data for Colorado, Part 1. Surface Water Records," Geological Survey, 1965-1966.

Voegeli, P.T. and Hershey, L.A., "Geology and Groundwater Resources of Prowers County, Colorado," Geological Survey Water-Supply Paper 1772, United States Government Printing Office, Washington D.C., 1965.

Walton, W.C., Groundwater Resource Evaluation, McGraw-Hill, New York, 1970.

APPENDIX A: DESCRIPTION AND LISTING OF COMPUTER PROGRAM

Description of Program and Subroutines

PROGRAM LINKFLO is the control program which directs the sequence of operations for solving the system of equations for flow in the stream-aquifer system. Appropriate subroutines are called from LINKFLO as needed for calculating the various components of flow, for adjusting boundary conditions, and for reading data. The time increment-loop is controlled by LINKFLO.

SUBROUTINE INITIAL reads in and prints out initial data, sets up the grid system for the groundwater flow equation, and establishes river channel geometry and canal distribution regions.

SUBROUTINE BCON reads in boundary conditions at the beginning of each time increment and computes discharge and head in each river grid, and surface inflow for every surface grid.

SUBROUTINE SCRIBE prints out intermediate and final results, including river discharges and water table elevations.

SUBROUTINE MATROP arranges two-dimensional and three-dimensional arrays in a standard form for printout.

SUBROUTINE MATSOL sets up the coefficient matrix and the right hand side column vector for solving the groundwater flow equations.

SUBROUTINE SIDE is called from MATSOL to compute coefficients and column vector values for those grids in the two-dimensional model segment that are surrounded on all sides by other two-dimensional grids.

SUBROUTINE STRAN is called from MATSOL to compute coefficients and column vector values for grids in the two-dimensional model segment that are adjacent on one side to a column of grids in the three-dimensional model segment.

SUBROUTINE CTRAN is called from MATSOL to compute coefficients and column vector values for grids in the three-dimensional model segment that are adjacent on one side to a grid in the two-dimensional model segment.

SUBROUTINE CENTER is called from MATSOL to compute coefficients and column vector values for grids in the three-dimensional model segment that are surrounded laterally by other three-dimensional grids.

SUBROUTINE BSOLVE is called from MATSOL to solve the matrix for new values of head in each groundwater grid using the Gauss-Elimination technique.

SUBROUTINE RIVBND computes seepage rates to and from the aquifer for each river grid of the model.

SUBROUTINE SPLIT is called from RIVBND to compute seepage rates in the river grids located in the three-dimensional model segment.

SUBROUTINE STORE computes the mass balance for the aquifer in all interior grids of the model at the end of each time increment.

SUBROUTINE ADJUST computes values for unsaturated hydraulic conductivity and derivative of saturation with respect to head for every grid in the three-dimensional model segment at the beginning of each time increment.

SUBROUTINE KFNP is called from CTRAN to compute values of unsaturated hydraulic conductivity above the water table for two-dimensional grids.

Table B-1 Initial Water Table Elevations in Feet, Upstream Segment

i \ j	1	2	3	4	5	6	7	8
1	3741	3736	3745	3765	3580	3790	3800	3815
2	3728	3727	3735	3763	3775	3781	3795	3812
3	3717	3719	3735	3760	3770	3772	3785	3810
4	3705	3705	3715	3740	3745	3750	3760	3795
5	3696	3695	3694	3720	3725	3730	3740	3775
6	3691	3686	3685	3701	3705	3710	3720	3760
7	3681	3674	3673	3680	3685	3690	3700	3745
8	3670	3665	3662	3660	3660	3665	3681	3721
9	3660	3650	3648	3649	3649	3655	3665	3680
10	3650	3641	3639	3637	3632	3635	3651	3680
11	3640	3633	3632	3629	3629	3628	3641	3681
12	3632	3629	3625	3624	3624	3625	3640	3660

Table B-2 Initial Heads in Feet, Center Segment

i \ j	1	2	3	4	5	6	7	8
1	3625	3620	3615	3616	3617	3618	3630	3655
2	3618	3612	3606	3608	3610	3611	3619	3656
3	3611	3605	3600	3603	3606	3608	3621	3651
4	3608	3602	3598	3600	3603	3607	3614	3630
5	3613	3600	3597	3599	3600	3604	3610	3625
6	3621	3598	3594	3595	3596	3600	3611	3621
7	3601	3595	3590	3589	3590	3592	3601	3621
8	3594	3588	3586	3588	3589	3588	3592	3616

Table B-3 Initial Water Table Elevations in Feet, Downstream Segment

i \ j	1	2	3	4	5	6	7	8
1	3600	3582	3581	3583	3583	3584	3589	3610
2	3590	3581	3574	3577	3577	3577	3580	3601
3	3580	3571	3564	3563	3565	3567	3575	3595
4	3570	3555	3554	3553	3555	3558	3570	3595
5	3560	3541	3542	3543	3544	3544	3550	3556
6	3541	3534	3534	3535	3537	3538	3541	3547
7	3525	3527	3525	3527	3529	3530	3532	3538
8	3517	3515	3513	3511	3511	3513	3518	3520
9	3506	3502	3500	3497	3496	3495	3502	3530
10	3489	3488	3484	3483	3483	3482	3500	3570
11	3477	3474	3477	3477	3478	3479	3485	3500
12	3453	3451	3454	3457	3460	3461	3475	3485
13	3438	3436	3437	3440	3442	3444	3450	3465
14	3426	3426	3428	3430	3432	3436	3435	3445
15	3417	3418	3419	3421	3423	3425	3428	3430
16	3405	3407	3408	3407	3408	3408	3410	3415
17	3393	3395	3394	3394	3395	3396	3398	3405
18	3383	3384	3382	3383	3383	3384	3387	3400
19	3368	3371	3372	3372	3371	3372	3373	3380
20	3354	3357	3358	3360	3360	3360	3360	3365
21	3345	3347	3348	3349	3350	3352	3355	3360
22	3336	3337	3338	3338	3340	3344	3350	3355

Table B-4 Bedrock Elevations in Feet, Upstream Segment

i \ j	1	2	3	4	5	6	7	8
1	3740	3710	3730	3750	3755	3760	3770	3790
2	3715	3700	3720	3762	3774	3780	3794	3811
3	3703	3680	3720	3750	3755	3760	3780	3800
4	3680	3670	3714	3739	3744	3749	3759	3794
5	3685	3660	3680	3719	3724	3729	3739	3774
6	3690	3670	3655	3700	3704	3709	3719	3759
7	3680	3655	3645	3679	3684	3689	3699	3744
8	3660	3636	3620	3630	3645	3655	3680	3720
9	3630	3610	3610	3632	3634	3645	3650	3660
10	3645	3610	3590	3600	3610	3520	3645	3675
11	3630	3611	3597	3686	3600	3620	3635	3670
12	3630	3704	3592	3580	3590	3600	3625	3640

Table B-5 Grid Center Elevations in Feet, Center Segment

Level 1

i \ j	1	2	3	4	5	6	7	8
1	3575	3572	3570	3570	3570	3570	3580	3605
2	3570	3565	3564	3563	3563	3563	3580	3610
3	3565	3563	3561	3560	3560	3560	3580	3605
4	3565	3560	3557	3557	3557	3557	3573	3595
5	3565	3557	3555	3555	3555	3555	3565	3585
6	3565	3553	3552	3552	3552	3552	3560	3575
7	3555	3548	3548	3548	3548	3548	3555	3570
8	3550	3545	3541	3540	3540	3540	3550	3565

Level 2

i \ j	1	2	3	4	5	6	7	8
1	3600	3597	3595	3595	3595	3595	3605	3630
2	3595	3590	3589	3588	3588	3588	3605	3635
3	3590	3588	3586	3585	3585	3585	3605	3630
4	3590	3585	3582	3582	3582	3582	3598	3620
5	3590	3582	3580	3580	3580	3580	3590	3610
6	3590	3578	3577	3577	3577	3577	3585	3600
7	3580	3573	3573	3573	3573	3573	3580	3595
8	3575	3570	3566	3565	3565	3565	3575	3590

Level 3

i \ j	1	2	3	4	5	6	7	8
1	3615	3612	3610	3610	3610	3610	3620	3645
2	3610	3605	3604	3603	3603	3603	3620	3650
3	3605	3603	3601	3600	3600	3600	3620	3645
4	3605	3600	3597	3597	3597	3597	3613	3635
5	3605	3597	3595	3595	3595	3595	3605	3625
6	3605	3593	3592	3592	3592	3592	3600	3615
7	3595	3588	3588	3588	3588	3588	3595	3610
8	3590	3585	3581	3580	3580	3580	3590	3605

Level 4

i \ j	1	2	3	4	5	6	7	8
1	3625	3622	3620	3620	3620	3620	3630	3655
2	3620	3615	3614	3613	3613	3613	3630	3660
3	3615	3613	3611	3610	3610	3610	3630	3655
4	3615	3610	3607	3607	3607	3607	3623	3645
5	3615	3607	3605	3605	3605	3605	3615	3635
6	3615	3603	3602	3602	3602	3602	3610	3625
7	3605	3598	3598	3598	3598	3598	3605	3620
8	3600	3595	3591	3590	3590	3590	3600	3615

Table B-6 Bedrock Elevations in Feet, Downstream Segment

i \ j	1	2	3	4	5	6	7	8
1	3599	3585	3565	3540	3520	3518	3570	3600
2	3589	3580	3560	3525	3515	3530	3560	3600
3	3579	3570	3520	3525	3530	3530	3570	3590
4	3569	3540	3490	3520	3530	3540	3555	3550
5	3559	3535	3480	3500	3505	3510	3520	3550
6	3540	3510	3480	3505	3510	3515	3525	3520
7	3515	3490	3465	3475	3475	3480	3500	3515
8	3490	3460	3455	3450	3460	3470	3500	3500
9	3495	3460	3440	3435	3445	3475	3510	3500
10	3480	3460	3420	3440	3450	3460	3450	3500
11	3455	3435	3410	3420	3430	3440	3470	3490
12	3450	3415	3380	3405	3420	3440	3450	3484
13	3410	3390	3360	3370	3400	3410	3420	3450
14	3420	3395	3365	3375	3405	3425	3430	3430
15	3410	3370	3320	3355	3375	3390	3410	3400
16	3340	3240	3280	3330	3370	3375	3365	3280
17	3260	3190	3280	3350	3355	3345	3370	3300
18	3260	3160	3280	3315	3325	3340	3350	3360
19	3180	3210	3270	3310	3320	3325	3350	3379
20	3280	3300	3320	3290	3300	3310	3330	3364
21	3330	3320	3300	3280	3280	3275	3305	3340
22	3330	3315	3300	3300	3300	3280	3305	3340

Table B-7 Hydraulic Conductivities in Feet Per Day, Upstream Segment

i \ j	1	2	3	4	5	6	7	8
1	0	360	445	357	214	178	223	214
2	360	396	178	0	0	0	0	0
3	481	410	267	267	178	223	535	267
4	535	382	0	0	0	0	0	0
5	365	611	191	0	0	0	0	0
6	0	1087	490	0	0	0	0	0
7	0	845	286	0	0	0	0	0
8	668	618	528	544	802	1070	920	344
9	401	480	528	786	758	1003	869	535
10	0	557	436	440	525	624	668	0
11	267	535	627	401	445	936	668	0
12	401	487	501	368	369	350	401	334

Table B-8 Hydraulic Conductivities in Feet Per Day, Center Segment

i \ j	1	2	3	4	5	6	7	8
1	267	520	586	270	167	184	107	67
2	201	771	1560	401	239	257	134	0
3	334	786	1470	342	273	334	802	67
4	753	826	1096	409	219	271	389	60
5	1337	1470	880	357	300	525	286	60
6	0	936	643	400	400	835	0	0
7	0	668	675	550	500	500	0	0
8	100	511	800	750	600	575	445	1070

Table B-9 Hydraulic Conductivities in Feet Per Day, Downstream Segment

i \ j	1	2	3	4	5	6	7	8
1	0	0	965	848	668	636	892	936
2	0	0	1337	683	623	578	612	1003
3	0	0	303	739	574	452	1337	445
4	0	743	564	810	807	928	972	445
5	0	1241	608	532	515	516	491	802
6	0	574	487	668	668	732	551	311
7	119	747	403	426	488	557	574	557
8	461	555	516	445	481	497	735	167
9	822	571	491	360	341	257	0	84
10	334	691	473	622	689	642	36	0
11	535	668	467	468	468	535	624	267
12	160	418	492	445	501	786	297	0
13	102	341	334	659	636	520	311	201
14	802	496	507	610	743	481	0	0
15	1226	535	378	365	426	418	257	0
16	229	356	443	616	786	579	372	229
17	295	289	567	1047	936	535	963	334
18	275	294	631	630	469	477	382	361
19	285	400	545	624	545	456	608	0
20	364	405	489	286	378	393	418	0
21	557	325	227	176	194	217	297	100
22	557	325	227	176	194	217	297	100

Table B-10 Mean Monthly Discharge below John Martin Dam, at Lamar, and at Coolidge, in Cubic Feet Per Second

Station	Month											
	Jan	Feb	Mar	Apr	May	Jun	Jul	Aug	Sep	Oct	Nov	Dec
1958												
John Martin Dam	7.7	5.9	5.8	39.5	115	401	529	896	805	520	9.6	6.8
Lamar	6.9	5.3	5.2	7.1	11.6	40	53	234	227	64	8.2	6.0
Coolidge	123	138	129	114	378	219	340	310	327	276	163	157
1959												
John Martin Dam	8.6	7.5	6.6	545	708	712	976	924	471	96.8	3.5	2.9
Lamar	120	82	46	147	261	199	381	379	237	27.6	26.6	16.2
Coolidge	142	144	140	198	367	266	374	470	423	246	177	159
1960												
John Martin Dam	2.8	3.4	3.5	136	844	358	422	22.6	33.8	98.1	56.8	2.8
Lamar	12.5	20.4	69.2	93.2	342	16.4	65.9	11.4	4.4	10.9	3.8	4.3
Coolidge	135	178	331	206	406	209	107	3.3	0.9	30.4	60.6	76.3
1961												
John Martin Dam	3.0	3.6	3.2	455	111	223	359	442	401	379	9.9	4.1
Lamar	3.8	4.2	20.8	188	8.1	107	72.7	63.7	7.4	21.2	45.4	52.1
Coolidge	103	114	106	198	35.1	346	138	142	70.4	199	149	137
1962												
John Martin Dam	3.4	3.8	4.1	627	438	426	572	267	41.7	69.8	47.8	3.3
Lamar	36.8	47.8	28.4	274	58.6	76.6	172	72.4	4.6	4.8	8.7	9.0
Coolidge	116	146	127	261	302	305	188	111	18.8	18.1	55.2	111
1963												
John Martin Dam	3.6	3.4	10.5	407	126	137	86.1	277	316	37.5	39.4	9.9
Lamar	21.4	45.1	25.9	175	6.4	20.8	47.7	30.7	61.8	4.8	2.2	2.3
Coolidge	92.1	160	119	175	6.6	98.9	59.5	14.4	63.2	19.0	29.2	34.7
1964												
John Martin Dam	2.9	2.5	2.9	185	128	235	133	167	47.9	31.6	27.0	14.1
Lamar	2.3	5.7	2.6	78.5	171	99.2	10.2	18.1	7.0	6.9	2.3	2.3
Coolidge	51.9	61.2	47.1	64.2	543	242	26.9	1.9	1.1	3.3	17.5	20.3
1965												
John Martin Dam	1.7	14.2	15.6	127	254	272	858	2127	857	144	217	281
Lamar	0.5	0.7	1.1	43.1	88.0	1359	480	1547	689	8.7	71.5	158
Coolidge	20.2	27.3	29.0	18.9	59.7	8221	741	1979	1079	200	229	270

Table B-11 Monthly Diversions to Major Canals and Inflows from Big Sandy Creek, in Acre-Feet

Canal or Tributary	Month											
	Jan	Feb	Mar	Apr	May	Jun	Jul	Aug	Sep	Oct	Nov	Dec
1958												
Fort Bent Canal	0	0	0	0	900	3000	4000	5400	4800	2700	0	0
Keesee Canal	0	0	0	0	100	500	1100	1200	800	600	0	0
Amity Canal	0	0	0	800	1900	15200	20800	24100	19800	17500	400	0
Lamar Canal	800	600	0	700	2800	4000	6200	9100	7500	4800	2200	1000
Hyde Canal	0	0	0	0	100	300	400	400	300	300	100	0
Manvel Canal	0	0	0	0	300	0	500	800	800	500	200	0
X-Y, Graham Canal	0	0	0	0	400	400	1900	1900	1600	1100	500	0
Buffalo Canal	1100	400	0	0	900	1900	1800	3200	2700	2300	1500	100
Sisson Canal	0	0	0	0	0	0	0	500	100	0	0	0
Big Sandy Creek	2028	2514	2287	2248	1207	660	832	537	974	967	3869	3857
1959												
Fort Bent Canal	0	0	0	1900	3500	4300	5300	4700	2200	500	0	0
Keesee Canal	0	0	0	300	900	600	1000	1000	600	0	0	0
Amity Canal	0	0	0	14900	18000	18100	22200	22200	9900	3900	0	0
Lamar Canal	0	0	0	5400	8200	8500	9700	8300	5500	1500	800	500
Hyde Canal	0	0	0	300	500	600	600	500	300	0	0	0
Manvel Canal	0	0	0	600	1500	900	1300	1400	700	0	0	0
X-Y, Graham Canal	0	0	0	900	2700	2400	3100	3000	1800	0	0	0
Buffalo Canal	0	0	0	1000	3000	2900	3100	3000	2200	300	0	0
Sisson Canal	0	0	0	0	0	0	0	0	0	0	0	0
Big Sandy Creek	3160	3917	3564	3503	1881	1029	1296	836	1518	380	1521	1516
1960												
Fort Bent Canal	0	0	0	300	3100	1700	3000	500	400	1000	200	0
Keesee Canal	0	0	0	100	500	200	700	600	400	0	0	0
Amity Canal	0	0	0	1400	21000	14900	14500	600	400	3100	3300	0
Lamar Canal	400	0	0	800	6100	5000	5400	1300	800	1400	900	900
Hyde Canal	0	0	0	100	500	400	300	100	100	200	100	0
Manvel Canal	0	0	0	0	900	0	100	0	0	0	0	0
X-Y, Graham Canal	0	0	0	200	1600	1300	1300	100	0	0	0	0
Buffalo Canal	0	0	0	1000	2200	1900	2100	1500	1000	1500	1400	1000
Sisson Canal	0	0	0	0	100	400	200	0	0	0	0	0
Big Sandy Creek	1242	1540	1401	1377	739	404	510	329	596	423	1694	1989
1961												
Fort Bent Canal	0	0	0	2300	1600	1200	2800	2200	2700	1200	600	0
Keesee Canal	0	0	0	100	600	200	300	700	500	300	0	0
Amity Canal	0	0	0	10400	2400	6000	14500	15900	16400	17500	500	0
Lamar Canal	500	400	100	2700	2300	2700	6200	5600	5500	4400	1900	900
Hyde Canal	0	0	0	200	200	300	400	300	200	200	200	0
Manvel Canal	0	0	0	300	100	400	300	0	0	0	0	0
X-Y, Graham Canal	0	0	0	900	600	300	1300	900	800	1300	100	0
Buffalo Canal	600	0	100	2600	2200	2200	3000	3000	1800	1300	1200	600
Sisson Canal	0	0	0	0	200	100	200	0	0	0	0	0
Big Sandy Creek	1383	1715	1560	1534	824	451	568	366	664	548	2195	2188
1962												
Fort Bent Canal	0	0	0	2600	2500	2200	3300	2300	1500	1200	900	0
Keesee Canal	0	0	0	300	900	600	900	800	600	700	200	0
Amity Canal	0	0	0	12400	16100	16400	19300	6600	0	400	900	0
Lamar Canal	0	0	0	5400	5300	5800	9100	5400	1100	1300	1800	1600
Hyde Canal	0	0	0	100	300	400	400	200	100	100	100	0
Manvel Canal	0	0	0	400	100	100	800	200	0	0	0	0
X-Y, Graham Canal	0	0	0	500	1000	1600	1900	800	500	700	700	500
Buffalo Canal	0	0	0	1700	2800	3100	3300	2200	1600	1000	800	600
Sisson Canal	0	0	0	0	0	0	0	0	0	0	100	300
Big Sandy Creek	1792	2222	2021	1987	1067	584	735	474	861	293	1174	1171

Table B-11 Continued

Canal or Tributary	Month											
	Jan	Feb	Mar	Apr	May	Jun	Jul	Aug	Sep	Oct	Nov	Dec
1963												
Fort Bent Canal	0	0	300	2300	900	1500	900	1900	2500	700	960	180
Keesee Canal	0	0	100	700	700	600	700	700	600	500	460	60
Amity Canal	0	0	0	7200	3100	2500	2200	7800	7500	0	0	0
Lamar Canal	0	100	100	3300	2100	3500	1400	3900	3900	900	760	520
Hyde Canal	0	0	0	200	200	200	100	200	200	100	120	100
Manvel Canal	0	0	0	100	0	100	0	100	0	0	0	0
X-Y, Graham Canal	0	0	0	1000	0	300	100	600	500	200	310	370
Buffalo Canal	0	0	1000	2900	2300	2000	1600	2600	2100	1600	980	680
Sisson Canal	100	0	0	200	300	100	0	0	0	200	160	0
Big Sandy Creek	959	1189	1082	1063	571	312	393	254	461	192	770	768
1964												
Fort Bent Canal	0	0	0	1270	520	1390	780	1030	0	0	210	130
Keesee Canal	0	0	0	640	730	230	650	630	710	550	410	0
Amity Canal	0	0	0	3360	2380	4500	2150	3020	0	0	0	0
Lamar Canal	400	210	490	1830	2470	2390	3780	2310	860	680	840	610
Hyde Canal	80	60	120	20	0	0	0	0	0	0	0	0
Manvel Canal	0	0	0	0	0	0	0	0	0	0	0	0
X-Y, Graham Canal	260	0	0	0	0	370	80	230	0	0	0	0
Buffalo Canal	430	390	750	2060	1380	2300	2820	2050	1160	600	850	850
Sisson Canal	0	0	0	270	170	180	180	60	0	0	0	0
Big Sandy Creek	629	780	709	697	374	205	258	166	302	909	3638	3627
1965												
Fort Bent Canal	0	0	0	530	1370	890	1480	3480	2090	410	210	0
Keesee Canal	0	0	270	820	860	330	390	790	550	0	0	0
Amity Canal	0	0	0	1500	6160	8960	18370	27670	13860	14040	10710	10880
Lamar Canal	330	490	420	1340	4680	2610	3510	5780	3410	2650	2320	2890
Hyde Canal	0	0	0	110	180	210	70	670	500	370	280	0
Manvel Canal	0	0	0	0	0	0	0	0	0	0	0	0
X-Y, Graham Canal	0	0	0	0	360	530	0	0	0	0	0	0
Buffalo Canal	0	0	0	2040	2940	1680	790	3080	1570	360	0	0
Sisson Canal	0	0	0	0	10	150	0	0	0	0	0	0
Big Sandy Creek	2971	3684	3551	3294	1769	968	1219	786	1427	1130	4524	4510

Table B-12 Parameters Defining Channel Geometry in Each River Grid of Model

River Grid	Channel Width, Feet	Channel Bed Elevation, Feet	Channel Bed Slope, Feet/Feet
1	115	3737	0.001033
2	144	3727	0.001225
3	144	3717	0.001065
4	115	3705	0.001112
5	144	3694	0.001125
6	173	3684	0.001065
7	144	3672	0.001291
8	58	3661	0.001488
9	86	3648	0.001420
10	85	3636	0.000985
11	85	3627	0.001052
12	85	3624	0.001136
13	85	3617	0.002156
14	85	3609	0.001452
15	85	3605	0.001205
16	43	3602	0.001488
17	64	3600	0.001263
18	85	3596	0.001049
19	85	3590	0.001077
20	85	3588	0.001296
21	85	3582	0.001291
22	68	3570	0.001114
23	79	3563	0.000947
24	113	3554	0.000968
25	113	3543	0.001285
26	90	3534	0.001136
27	113	3525	0.001291
28	90	3509	0.001470
29	101	3499	0.001768
30	113	3484	0.000988
31	124	3470	0.001398
32	145	3456	0.001296
33	145	3444	0.001488
34	242	3433	0.001420
35	242	3422	0.001448
36	242	3408	0.001263
37	217	3399	0.001389
38	169	3385	0.001560
39	145	3373	0.001420
40	145	3360	0.001556
41	145	3349	0.001405
42	133	3338	0.001403

Table B-13 Monthly Precipitation at Lamar, in Inches

Month \ Year	1958	1959	1960	1961	1962	1963	1964	1965
January	.73	.79	1.43	0	.89	.42	0	.36
February	.21	.16	2.07	.84	.11	.14	.75	.49
March	1.75	.29	.50	.90	.34	1.01	.19	1.21
April	.94	.94	1.77	.44	.68	0	1.07	.03
May	3.62	2.25	1.91	.97	2.20	.58	6.97	2.40
June	3.05	2.58	.64	4.27	1.97	1.93	.77	6.60
July	3.84	.87	1.68	3.21	4.36	1.81	.32	1.14
August	.75	2.08	.26	3.22	.64	2.09	.42	2.50
September	.57	1.60	.99	.92	.66	1.18	.96	1.13
October	.04	1.58	1.76	.52	.41	.10	.17	1.82
November	.72	.16	.18	1.18	.54	.29	.36	.05
December	.08	.08	.87	.23	.12	.38	.21	1.75

Table B-14 Estimated Monthly Evapotranspiration for Study Area, in Inches

Month \ Year	1958	1959	1960	1961	1962	1963	1964	1965
January	0	0	0	0	0	0	0	0
February	0	0	0	0	0	0	0	0
March	0	0	0	0	0	0	0	0
April	1.08	1.21	1.51	1.18	1.51	1.60	1.25	1.55
May	3.12	2.88	2.69	2.81	3.25	3.29	3.00	3.00
June	6.37	6.80	6.30	3.61	5.89	7.04	6.19	5.84
July	7.68	8.05	7.95	8.08	7.95	9.54	9.38	8.67
August	6.24	6.25	6.40	5.94	6.24	6.40	5.94	5.63
September	3.18	2.55	3.01	2.47	2.82	3.49	2.86	2.32
October	0	0	0	0	0	0	0	0
November	0	0	0	0	0	0	0	0
December	0	0	0	0	0	0	0	0

Table B-15 Canal Distribution Region Parameters

Canal	Percentage of Distribution Region Lying Inside the Study Area	Area of Portion of Distributed Region Lying Inside the Study Area, Square Miles
Keesee	0.60	0.9
Fort Bent	1.00	2.7
Amity	0.25	16.2
Lamar	0.15	7.3
Hyde	1.00	4.4
Manvel	0.80	3.9
X-Y, Graham	1.00	14.4
Buffalo	1.00	18.6
Sisson	1.00	2.6

PROGRAM LISTING

```
      PROGRAM LINKFLO(INPUT,OUTPUT,TAPE5=INPUT,TAPE6=OUTPUT)
      COMMON LC,M,N,LRL,LRM,LRIV,NADJ,NCAN,HPB,SK,TH,SY,AN,BSC,VT,POR,
     2TIME,TCON,DT,C(384),DXC(8),DY(8),DZ(4),DB(8),IRIV(47),JRIV(47),
     3RBED(47),RWID(47),RSLP(47),QRIV(47),DIV(47),RSO(47),VMS(47),
     4VMB(47),SDRIV(20),FKFAC(20),CDV(9),PCT(9),AREA(9),LCAN(10),
     5QJMD(3),QLAM(3),QKAN(3),CM(384,49),NDL(12,8),NDC(8,8),NDR(22,8),
     6HTEMP(8,8),QIC(8,8),KODC(8,8,4),HCP(8,8,4),ZC(8,8,4),CKC(8,8,4),
     7CKSAT(8,8,4),DSDHP(8,8,4)
      COMMON /A/ LL,DXL(12),KODL(12,8),CKL(12,8),HLP(12,8),ZBL(12,8),
     2QIL(12,8)
      COMMON /B/ LR,DXR(22),KODR(22,8),CKR(22,8),HRP(22,8),ZBR(22,8),
     2QIR(22,8)
C
C  ***********************************************************************
C  THIS IS THE CONTROL PROGRAM WHICH DIRECTS THE SEQUENCE OF OPERATIONS
C  FOR SOLVING THE SYSTEM OF EQUATIONS FOR FLOW IN THE STREAM-AQUIFER
C  SYSTEM.  APPROPRIATE SUBROUTINES ARE CALLED FROM LINKFLO AS NEEDED
C  FOR CALCULATING THE VARIOUS COMPONENTS OF FLOW, FOR ADJUSTING
C  BOUNDARY CONDITIONS, AND FOR READING DATA.  THE TIME INCREMENTING
C  LOOP IS CONTROLLED BY LINKFLO.
C  ***********************************************************************
C
      JUMP=1
      TIME=0.0
      TBEG=0.0
      TEND=2520.0
C     DT=10.0
      DT=30.0
      TW=60.0
      TW=30.0
      NT=84
      TIME=TBEG+DT
      TCON=TBEG+TW
      CALL INITIAL
      DO 7 ITIME=1,NT
      CALL BCON(JUMP)
      CALL ADJUST
      CALL MATSOL
      CALL RIVBND
      CALL STORE
      IF(TIME.LT.TCON) GO TO 6
      CALL SCRIBE
      TCON=TIME+TW
      WRITE(6,107) TIME
  107 FORMAT(10X,*TIME=*,F10.2,5X,*DAYS*,/)
    6 TIME=TIME +DT
    7 CONTINUE
      CALL EXIT
      END
      SUBROUTINE INITIAL
      COMMON LC,M,N,LRL,LRM,LRIV,NADJ,NCAN,HPB,SK,TH,SY,AN,BSC,VT,POR,
     2TIME,TCON,DT,C(384),DXC(8),DY(8),DZ(4),DB(8),IRIV(47),JRIV(47),
     3RBED(47),RWID(47),RSLP(47),QRIV(47),DIV(47),RSO(47),VMS(47),
     4VMB(47),SDRIV(20),FKFAC(20),CDV(9),PCT(9),AREA(9),LCAN(10),
     5QJMD(3),QLAM(3),QKAN(3),CM(384,49),NDL(12,8),NDC(8,8),NDR(22,8),
     6HTEMP(8,8),QIC(8,8),KODC(8,8,4),HCP(8,8,4),ZC(8,8,4),CKC(8,8,4),
     7CKSAT(8,8,4),DSDHP(8,8,4)
      COMMON /A/ LL,DXL(12),KODL(12,8),CKL(12,8),HLP(12,8),ZBL(12,8),
     2QIL(12,8)
      COMMON /B/ LR,DXR(22),KODR(22,8),CKR(22,8),HRP(22,8),ZBR(22,8),
     2QIR(22,8)
C
C  ***********************************************************************
C  SYSTEM FOR THE GROUNDWATER FLOW EQUATION, AND ESTABLISHES RIVER
C  THIS SUBROUTINE READS IN AND PRINTS OUT INITIAL DATA, SETS UP THE GRID
C  CHANNEL GEOMETRY AND CANAL DISTRIBUTION REGIONS.  DATA VALUES ARE READ
C  FROM PUNCHED CARDS.  CARD FORMATS ARE INDICATED IN THIS SUBROUTINE
C  FOR EACH INITIAL PARAMETER.
C  ***********************************************************************
C
      WRITE(6,2)
    2 FORMAT(1H1,50X,*INITIAL DATA*,/)
      READ(5,10)LL,LC,LR,M,N,LRL,LRM,LRIV,NCAN,NADJ
C  LL - NUMBER OF GRIDS IN THE I DIRECTION - UPSTREAM 2-D SEGMENT
C  LC - NUMBER OF GRIDS IN THE I DIRECTION - CENTER SEGMENT
C  LR - NUMBER OF GRIDS IN THE I DIRECTION - DOWNSTREAM 2-D SEGMENT
```

```
C  M -  NUMBER OF GRIDS IN THE J DIRECTION -
C  N - NUMBER OF GRIDS IN THE K DIRECTION
C  LRL - DIMENSION OF FURTHES DOWNSTREAM RIVER GRID IN THE UPSTREAM 2-D SEGMENT
C  LRM - DIMENSION OF FURTHES DOWNSTREAM RIVER GRID IN THE CENTER SEGMENT
C  LRIV - DIMENSION OF FURTHEST DOWNSTREAM RIVER GRID IN THE DOWNSTREAM 2-D SEG.
C  NCAN - NUMBER OF CANALS DIVERTING FROM THE RIVER IN THE STUDY AREA
C  NADJ - ARRAY SIZE OF DISCRETIZED PLOTS OF RELATIVE PERMEABILITY AND
C      SATURATION DERIVATIVE.
       WRITE(6,3)
     3 FORMAT(3X,*LL*,3X,*LC*,3X,*LR*,4X,*M*,4X,*N*,2X,*LRL*,2X,*LRM*,1X,
      2*LRIV*,1X,*NCAN*,1X,*NADJ*)
       WRITE(6,10) LL,LC,LR,M,N,LRL,LRM,LRIV,NCAN,NADJ
    10 FORMAT(10I5)
       READ(5,20) HPB,AN,POR,SY,SK,TH
C  HPB - SILT LAYER BUBBLING PRESSURE HEAD
C  AN - MANNING ROUGHNESS COEFFICIENT
C  POR - POROSITY
C  SY - SPECIFIC YIELD
C  SK - SILT LAYER HYDRAULIC CONDUCTIVITY
C  TH - SILT LAYER THICKNESS
    20 FORMAT(6F5.2)
       WRITE(6,4)
     4 FORMAT(2X,*HPB*,3X,*AN*,2X,*POR*,3X,*SY*,3X,*SK*,3X,*TH*)
       WRITE(6,20) HPB,AN,POR,SY,SK,TH
C  GRID PARAMETERS - UPSTREAM SEGMENT
       DO 7 I=1,LL
C  HLP - HEAD
       READ(5,11) (HLP(I,J),J=1,M)
C  ZBL - BEDROCK ELEVATION
       READ(5,11) (ZBL(I,J),J=1,M)
C  CKL - HYDRAULIC CONDUCTIVITY
       READ(5,11) (CKL(I,J),J=1,M)
C  KODL - BOUNDARY CONDITION INDICATOR
       READ(5,12) (KODL(I,J),J=1,M)
C  NDL - CANAL DISTRIBUTION AREA INDICATOR
       READ(5,12) (NDL(I,J),J=1,M)
    11 FORMAT(8F8.0)
    12 FORMAT(8I8)
     7 CONTINUE
C  GRID PARAMETERS - CENTER SEGMENT
       DO 8 I=1,LC
       DO 9 K=1,N
       READ(5,11) (HCP(I,J,K),J=1,M)
C  ZC - GRID CENTER ELEVATION
       READ(5,11) (ZC(I,J,K),J=1,M)
C  CKSAT - HYDRAULIC CONDUCTIVITY UNDER FULLY SATURATED CONDITIONS
       READ(5,11) (CKSAT(I,J,K),J=1,M)
       READ(5,12) (KODC(I,J,K),J=1,M)
     9 CONTINUE
       READ(5,12) (NDC(I,J),J=1,M)
     8 CONTINUE
C  GRID PARAMETERS - DOWNSTREAM SEGMENT
       DO 17 I=1,LR
       READ(5,11) (HRP(I,J),J=1,M)
       READ(5,11) (ZBR(I,J),J=1,M)
       READ(5,11) (CKR(I,J),J=1,M)
       READ(5,12) (KODR(I,J),J=1,M)
       READ(5,12) (NDR(I,J),J=1,M)
    17 CONTINUE
       WRITE(6,5)
     5 FORMAT(40X,*INITIAL WATER TABLE - UPSTREAM*,/)
       CALL MATROP(LL,M,HLP)
       DO 85 K=1,N
       DO 86 I=1,LC
       DO 86 J=1,M
       HTEMP(I,J)=HCP(I,J,K)
    86 CONTINUE
       WRITE(6,77) K
    77 FORMAT(48X,*INITIAL HEADS AT LEVEL*,I4,* OF CENTER*,/)
       CALL MATROP(LC,M,HTEMP)
    85 CONTINUE
       WRITE(6,105)
   105 FORMAT(40X,*INITIAL WATER TABLE - DOWNSTREAM*,/)
       CALL MATROP(LR,M,HRP)
       WRITE(6,106)
```

```
  106 FORMAT(40X,*BEDROCK ELEVATIONS - UPSTREAM*,/)
      CALL MATROP(LL,M,ZBL)
      DO 185 K=1,N
      DO 186 I=1,LC
      DO 186 J=1,M
      HTEMP(I,J)=ZC(I,J,K)
  186 CONTINUE
      WRITE(6,177) K
  177 FORMAT(40X,*GRID CENTER ELEVATIONS AT LEVEL*,I4,* OF CENTER*,/)
       CALL MATROP(LC,M,HTEMP)
  185 CONTINUE
      WRITE(6,107)
  107 FORMAT(40X,*BEDROCK ELEVATIONS - DOWNSTREAM*,/)
      CALL MATROP(LR,M,ZBR)
      WRITE(6,205)
  205 FORMAT(40X,*HYDRAULIC CONDUCTIVITIES UPSTREAM*,/)
      CALL MATROP(LL,M,CKL)
      DO 241 K=1,N
      DO 242 I=1,LC
      DO 242 J=1,M
      HTEMP(I,J)=CKSAT(I,J,K)
  242 CONTINUE
      WRITE(6,203) K
  203 FORMAT(40X,*SAT. HYDR. CONDUCTIVITIES AT LEVEL*,I4,* OF CENTER*,/)
      CALL MATROP(LC,M,HTEMP)
  241 CONTINUE
      WRITE(6,202)
  202 FORMAT(40X,*HYDRAULIC CONDUCTIVITIES DOWNSTREAM*,/)
      CALL MATROP(LR,M,CKR)
      WRITE(6,560)
  560 FORMAT(20X,*KODL*,/)
      DO 570 I=1,LL
      WRITE(6,565) (KODL(I,J),J=1,M)
  570 CONTINUE
      DO 571 K=1,N
      WRITE(6,561) K
  561 FORMAT(20X,*KODC AT LEVEL*,I5,/)
      DO 571 I=1,LC
      WRITE(6,565) (KODC(I,J,K),J=1,M)
  565 FORMAT(8I12)
  571 CONTINUE
      WRITE(6,562)
  562 FORMAT(20X,*KODR*,/)
      DO 572 I=1,LR
      WRITE(6,565) (KODR(I,J),J=1,M)
  572 CONTINUE
      WRITE(6,660)
  660 FORMAT(40X,*NDL*,/)
      DO 670 I=1,LL
      WRITE(6,565) (NDL(I,J),J=1,M)
  670 CONTINUE
      WRITE(6,661)
  661 FORMAT(40X,*NDC*,/)
      DO 671 I=1,LC
      WRITE(6,565) (NDC(I,J),J=1,M)
  671 CONTINUE
      WRITE(6,662)
  662 FORMAT(40X,*NDR*,/)
      DO 672 I=1,LR
      WRITE(6,565) (NDR(I,J),J=1,M)
  672 CONTINUE
C  GRID SIZE IN I DIRECTION
C   UPSTREAM SEGMENT
      READ(5,11) (DXL(I),I=1,LL)
      WRITE(6,801)
  801 FORMAT(20X,*DXL*)
      WRITE(6,802) (DXL(I),I=1,12)
  802 FORMAT(2X,12F8.0)
C   CENTER SEGMENT
      READ(5,11) (DXC(I),I=1,LC)
      WRITE(6,803)
  803 FORMAT(20X,*DXC*)
      WRITE(6,804) (DXC(I),I=1,8)
  804 FORMAT(2X,8F8.0)
C   DOWNSTREAM SEGMENT
      READ(5,11) (DXR(I),I=1,LR)
      WRITE(6,805)
```

```
  805 FORMAT(20X,*DXR*)
      WRITE(6,806) (DXR(I),I=1,11)
  806 FORMAT(2X,11F8.0)
      WRITE(6,806) (DXR(I),I=12,22)
C  GRID SIZE IN J DIRECTION
      READ(5,11) (DY(J),J=1,M)
      WRITE(6,807)
  807 FORMAT(20X,*DY*)
      WRITE(6,804) (DY(J),J=1,8)
C  GRID SIZE IN K DIRECTION
      READ(5,11) (DZ(K),K=1,N)
      WRITE(6,809)
  809 FORMAT(20X,*DZ*)
      WRITE(6,810) (DZ(K),K=1,4)
  810 FORMAT(2X,4F8.0)
C  GRID SIZE IN I DIRECTION AT RIVER BEND
      READ(5,11) (DB(J),J=1,M)
      WRITE(6,811)
  811 FORMAT(20X,*DB*)
      WRITE(6,804) (DB(J),J=1,8)
C  CANAL DISTRIBUTION AREA PARAMETERS
C  PERCENT INSIDE STUDY REGION
      READ(5,130) (PCT(I),I=1,9)
  130 FORMAT(9F8.2)
      WRITE(6,900)
  900 FORMAT(20X,*PCT*)
      WRITE(6,130) (PCT(I),I=1,9)
C  AREA INSIDE STUDY REGION
      READ(5,13) (AREA(I),I=1,9)
   13 FORMAT(6F10.0)
      WRITE(6,902)
  902 FORMAT(20X,*AREA*)
      WRITE(6,901) (AREA(I),I=1,9)
  901 FORMAT(5X,9F12.0)
C  RIVER GRID IN WHICH DIVERSION POINT IS LOCATED
      READ(5,14) (LCAN(I),I=1,10)
   14 FORMAT(10I5)
      WRITE(6,904)
  904 FORMAT(20X,*LCAN*)
      WRITE(6,905) (LCAN(I),I=1,10)
  905 FORMAT(5X,10I10)
      WRITE(6,950)
C  RIVER PARAMETERS
  950 FORMAT(35X,*RIVER PARAMETERS*,/)
      WRITE(6,951)
  951 FORMAT(2X,*IRIV*,4X,*JRIV*,4X,*RWID*,4X,*RBED*,4X,*RSLP*)
C  RIVER GRID NUMBERING BEGINS WITH 6 IN THE FURTHEST UPSTREAM GRID OF THE MODEL
C  THE FIRST 5 NUMBERS ARE RESERVED FOR INDICATION BOUNDARY CONDITIONS IN
C  AQUIFER GRIDS.
      DO 22 I=6,LRIV
C  I=RIVER GRID SUBSCRIPT (USED AS BOUNDARY CONDITION INDICATOR)
C  IRIV,JRIV - GRID LOCATION IN I,J,DIRECTIONS  ( IN 3-D SEGMENT RIVER GRIDS
C       ARE LOCATED IN THE UPPERMOST LAYER OF GRIDS )
C  RWID - WIDTH OF CHANNEL
C  RBED - ELEVATION OF CHANNEL BED
C  RSLP - CHANNEL BED SLOPE
      READ(5,15) IRIV(I),JRIV(I),RWID(I),RBED(I),RSLP(I)
      WRITE(6,15) IRIV(I),JRIV(I),RWID(I),RBED(I),RSLP(I)
   15 FORMAT(2I8,2F8.0,F8.6)
C  RSO - RATE OF SEEPAGE FROM RIVER
      RSO(I)=0.0
   22 CONTINUE
      DO 23 I=1,5
      IRIV(I)=IRIV(6)
      JRIV(I)=JRIV(6)
      RWID(I)=RWID(6)
      RBED(I)=RBED(6)
      RSLP(I)=RSLP(6)
      RSO(I)=0.0
   23 CONTINUE
C  ARRAYS OF VALUES OF DISCRETIZED CURVES OF RELATIVE PERMEABILITY AND
C  SATURATION AS FUNCTIONS OF HEAD
C  RELATIVE PERMEABILITY
      READ(5,16) (FKFAC(I),I=1,NADJ)
   16 FORMAT(10F5.3)
      WRITE(6,960)
C     HSTEP=STEP=0.5 FEET----DEFINED IN KFNP AND ADJUST
```

```
  960 FORMAT(20X,*FKFAC*)
      WRITE(6,961) (FKFAC(I),I=1,NADJ)
  961 FORMAT(10X,20F6.3)
C  SATURATION DERIVATIVE
      READ(5,16) (SDRIV(I),I=1,NADJ)
      WRITE(6,962)
  962 FORMAT(20X,*SDRIV*)
      WRITE(6,961) (SDRIV(I),I=1,NADJ)
      CONTINUE
      RETURN
      END
      SUBROUTINE BCON(JUMP)
      COMMON LC,M,N,LRL,LRM,LRIV,NADJ,NCAN,HPB,SK,TH,SY,AN,BSC,VT,POR,
     2TIME,TCON,DT,C(384),DXC(8),DY(8),DZ(4),DB(8),IRIV(47),JRIV(47),
     3RBED(47),RWID(47),RSLP(47),QRIV(47),DIV(47),RSO(47),VMS(47),
     4VMB(47),SDRIV(20),FKFAC(20),CDV(9),PCT(9),AREA(9),LCAN(10),
     5QJMD(3),QLAM(3),QKAN(3),CM(384,49),NDL(12,8),NDC(8,8),NDR(22,8),
     6HTEMP(8,8),QIC(8,8),KODC(8,8,4),HCP(8,8,4),ZC(8,8,4),CKC(8,8,4),
     7CKSAT(8,8,4),DSDHP(8,8,4)
      COMMON /A/ LL,DXL(12),KODL(12,8),CKL(12,8),HLP(12,8),ZBL(12,8),
     2QIL(12,8)
      COMMON /B/ LR,DXR(22),KODR(22,8),CKR(22,8),HRP(22,8),ZBR(22,8),
     2QIR(22,8)
C
C  ************************************************************************
C  THIS SUBROUTINE READS IN BOUNDARY CONDITIONS AT THE BEGINNING OF
C  EACH TIME INCREMENT AND COMPUTES DISCHARGE AND HEAD IN EACH RIVER GRID,
C  AND SURFACE INFLOW FOR EVERY SURFACE GRID.  DATA VALUES ARE READ FROM
C  PUNCHED CARDS.  CARD FORMATS ARE INDICATED IN THIS SUBROUTINE FOR EACH
C  BOUNDARY PARAMETER.
C  ************************************************************************
C
      JUMP=1
C     IF(JUMP.GT.1) GO TO 16
      QT=0.0
      READ(5,10) (QJMD(I),QLAM(I),QKAN(I),I=1,3)
   10 FORMAT(9F8.1)
      QT=QJMD(1)+QJMD(2)+QJMD(3)
      QJMD(JUMP)=(QJMD(1)+QJMD(2)+QJMD(3))/3.0
      QLAM(JUMP)=(QLAM(1)+QLAM(2)+QLAM(3))/3.0
      QKAN(JUMP)=(QKAN(1)+QKAN(2)+QKAN(3))/3.0
      READ(5,11) ET,PRECIP
   11 FORMAT(2F8.2)
      READ(5,12)  (CDV(I),I=1,NCAN), BSC
      BSC=BSC*1.25
   12 FORMAT(10F6.0)
C  CONVERSION TO CUBIC FEET PER DAY OR FEET PER DAY
C  INCHES PER MONTH TO FEET PER DAY
      ET=ET/360.0
      PRECIP=PRECIP/360.0
      DO 8 I=1,NCAN
C  ACRE FEET PER MONTH TO CUBIC FEET PER DAY
      CDV(I)=CDV(I)*43560.0/30.0
    8 CONTINUE
C  ACRE FEET PER MONTH TO CUBIC FEET PER DAY
      BSC=BSC*43560.0/30.0
C  ADDITION OF 10 CFS TO LAMAR CANAL FROM POWER PLANT
      CDV(4)=CDV(4)+864000.0
C  WATER TABLE FLUCTUATIONS IN EDGE GRIDS
      HLP(9,1)=HLP(9,1)-0.05
      HLP(10,1)=HLP(10,1)-0.05
      HLP(12,1)=HLP(12,1)+0.03
      HLP(8,8)=HLP(8,8)+0.10
      HLP(9,8)=HLP(9,8)-0.05
      HLP(11,8)=HLP(11,8)-0.10
      HCP(2,1)=HCP(2,1)+0.04
      HCP(4,1)=HCP(4,1)+0.04
      HCP(5,1)=HCP(5,1)+0.09
      HCP(8,1)=HCP(8,1)+0.06
      HCP(1,8)=HCP(1,8)+0.05
      HCP(3,8)=HCP(3,8)+0.10
      HCP(4,8)=HCP(4,8)+0.05
      HCP(6,8)=HCP(6,8)+0.07
      HCP(8,8)=HCP(8,8)+0.10
      HRP(7,1)=HRP(7,1)+0.07
      DO 26 I=8,11
      HRP(I,1)=HRP(I,1)+0.02
```

```
   26 CONTINUE
      HRP(I,1)=HRP(I,1)+0.02
   26 CONTINUE
      HRP(12,1)=HRP(12,1)+0.07
      DO 27 I=13,18
      HRP(I,1)=HRP(I,1)+0.04
   27 CONTINUE
      HRP(19,1)=HRP(19,1)+0.12
      HRP(20,1)=HRP(20,1)+0.18
      HRP(21,1)=HRP(21,1)+0.15
      HRP(2,8)=HRP(2,8)+0.08
      HRP(3,8)=HRP(3,8)+0.10
      HRP(5,8)=HRP(5,8)+0.09
      HRP(6,8)=HRP(6,8)+0.03
      HRP(7,8)=HRP(7,8)+0.07
      HRP(8,8)=HRP(8,8)+0.20
      HRP(13,8)=HRP(13,8)+0.05
      HRP(16,8)=HRP(16,8)-0.06
      HRP(17,8)=HRP(17,8)-0.05
      HRP(18,8)=HRP(18,8)-0.03
      HRP(21,2)=HRP(21,2)+0.10
      HRP(21,3)=HRP(21,3)+0.02
      HRP(21,4)=HRP(21,4)-0.01
      HRP(21,5)=HRP(21,5)-0.01
      HRP(21,6)=HRP(21,6)-0.03
      HRP(21,7)=HRP(21,7)-0.05
C     WEIGHTING FACTOR FOR DIVERSIONS BASED ON JMD RELEASES
   16 FAC=3.0*QJMD(JUMP)/QT
C  COMPUTATION OF SURFACE INPUT    (CUBIC FEET PER DAY)
      DO 20 I=1,LL
      DO 20 J=1,M
      NA=NDL(I,J)
      IF(NA.EQ.0) GO TO 21
      QIL(I,J)=(PRECIP-ET)*DXL(I)*DY(J)+CDV(NA)*FAC*PCT(NA)*DXL(I)*
     2DY(J)/AREA(NA)
      GO TO 20
   21 QIL(I,J)=(PRECIP-ET)*DXL(I)*DY(J)
   20 CONTINUE
      DO 30 I=1,LC
      DO 30 J=1,M
      NA=NDC(I,J)
      IF(NA.EQ.0) GO TO 31
      QIC(I,J)=(PRECIP-ET)*DXC(I)*DY(J)+CDV(NA)*FAC*PCT(NA)*DXC(I)*
     2DY(J)/AREA(NA)
      GO TO 30
   31 QIC(I,J)=(PRECIP-ET)*DXC(I)*DY(J)
   30 CONTINUE
      DO 40 I=1,LR
      DO 40 J=1,M
      NA=NDR(I,J)
      IF(I.EQ.8) DXR(I)=DR(J)
      IF(NA.EQ.0) GO TO 41
      QIR(I,J)=(PRECIP-ET)*DXR(I)*DY(J)+CDV(NA)*FAC*PCT(NA)*DXR(I)*
     2DY(J)/AREA(NA)
      GO TO 40
   41 QIR(I,J)=(PRECIP-ET)*DXR(I)*DY(J)
   40 CONTINUE
C  SPECIAL CASES
C  LAMAR WELLS
C     QIC(4,3)=QIC(4,3)-432000.0
C     QIC(4,4)=QIC(4,4)-432000.0
C  BIG SANDY CREEK DISCHARGE FROM GRIDS
      QIR(5,6)=QIR(5,6)-0.05*BSC
      QIR(5,7)=QIR(5,7)-0.10*BSC
      DO 601 I=1,LL
      DO 601 J=1,M
      IF(NDL(I,J).EQ.0) QIL(I,J)=0.0
  601 CONTINUE
      DO 602 I=1,LC
      DO 602 J=1,M
      IF(NDC(I,J).EQ.0) QIC(I,J)=0.0
  602 CONTINUE
      DO 603 I=1,LR
      DO 603 J=1,M
      IF(NDR(I,J).EQ.0) QIR(I,J)=0.0
```

```
  603 CONTINUE
C      RIVER FLOW CALCULATIONS
C     LAMAR GAGING STATION IS LOCATED AT RIVER GRID NO. 20
C      DIVERSIONS - CONVERT TO CFS
       DO 47 I=1,LRIV
       DIV(I)=0.0
   47  CONTINUE
       DO 57 I=1,NCAN
       L=LCAN(I)
C   CANAL DIVERSIONS CONVERTED TO CFS
       DIV(L)=DIV(L)+CDV(I)*FAC/86400.0
   57  CONTINUE
       L=LCAN(10)
C   BIG SANDY CREEK TRIBUTARY INFLOW
C   BIG SANDY CREEK DISCHARGE CONVERTED TO CFS
       DIV(L)=DIV(L)-BSC/86400.0
C     CALCULATIONS OF FLOW AT ALL RIVER SECTIONS
       QRIV(20)=QLAM(JUMP)
       D=(QRIV(20)*AN/(1.486*RWID(20)*SQRT(RSLP(20))))**0.6
       I=IRIV(20)
       J=JRIV(20)
       HCP(I,J,N)=RBED(20)+D
       DO 67 I=1,14
C   RIVER FLOWS UPSTREAM FROM LAMAR
       L=20-I
       QRIV(L)=QRIV(L+1)+DIV(L+1)+0.5/86400.0*(RSO(L+1)+RSO(L))
       IF(QRIV(L).LT.0.0) QRIV(L)=0.0
       D=(QRIV(L)*AN/(1.486*RWID(L)*SQRT(RSLP(L))))**0.6
       IG=IRIV(L)
       JG=JRIV(L)
       IF(L.GT.LRL) GO TO 62
       HLP(IG,JG)=RBED(L)+D
       GO TO 67
   62  HCP(IG,JG,N)=RBED(L)+D
   67  CONTINUE
       DO 77 L=21,47
C   RIVER FLOWS DOWNSTREAM FROM LAMAR
       QRIV(L)=QRIV(L-1)-DIV(L)-0.5/86400.0*(RSO(L-1)+RSO(L))
       IF(QRIV(L).LT.0.0) QRIV(L)=0.0
       D=(QRIV(L)*AN/(1.486*RWID(L)*SQRT(RSLP(L))))**0.6
       IG=IRIV(L)
       JG=JRIV(L)
       IF(L.GT.LRM) GO TO 72
       HCP(IG,JG,N) =RBED(L)+D
       GO TO 77
   72  HRP(IG,JG)=RBED(L)+D
   77  CONTINUE
       WRITE(6,206)
  206  FORMAT(12X,*QJMD*,9X,*QRIV(L)*,12X,*QLAM*,12X,*QKAN*,8X,*QRIV(47)*
     2,2X,*JUMP*,4X,*TIME*)
       WRITE(6,207) QJMD(JUMP),QRIV(6),QLAM(JUMP),QKAN(JUMP),QRIV(LRIV),
     2JUMP,TIME
  207  FORMAT(5F16.2,I5,F10.2)
       JUMP=JUMP+1
       IF(JUMP.GT.3)  JUMP=1
       RETURN
       END
       SUBROUTINE SCRIBE
       COMMON LC,M,N,LRL,LRM,LRIV,NADJ,NCAN,HPB,SK,TH,SY,AN,BSC,VT,POR,
     2TIME,TCON,DT,C(384),DXC(8),DY(8),DZ(4),DB(8),IRIV(47),JRIV(47),
     3RBED(47),RWID(47),RSLP(47),QRIV(47),DIV(47),RSO(47),VMS(47),
     4VMB(47),SDRIV(20),FKFAC(20),CDV(9),PCT(9),AREA(9),LCAN(10),
     5QJMD(3),QLAM(3),QKAN(3),CM(384,49),NDL(12,8),NDC(8,8),NDR(22,8),
     6HTEMP(8,8),QIC(8,8),KODC(8,8,4),HCP(8,8,4),ZC(8,8,4),CKC(8,8,4),
     7CKSAT(8,8,4),DSDHP(8,8,4)
       COMMON /A/ LL,DXL(12),KODL(12,8),CKL(12,8),HLP(12,8),ZBL(12,8),
     2QIL(12,8)
       COMMON /B/ LR,DXR(22),KODR(22,8),CKR(22,8),HRP(22,8),ZBR(22,8),
     2QIR(22,8)
C
C  ***************************************************************************
C  THIS SUBROUTINE PRINTS OUT INTERMEDIATE AND FINAL RESULTS, INCLUDING
C  RIVER DISCHARGES AND WATER TABLE ELEVATIONS.
C  ***************************************************************************
C
```

```
      WRITE(6,987)
  987 FORMAT(///,5X,*XXXXXXXXXXXXXXXXXXXXXXXXXXXXXXXXXXXXXXXXXXXXXXXXXXXX
     2XXXXXXXXXXXXXXXXXXXXXXXXXXXXXXXXX*,/)
      WRITE(6,74) TIME
   74 FORMAT(5X,*TIME=*,F10.2,//)
      WRITE(6,75)
   75 FORMAT(40X,*WATER TABLE ELEVATIONS UPSTREAM*,/)
      CALL MATROP(LL,M,HLP)
      DO 85 K=1,N
      DO 86 I=1,LC
      DO 86 J=1,M
      HTEMP(I,J)=HCP(I,J,K)
   86 CONTINUE
      WRITE(6,77) K
   77 FORMAT(48X,*HEADS AT LEVEL*,I5,2X,*OF CENTER*,/)
      CALL MATROP(LC,M,HTEMP)
   85 CONTINUE
      WRITE(6,76)
   76 FORMAT(40X,*WATER TABLE ELEVATIONS DOWNSTREAM*,/)
      CALL MATROP(LR,M,HRP)
      DO 41 K=1,N
      DO 42 I=1,LC
      DO 42 J=1,M
      HTEMP(I,J)=CKC(I,J,K)
   42 CONTINUE
      WRITE(6,103) K
  103 FORMAT(40X,*CONDUCTIVITIES AT LEVEL*,I5,2X,*OF CENTER (FT/DAY)*,/)
      CALL MATROP(LC,M,HTEMP)
   41 CONTINUE
      WRITE(6,400)
  400 FORMAT(40X,*SURFACE FLUX UPSTREAM,  CFD*,/)
      CALL MATROP(LL,M,QIL)
      WRITE(6,401)
  401 FORMAT(40X,*SURFACE FLUX CENTER,  CFD*,/)
      CALL MATROP(LC,M,QIC)
      WRITE(6,402)
  402 FORMAT(40X,*SURFACE FLUX DOWNSTREAM,  CFD*,/)
      CALL MATROP(LR,M,QIR)
      DO 571 K=1,N
      WRITE(6,561) K
  561 FORMAT(20X,*KODC AT LEVEL*,I5,/)
      DO 571 I=1,LC
      WRITE(6,565) (KODC(I,J,K),J=1,M)
  565 FORMAT(8I12)
  571 CONTINUE
      WRITE(6,70)
   70 FORMAT(10X,*SECTION*,10X,*RIVER FLOW, CFS*,10X,*SEEPAGE RATE OUT,
     2ACRE-FEET/DAY*,/)
      DO 72 L=6,LRIV
      RSO(L)=RSO(L)/43560.0
      WRITE(6,71) L,QRIV(L),RSO(L)
   71 FORMAT(5X,I10,F25.2,F30.2)
      RSO(L)=RSO(L)*43560.0
   72 CONTINUE
      VT=VT/43560.0
      WRITE(6,22) TIME,VT
   22 FORMAT(5X,*TIME=*,F10.2,5X,*TOTAL VOLUME OF SEEPAGE IN TIME INCREM
     2ENT=*,F20.3,5X,*ACRE-FEET*,/)
      VT=VT*43560.0
      RETURN
      END
      SUBROUTINE MATROP (NR, NC, B)
      DIMENSION B(NR,NC),A(8)
C DIMENSIONS OF B MUST MATCH DIMENSIONS OF VARIABLE CALLED FROM MAIN PROGRAM
C
C  ***************************************************************************
C  THIS SUBROUTINE ARRANGES TWO-DIMENSIONAL AND THREE-DIMENSIONAL ARRAYS
C  IN A STANDARD FORM FOR PRINTOUT.
C  ***************************************************************************
C
      DO 11 I=1,NC,8
      IN=I/8
      DO 9 J=1,NR
      IF((IN+1)*8.LE.NC) 1,3
    1 DO 2 JJ=1,8
      JJJ=IN*8+JJ
```

```
    2 A(JJ)=B(J,JJJ)
      GO TO 6
    3 LL=NC-8*IN
      DO 4 JJ=1,LL
      JJJ=IN*8+JJ
    4 A(JJ)=B(J,JJJ)
      LL=LL+1
      DO 5 JJ=LL,8
    5 A(JJ)=0.0
    6 IF (A(1).LT.0.001) GO TO 14
      IF (IN) 7,7,8
    7 WRITE(6,12) (A(II),II=1,8),J
      GO TO 9
    8 WRITE (6,12) (A(II),II=1,8), IN
      GO TO 9
   14 IF(IN) 15,15,16
   15 WRITE (6,17) (A(II),II=1,8), J
      GO TO 9
   16 WRITE (6,17) (A(II),II=1,8), IN
    9 CONTINUE
      IF(NC.LE.(IN+1)*8) 11,10
   10 WRITE (6,13)
   11 CONTINUE
   12 FORMAT(1H ,8F15.2,I4)
   13 FORMAT (1H0,//)
   17 FORMAT (1H ,8F15.2,I4)
      RETURN
      END
      SUBROUTINE MATSOL
      COMMON LC,M,N,LRL,LRM,LRIV,NADJ,NCAN,HPB,SK,TH,SY,AN,BSC,VT,POR,
     2TIME,TCON,DT,C(384),DXC(8),DY(8),DZ(4),DB(8),IRIV(47),JRIV(47),
     3RBED(47),RWID(47),RSLP(47),QRIV(47),DIV(47),RSO(47),VMS(47),
     4VMB(47),SDRIV(20),FKFAC(20),CDV(9),PCT(9),AREA(9),LCAN(10),
     5QJMD(3),QLAM(3),QKAN(3),CM(384,49),NDL(12,8),NDC(8,8),NDR(22,8),
     6HTEMP(8,8),QIC(8,8),KODC(8,8,4),HCP(8,8,4),ZC(8,8,4),CKC(8,8,4),
     7CKSAT(8,8,4),DSDHP(8,8,4)
      COMMON /A/ LL,DXL(12),KODL(12,8),CKL(12,8),HLP(12,8),ZBL(12,8),
     2QIL(12,8)
      COMMON /B/ LR,DXR(22),KODR(22,8),CKR(22,8),HRP(22,8),ZBR(22,8),
     2QIR(22,8)
C
C   ***********************************************************************
C   THIS SUBROUTINE SETS UP THE COEFFICIENT MATRIX AND THE RIGHT HAND SIDE
C   COLUMN VECTOR FOR SOLVING THE GROUNDWATER FLOW EQUATIONS. THIS
C   SUBROUTINE IS ARRANGED FOR SETTING UP A COEFFICIENT MATRIX FOR A THREE-
C   DIMENSIONAL GRID SYSTEM INTERFACED ON EACH END IN THE I DIRECTION
C   WITH TWO-DIMENSIONAL GRID SYSTEMS.  THE VALUE OF M MUST BE EQUAL TO THE
C   NUMBER OF GRIDS IN A ROW ACROSS THE MODEL IN THE J DIRECTION.  TO MINIMIZE
C   COMPUTER TIME AND STORAGE NEEDED TO SOLVE THE MATRIX OF GROUNDWATER FLOW
C   EQUATIONS, THE VALUE OF M SHOULD, IF POSSIBLE, CORRESPOND TO
C   THE SMALLEST LATERAL GRID DIMENSION OF THE ENTIRE MODEL GRID SYSTEM.
C   ***********************************************************************
C
      ISIDE=1
      NA=(M-2)*((LL-1)+LC*N+(LR-1))
      NB=2*(M-2)*N+1
      MSUB=M
      DO 7 I=1,NA
      C(I)=0.0
      DO 7 J=1,NB
      CM(I,J)=0.0
    7 CONTINUE
      LRLL=LRL+1
      DO 8 L=LRLL,LRM
      I=IRIV(L)
      J=JRIV(L)
      VMB(L)=SK*(((HCP(I,J,N)-RBED(L))-HPB)+TH)/TH
      VMS(L)=SK*((HCP(I,J,N)-RBED(L))-HPB)*0.5/TH
    8 CONTINUE
      LBEG=1
      LEND=(M-2)*(LL-2)
      CALL SIDE (LBEG,LEND,LL,KODL,CKL,HLP,ZBL,DXL,QIL,MSUB)
      LBEG=LEND+1
      LEND=LEND+(M-2)
      CALL STRAN (LBEG,LEND,LL,KODL,CKL,HLP,ZBL,DXL,QIL,MSUB,ISIDE)
      LBEG=LEND+1
```

```
      LEND=LEND+(M-2)*N
      CALL CTRAN (LBEG,LEND,LL,KODL,CKL,HLP,ZBL,DXL,QIL,MSUB,ISIDE)
      LBEG=LEND+1
      LEND=LEND+(M-2)*N*(LC-2)
      CALL CENTER (LBEG,LEND)
      LBEG=LEND+1
      LEND=LEND+(M-2)*N
      ISIDE=2
      CALL CTRAN (LBEG,LEND,LR,KODR,CKR,HRP,ZBR,DXR,QIR,MSUB,ISIDE)
      LBEG=LEND+1
      LEND=LEND+(M-2)
      CALL STRAN (LBEG,LEND,LR,KODR,CKR,HRP,ZBR,DXR,QIR,MSUB,ISIDE)
      LBEG=LEND+1
      LEND=LEND+(M-2)*(LR-2)
      CALL SIDE (LBEG,LEND,LR,KODR,CKR,HRP,ZBR,DXR,QIR,MSUB)
      CALL BSOLVE(CM,NA,NB,C)
      LRR=LR-1
      MR=M-1
      NT=0
      DO 70 I=2,LL
      DO 70 J=2,MR
      NT=NT+1
      HLP(I,J)=C(NT)
   70 CONTINUE
      DO 71 I=1,LC
      DO 71 J=2,MR
      DO 71 K=1,N
      NT=NT+1
      HCP(I,J,K)=C(NT)
   71 CONTINUE
      DO 72 I=1,LRR
      DO 72 J=2,MR
      NT=NT+1
      HRP(I,J)=C(NT)
   72 CONTINUE
      RETURN
      END
      SUBROUTINE SIDE (LB,LE,LS,KODS,CKS,HSP,ZBS,DXS,QIS,MS)
      DIMENSION KODS(LS,MS),CKS(LS,MS),HSP(LS,MS),ZBS(LS,MS),DXS(LS),
     2QIS(LS,MS)
      COMMON LC,M,N,LRL,LRM,LRIV,NADJ,NCAN,HPB,SK,TH,SY,AN,BSC,VT,POR,
     2TIME,TCON,DT,C(384),DXC(8),DY(8),DZ(4),DB(8),IRIV(47),JRIV(47),
     3RBED(47),RWID(47),RSLP(47),QRIV(47),DIV(47),RSO(47),VMS(47),
     4VMB(47),SDRIV(20),FKFAC(20),CDV(9),PCT(9),AREA(9),LCAN(10),
     5QJMD(3),QLAM(3),QKAN(3),CM(384,49),NDL(12,8),NDC(8,8),NDR(22,8),
     6HTEMP(8,8),QIC(8,8),KODC(8,8,4),HCP(8,8,4),ZC(8,8,4),CKC(8,8,4),
     7CKSAT(8,8,4),DSDHP(8,8,4)
C
C  ***************************************************************************
C  THIS SUBROUTINE IS CALLED FROM MATSOL TO COMPUTE COEFFICIENTS AND COLUMN
C  VECTOR VALUES FOR THOSE GRIDS IN THE TWO-DIMENSIONAL MODEL SEGMENT THAT
C  ARE SURROUNDED ON ALL SIDES BY OTHER TWO-DIMENSIONAL GRIDS.
C  ***************************************************************************
C
      PERM(CK1,CK2,H1,Z1,H2,Z2,XY,DXY1,DXY2)=(2.0*CK1*CK2*(H1-Z1)*(H2-Z2
     2)*XY)/(DXY2*CK1*(H1-Z1)+DXY1*CK2*(H2-Z2))
      IM=(M-2)*N+1
      IC=IM-1
      ID=IM+1
      IA=IM-(M-2)
      IB=IM+(M-2)
      LSR=LS-1
      MR=M-1
      DO 8 I=2,LSR
      DO 8 J=2,MR
      IF(ISIDE.EQ.2.AND.I.EQ.8) DXS(I)=DB(J)
      IF(KODS(I,J).EQ.1.OR.KODS(I,J).GE.6) GO TO 60
      IF(CKS(I,J).LT.0.005) GO TO 60
      CM(LB,IA)=PERM(CKS(I,J),CKS(I-1,J),HSP(I,J),ZBS(I,J),HSP(I-1,J),
     2ZBS(I-1,J),DY(J),DXS(I),DXS(I-1))
      IF(KODS(I-1,J).NE.1.AND.KODS(I-1,J).LT.6) GO TO 20
      CM(LB,IM)=CM(LB,IM)-CM(LB,IA)
      C(LB)=C(LB)-HSP(I-1,J)*CM(LB,IA)
      CM(LB,IA)=0.0
   20 CM(LB,IB)=PERM(CKS(I,J),CKS(I+1,J),HSP(I,J),ZBS(I,J),HSP(I+1,J),
     2ZBS(I+1,J),DY(J),DXS(I),DXS(I+1))
```

```
      IF(KODS(I+1,J).NE.1.AND.KODS(I+1,J).LT.6) GO TO 30
      CM(LB,IM)=CM(LB,IM)-CM(LB,IB)
      C(LB)=C(LB)-HSP(I+1,J)*CM(LB,IB)
      CM(LB,IB)=0.0
   30 CM(LB,IC)=PERM(CKS(I,J),CKS(I,J-1),HSP(I,J),ZBS(I,J),HSP(I,J-1),
     2ZBS(I,J-1),DXS(I),DY(J),DY(J-1))
      IF(KODS(I,J-1).NE.1.AND.KODS(I,J-1).LT.6) GO TO 40
      CM(LB,IM)=CM(LB,IM)-CM(LB,IC)
      C(LB)=C(LB)-HSP(I,J-1)*CM(LB,IC)
      CM(LB,IC)=0.0
   40 CM(LB,ID)=PERM(CKS(I,J),CKS(I,J+1),HSP(I,J),ZBS(I,J),HSP(I,J+1),
     2ZBS(I,J+1),DXS(I),DY(J),DY(J+1))
      IF(KODS(I,J+1).NE.1.AND.KODS(I,J+1).LT.6) GO TO 50
      CM(LB,IM)=CM(LB,IM)-CM(LB,ID)
      C(LB)=C(LB)-HSP(I,J+1)*CM(LB,ID)
      CM(LB,ID)=0.0
   50 CM(LB,IM)=CM(LB,IM)-(CM(LB,IA)+CM(LB,IB)+CM(LB,IC)+CM(LB,ID))-
     2DXS(I)*DY(J)*SY/DT
      C(LB)=C(LB)-HSP(I,J)*(DXS(I)*DY(J)*SY/DT)-QIS(I,J)
      GO TO 70
   60 CM(LB,IM)=1.0
      C(LB)=HSP(I,J)
   70 LB=LB+1
      LBB=LB-1
    8 CONTINUE
      LCK=LB-1
      IF(LCK.NE.LE) WRITE(6,77)
   77 FORMAT(5X,*ERROR IN LOOP INDEX IN SUBROUTINE SIDE*,/)
      RETURN
      END
      SUBROUTINE  STRAN (LB,LE,LS,KODS,CKS,HSP,ZBS,DXS,QIS,MS,ISIDE)
      DIMENSION KODS(LS,MS),CKS(LS,MS),HSP(LS,MS),ZBS(LS,MS),DXS(LS),
     2QIS(LS,MS)
      COMMON LC,M,N,LRL,LRM,LRIV,NADJ,NCAN,HPB,SK,TH,SY,AN,BSC,VT,POR,
     2TIME,TCON,DT,C(384),DXC(8),DY(8),DZ(4),DB(8),IRIV(47),JRIV(47),
     3RBED(47),RWID(47),RSLP(47),QRIV(47),DIV(47),RSO(47),VMS(47),
     4VMB(47),SDRIV(20),FKFAC(20),CDV(9),PCT(9),AREA(9),LCAN(10),
     5QJMD(3),QLAM(3),QKAN(3),CM(384,49),NDL(12,8),NDC(8,8),NDR(22,8),
     6HTEMP(8,8),QIC(8,8),KODC(8,8,4),HCP(8,8,4),ZC(8,8,4),CKC(8,8,4),
     7CKSAT(8,8,4),DSDHP(8,8,4)
C
C  ***********************************************************************
C  THIS SUBROUTINE IS CALLED FROM MATSOL TO COMPUTE COEFFICIENTS AND COLUMN
C  VECTOR VALUES FOR GRIDS IN THE TWO-DIMENSIONAL MODEL SEGMENT THAT ARE
C  ADJACENT ON ONE SIDE TO A COLUMN OF GRIDS IN THE THREE-DIMENSIONAL MODEL
C  SEGMENT.
C  ***********************************************************************
C
      PERM(CK1,CK2,H1,Z1,H2,Z2,XY,DXY1,DXY2)=(2.0*CK1*CK2*(H1-Z1)*(H2-Z2
     2)*XY)/(DXY2*CK1*(H1-Z1)+DXY1*CK2*(H2-Z2))
      TPERM(CK1,CK2,H1,Z1,STA,XY,DX1,DX2)=(2.0*CK1*CK2*(H1-Z1)*STA*XY)/
     2(DX2*CK1*(H1-Z1)+DX1*CK2*STA)
      IM=(M-2)*N+1
      IC=IM-1
      ID=IM+1
      MR=M-1
      GO TO (15,16) ISIDE
   15 IS=LS
      I=1
      IA=IM-(M-2)
      GO TO 17
   16 IS=1
      I=LC
      IB=IM+(M-2)
   17 DO 8 J=2,MR
      IF(KODS(IS,J).EQ.1.OR.KODS(IS,J).GE.6) GO TO 90
      IF(CKS(IS,J).LT.0.005) GO TO 90
      CM(LB,IC)=PERM(CKS(IS,J),CKS(IS,J-1),HSP(IS,J),ZBS(IS,J),HSP(IS,J-
     21),ZBS(IS,J-1),DXS(IS),DY(J),DY(J-1))
      IF(KODS(IS,J-1).NE.1.AND.KODS(IS,J-1).LT.6) GO TO 20
      CM(LB,IM)=CM(LB,IM)-CM(LB,IC)
      C(LB)=C(LB)-HSP(IS,J-1)*CM(LB,IC)
      CM(LB,IC)=0.0
   20 CM(LB,ID)=PERM(CKS(IS,J),CKS(IS,J+1),HSP(IS,J),ZBS(IS,J),HSP(IS,J+
     21),ZBS(IS,J+1),DXS(IS),DY(J),DY(J+1))
      IF(KODS(IS,J+1).NE.1.AND.KODS(IS,J+1).LT.6) GO TO 30
```

```
      CM(LB,IM)=CM(LB,IM)-CM(LB,ID)
      C(LB)=C(LB)-HSP(IS,J+1)*CM(LB,ID)
      CM(LB,ID)=0.0
   30 CM(LB,IM)=CM(LB,IM)-(CM(LB,IC)+CM(LB,ID))
      GO TO (40,60) ISIDE
   40 CM(LB,IA)=PERM(CKS(IS,J),CKS(IS-1,J),HSP(IS,J),ZBS(IS,J),HSP(IS-1,
     2J),ZBS(IS-1,J),DY(J),DXS(IS),DXS(IS-1))
      IF(KODS(IS-1,J).NE.1.AND.KODS(IS-1,J).LT.6) GO TO 45
      CM(LB,IM)=CM(LB,IM)-CM(LB,IA)
      C(LB)=C(LB)-HSP(IS-1,J)*CM(LB,IA)
      CM(LB,IA)=0.0
   45 CM(LB,IM)=CM(LB,IM)-CM(LB,IA)
      BRK=ZC(I,J,1)-0.5*DZ(1)
      DO 107 KI=1,N
      IF(CKSAT(I,J,KI).LT.0.005) BRK=BRK+DZ(KI)
  107 CONTINUE
      STC=HCP(I,J,N)-BRK
      DO 55 K=1,N
      IB=IM+((M-1-J)+(J-2)*N+K)
      IF(STC.LE.0.0) GO TO 49
      TOP=ZC(I,J,K)+0.5*DZ(K)
      BOT=ZC(I,J,K)-0.5*DZ(K)
      IF(BOT.GE.HCP(I,J,K)) GO TO 49
      IF(TOP.GT.HCP(I,J,K).AND.BOT.LT.HCP(I,J,K)) GO TO 46
      CM(LB,IB)=DZ(K)/STC*TPERM(CKS(IS,J),CKSAT(I,J,K),HSP(IS,J),ZBS(IS,
     2J),STC,DY(J),DXS(IS),DXC(I))
      GO TO 47
   46 DZR=HCP(I,J,K)-BOT
      CM(LB,IB)=DZR/STC*TPERM(CKS(IS,J),CKSAT(I,J,K),HSP(IS,J),ZBS(IS,J)
     2,STC,DY(J),DXS(IS),DXC(I))
   47 IF(KODC(I,J,K).NE.1) GO TO 50
      CM(LB,IM)=CM(LB,IM)-CM(LB,IB)
      C(LB)=C(LB)-HCP(I,J,K)*CM(LB,IB)
   49 CM(LB,IB)=0.0
   50 CM(LB,IM)=CM(LB,IM)-CM(LB,IB)
   55 CONTINUE
      GO TO 80
   60 CM(LB,IB)=PERM(CKS(IS,J),CKS(IS+1,J),HSP(IS,J),ZBS(IS,J),HSP(IS+1,
     2J),ZBS(IS+1,J),DY(J),DXS(IS),DXS(IS+1))
      IF(KODS(IS+1,J).NE.1.AND.KODS(IS+1,J).LT.6) GO TO 65
      CM(LB,IM)=CM(LB,IM)-CM(LB,IB)
      C(LB)=C(LB)-HSP(IS+1,J)*CM(LB,IB)
   65 CM(LB,IM)=CM(LB,IM)-CM(LB,IB)
      BRK=ZC(I,J,1)-0.5*DZ(1)
      DO 207 KI=1,N
      IF(CKSAT(I,J,KI).LT.0.005) BRK=BRK+DZ(KI)
  207 CONTINUE
      STC=HCP(I,J,N)-BRK
      DO 75 K=1,N
      IA=IM-((J-1)+(M-1-J)*N+(N-K))
      IF(STC.LE.0.0) GO TO 69
      TOP=ZC(I,J,K)+0.5*DZ(K)
      BOT=ZC(I,J,K)-0.5*DZ(K)
      IF(BOT.GE.HCP(I,J,K)) GO TO 69
      IF(TOP.GT.HCP(I,J,K).AND.BOT.LT.HCP(I,J,K)) GO TO 66
      CM(LB,IA)=DZ(K)/STC*TPERM(CKS(IS,J),CKSAT(I,J,K),HSP(IS,J),ZBS(IS,
     2J),STC,DY(J),DXS(IS),DXC(I))
      GO TO 67
   66 DZR=HCP(I,J,K)-BOT
      CM(LB,IA)=DZR/STC*TPERM(CKS(IS,J),CKSAT(I,J,K),HSP(IS,J),ZBS(IS,J)
     2,STC,DY(J),DXS(IS),DXC(I))
   67 IF(KODC(I,J,K).NE.1) GO TO 70
      CM(LB,IM)=CM(LB,IM)-CM(LB,IA)
      C(LB)=C(LB)-HCP(I,J,K)*CM(LB,IA)
   69 CM(LB,IA)=0.0
   70 CM(LB,IM)=CM(LB,IM)-CM(LB,IA)
   75 CONTINUE
   80 CM(LB,IM)=CM(LB,IM)-DXS(IS)*DY(J)*SY/DT
      C(LB)=C(LB)-HSP(IS,J)*DXS(IS)*DY(J)*SY/DT-QIS(IS,J)
      GO TO 99
   90 CM(LB,IM)=1.0
      C(LB)=HSP(IS,J)
   99 LB=LB+1
    8 CONTINUE
      LCK=LB-1
      IF(LCK.NE.LE) WRITE(6,77)
```

```
   77 FORMAT(5X,*ERROR IN LOOP INDEX IN SUBROUTINE STRAN*/)
      RETURN
      END
      SUBROUTINE CTRAN  (LB,LE,LS,KODS,CKS,HSP,ZBS,DXS,QIS,MS,ISIDE)
      DIMENSION KODS(LS,MS),CKS(LS,MS),HSP(LS,MS),ZBS(LS,MS),DXS(LS),
     2QIS(LS,MS)
      COMMON LC,M,N,LRL,LRM,LRIV,NADJ,NCAN,HPB,SK,TH,SY,AN,BSC,VT,POR,
     2TIME,TCON,DT,C(384),DXC(8),DY(8),DZ(4),DB(8),IRIV(47),JRIV(47),
     3RBED(47),RWID(47),RSLP(47),QRIV(47),DIV(47),RSO(47),VMS(47),
     4VMB(47),SDRIV(20),FKFAC(20),CDV(9),PCT(9),AREA(9),LCAN(10),
     5QJMD(3),QLAM(3),QKAN(3),CM(384,49),NDL(12,8),NDC(8,8),NDR(22,8),
     6HTEMP(8,8),QIC(8,8),KODC(8,8,4),HCP(8,8,4),ZC(8,8,4),CKC(8,8,4),
     7CKSAT(8,8,4),DSDHP(8,8,4)
C
C  ***************************************************************************
C  THIS SUBROUTINE IS CALLED FROM MATSOL TO COMPUTE COEFFICIENTS AND COLUMN
C  VECTOR VALUES FOR GRIDS INT HE THREE-DIMENSIONAL MODEL SEGMENT THAT ARE
C  ADJACENT ON ONE SIDE TO A GRID IN THE TWO-DIMENSIONAL MODEL SEGMENT.
C  ***************************************************************************
C
      PERM(CK1,CK2,SA1,SA2,DIST1,DIST2)=(2.0*CK1*CK2*SA1*SA2)/(DIST2*
     2CK1+DIST1*CK2)
      CPERM(CK1,CK2,CO,BK,SA1,SA2,DIST1,DIST2)=(2.0*CK1*CK2*CO*BK*SA1*SA
     22)/(DIST2*CK1+DIST1*CK2*CO*BK)
      RPERM(CK1,CK2,SA1,SA2,DIST1,DIST2) = (2.0*CK1*CK2*SA1*SA2)/(DIST2
     2*CK1+2.0*DIST1*CK2)
      TPERM(CKB,SA1,SA2,SL)=2.0*CKB*SA1*SA2/SL
      MR=M-1
      IM=(M-2)*N+1
      IE=IM-1
      IF=IM+1
      IC=IM-N
      ID=IM+N
      GO TO (10,15) ISIDE
   10 IB=IM+N*(M-2)
      IS=LS
      I=1
      GO TO 20
   15 IA=IM-N*(M-2)
      IS=1
      I=LC
   20 DO 8 J=2,MR
      DO 8 K=1,N
      FK=1.0
      BKR=1.0
      IF(KODC(I,J,K).EQ.1.OR.KODC(I,J,K).GE.6) GO TO 90
      IF(CKC(I,J,K).LT.0.005) GO TO 90
C     CCCCCCCCCCCCCCCCCCCCCCCCCCCCCCCCCCCCCCCCCCCCCCCCCCCCCCCCCCCCCCCCCCCCCCCCCC
      IF(KODC(I,J-1,K).GE.6.AND.KODC(I,J,K).EQ.3) GO TO 25
      IF(KODC(I,J-1,K).GE.6.AND.KODC(I,J,K).NE.3) GO TO 28
      CM(LB,IC)=PERM(CKC(I,J,K),CKC(I,J-1,K),DXC(I),DZ(K),DY(J),DY(J-1))
      IF(KODC(I,J-1,K).NE.1) GO TO 22
      GO TO 21
   28 IF(HCP(I,J,K).GE.HCP(I,J-1,K)) CM(LB,IC)=TPERM(CKC(I,J,K),DXC(I),D
     2Z(K),DY(J))
      IF(HCP(I,J,K).LT.HCP(I,J-1,K)) CM(LB,IC)=RPERM(SK,CKC(I,J,K),DXC(I
     2),DZ(K),TH,DY(J))
   21 CM(LB,IM)=CM(LB,IM)-CM(LB,IC)
      C(LB)=C(LB)-HCP(I,J-1,K)*CM(LB,IC)
      CM(LB,IC)=0.0
   22 GO TO 30
   25 CM(LB,IC)=0.0
      IJK=KODC(I,J-1,K)
      HT=HCP(I,J-1,K)-(ZC(I,J-1,K)-0.5*DZ(K))
      C(LB)=C(LB)-VMS(IJK)*DXC(I)*HT
C     DDDDDDDDDDDDDDDDDDDDDDDDDDDDDDDDDDDDDDDDDDDDDDDDDDDDDDDDDDDDDDDDDDDDDDDDDD
   30 IF(KODC(I,J+1,K).GE.6.AND.KODC(I,J,K).EQ.3) GO TO 35
      IF(KODC(I,J+1,K).GE.6.AND.KODC(I,J,K).NE.3) GO TO 38
      CM(LB,ID)=PERM(CKC(I,J,K),CKC(I,J+1,K),DXC(I),DZ(K),DY(J),DY(J+1))
      IF(KODC(I,J+1,K).NE.1) GO TO  32
      GO TO 31
   38 IF(HCP(I,J,K).GE.HCP(I,J+1,K)) CM(LB,ID)=TPERM(CKC(I,J,K),DXC(I),D
     2Z(K),DY(J))
      IF(HCP(I,J,K).LT.HCP(I,J+1,K)) CM(LB,ID)=RPERM(SK,CKC(I,J,K),DXC(I
     2),DZ(K),TH,DY(J))
```

```
   31 CM(LB,IM)=CM(LB,IM)-CM(LB,ID)
      C(LB)=C(LB)-HCP(I,J+1,K)*CM(LB,ID)
      CM(LB,ID)=0.0
   32 GO TO 40
   35 CM(LB,ID)=0.0
      IJK=KODC(I,J+1,K)
      HT=HCP(I,J+1,K)-(ZC(I,J+1,K)-0.5*DZ(K))
      C(LB)=C(LB)-VMS(IJK)*DXC(I)*HT
C     FFFFFFFFFFFFFFFFFFFFFFFFFFFFFFFFFFFFFFFFFFFFFFFFFFFFFFFFFFFFFFFFFFF
   40 IF(K.EQ.N) GO TO 49
      IF(KODC(I,J,K+1).EQ.5) GO TO 49
      IF(CKC(I,J,K+1).LT.0.005) GO TO 49
      IF(KODC(I,J,K+1).GE.6.AND.KODC(I,J,K).EQ.4) GO TO 45
      IF(KODC(I,J,K+1).GE.6.AND.KODC(I,J,K).NE.4) GO TO 48
      CM(LB,IF)=PERM(CKSAT(I,J,K),CKSAT(I,J,K+1),DXC(I),DY(J),DZ(K),
     2DZ(K+1))
      IF(KODC(I,J,K+1).NE.1) GO TO 42
      GO TO 41
   48 IF(HCP(I,J,K).LT.HCP(I,J,K+1)) CM(LB,IF)=TPERM(CKC(I,J,K),DXC(I),D
     2Y(J),DZ(K))
      IF(HCP(I,J,K).LT.HCP(I,J,K+1)) CM(LB,IF)=RPERM(SK,CKC(I,J,K),DXC(I
     2),DY(J),TH,DZ(K))
   41 CM(LB,IM)=CM(LB,IM)-CM(LB,IF)
      C(LB)=C(LB)-HCP(I,J,K+1)*CM(LB,IF)
      CM(LB,IF)=0.0
   42 GO TO 50
   45 CM(LB,IF)=0.0
      IJK=KODC(I,J,K+1)
      C(LB)=C(LB)-VMB(IJK)*DXC(I)*DY(J)
      GO TO 50
   49 CM(LB,IF)=0.0
      C(LB)=C(LB)-QIC(I,J)
C     EEEEEEEEEEEEEEEEEEEEEEEEEEEEEEEEEEEEEEEEEEEEEEEEEEEEEEEEEEEEEEEEEEE
   50 IF(K.EQ.1) GO TO 55
      CM(LB,IE)=PERM(CKSAT(I,J,K),CKSAT(I,J,K-1),DXC(I),DY(J),DZ(K),
     2DZ(K-1))
      IF(KODC(I,J,K-1).NE.1) GO TO 52
      CM(LB,IM)=CM(LB,IM)-CM(LB,IE)
      C(LB)=C(LB)-HCP(I,J,K-1)*CM(LB,IE)
      CM(LB,IE)=0.0
   52 GO TO 60
   55 CM(LB,IE)=0.0
   60 GO TO (70,80) ISIDE
C  A AND B COEFFICIENTS FOR LEFT SIDE (UPSTREAM)
C     BBBBBBBBBBBBBBBBBBBBBBBBBBBBBBBBBBBBBBBBBBBBBBBBBBBBBBBBBBBBBBBBBBB
   70 IA=IM-((M-1-J)+(J-2)*N+K)
      IF(KODC(I+1,J,K).GE.6.AND.KODC(I,J,K).EQ.2) GO TO 75
      IF(KODC(I+1,J,K).GE.6.AND.KODC(I,J,K).NE.2) GO TO 78
      CM(LB,IB)=PERM(CKC(I,J,K),CKC(I+1,J,K),DY(J),DZ(K),DXC(I),DXC(I+1)
     2)
      IF(KODC(I+1,J,K).NE.1) GO TO 72
      GO TO 71
   78 IF(HCP(I,J,K).GE.HCP(I+1,J,K)) CM(LB,IB)=TPERM(CKC(I,J,K),DY(J),DZ
     2(K),DXC(I))
      IF(HCP(I,J,K).LT.HCP(I+1,J,K)) CM(LB,IB)=RPERM(SK,CKC(I,J,K),DY(J)
     2,DZ(K),TH,DXC(I))
   71 CM(LB,IM)=CM(LB,IM)-CM(LB,IB)
      C(LB)=C(LB)-HCP(I+1,J,K)*CM(LB,IB)
      CM(LB,IB)=0.0
   72 GO TO 73
   75 CM(LB,IB)=0.0
      IJK=KODC(I+1,J,K)
      HT=HCP(I+1,J,K)-(ZC(I+1,J,K)-0.5*DZ(K))
      C(LB)=C(LB)-VMS(IJK)*DY(J)*HT
C     AAAAAAAAAAAAAAAAAAAAAAAAAAAAAAAAAAAAAAAAAAAAAAAAAAAAAAAAAAAAAAAAAAAAAA
   73 TOP=ZC(I,J,K)+0.5*DZ(K)
      BOT=ZC(I,J,K)-0.5*DZ(K)
      IF(TOP.GT.HSP(IS,J)) CALL KFNP(ZC(I,J,K),HSP(IS,J),FK,TOP,BOT)
      BKR=(TOP-ZBS(IS,J))/DZ(K)
      IF(BKR.LT.0.0) BKR=0.0
      IF(BKR.GT.1.0) BKR=1.0
      CM(LB,IA)=CPERM(CKC(I,J,K),CKS(IS,J),FK,BKR,DY(J),DZ(K),DXC(I),DXS
     2(IS))
      IF(KODS(IS,J).NE.1.AND.KODS(IS,J).LT.6) GO TO 74
      CM(LB,IM)=CM(LB,IM)-CM(LB,IA)
      C(LB)=C(LB)-HSP(IS,J)*CM(LB,IA)
      CM(LB,IA)=0.0
```

```
   74 GO TO 84
C     A AND B COEFFICIENTS FOR RIGHT SIDE   (DOWNSTREAM)
C     AAAAAAAAAAAAAAAAAAAAAAAAAAAAAAAAAAAAAAAAAAAAAAAAAAAAAAAAAAAAAAAA
   80 IB=IM+((M-1-J)*N+(N-K)+(J-1))
      IF(KODC(I-1,J,K).GE.6.AND.KODC(I,J,K).EQ.2) GO TO 85
      IF(KODC(I-1,J,K).GE.6.AND.KODC(I,J,K).NE.2) GO TO 88
      CM(LB,IA)=PERM(CKC(I,J,K),CKC(I-1,J,K),DY(J),DZ(K),DXC(I),DXC(I-1)
     2)
      IF(KODC(I-1,J,K).NE.1) GO TO 82
      GO TO 81
   88 IF(HCP(I,J,K).GE.HCP(I-1,J,K)) CM(LB,IA)=TPERM(CKC(I,J,K),DY(J),DZ
     2(K),DXC(I))
      IF(HCP(I,J,K).LT.HCP(I-1,J,K)) CM(LB,IA)=RPERM(SK,CKC(I,J,K),DY(J)
     2,DZ(K),TH,DXC(I))
   81 CM(LB,IM)=CM(LB,IM)-CM(LB,IA)
      C(LB)=C(LB)-HCP(I-1,J,K)*CM(LB,IA)
      CM(LB,IA)=0.0
   82 GO TO 83
   85 CM(LB,IA)=0.0
      IJK=KODC(I-1,J,K)
      HT=HCP(I-1,J,K)-(ZC(I-1,J,K)-0.5*DZ(K))
      C(LB)=C(LB)-VMS(IJK)*DY(J)*HT
C     BBBBBBBBBBBBBBBBBBBBBBBBBBBBBBBBBBBBBBBBBBBBBBBBBBBBBBBBBBBBBBBBBBBBBB
   83 TOP=ZC(I,J,K)+0.5*DZ(K)
      BOT=ZC(I,J,K)-0.5*DZ(K)
      IF(TOP.GT.HSP(IS,J)) CALL KFNP(ZC(I,J,K),HSP(IS,J),FK,TOP,BOT)
      BKR=(TOP-ZBS(IS,J))/DZ(K)
      IF(BKR.LT.0.0) BKR=0.0
      IF(BKR.GT.1.0) BKR=1.0
      CM(LB,IB)=CPERM(CKC(I,J,K),CKS(IS,J),FK,BKR,DY(J),DZ(K),DXC(I),DXS
     2(IS))
      IF(KODS(IS,J).NE.1.AND.KODS(IS,J).LT.6) GO TO 84
      CM(LB,IM)=CM(LB,IM)-CM(LB,IB)
      C(LB)=C(LB)-HSP(IS,J)*CM(LB,IB)
      CM(LB,IB)=0.0
   84 CM(LB,IM)=CM(LB,IM)-(CM(LB,IA)+CM(LB,IB)+CM(LB,IC)+CM(LB,ID)+
     2CM(LB,IE)+CM(LB,IF)  +POR*DXC(I)*DY(J)*DZ(K)*DSDHP(I,J,K)/DT)
      C(LB)=C(LB)-HCP(I,J,K)*POR*DXC(I)*DY(J)*DZ(K)*DSDHP(I,J,K)/DT
      GO TO 99
   90 CM(LB,IM)=1.0
      C(LB)=HCP(I,J,K)
   99 LB=LB+1
    8 CONTINUE
      LCK=LB-1
      IF(LCK.NE.LE) WRITE(6,7)
    7 FORMAT(5X,*ERROR IN LOOP INDEX IN SUBROUTINE CTRAN*,/)
      RETURN
      END
      SUBROUTINE CENTER(LB,LE)
      COMMON LC,M,N,LRL,LRM,LRIV,NADJ,NCAN,HPB,SK,TH,SY,AN,BSC,VT,POR,
     2TIME,TCON,DT,C(384),DXC(8),DY(8),DZ(4),DB(8),IRIV(47),JRIV(47),
     3RBED(47),RWID(47),RSLP(47),QRIV(47),DIV(47),RSO(47),VMS(47),
     4VMB(47),SDRIV(20),FKFAC(20),CDV(9),PCT(9),AREA(9),LCAN(10),
     5QJMD(3),QLAM(3),QKAN(3),CM(384,49),NDL(12,8),NDC(8,8),NDR(22,8),
     6HTEMP(8,8),QIC(8,8),KODC(8,8,4),HCP(8,8,4),ZC(8,8,4),CKC(8,8,4),
     7CKSAT(8,8,4),DSDHP(8,8,4)
      COMMON /A/ LL,DXL(12),KODL(12,8),CKL(12,8),HLP(12,8),ZBL(12,8),
     2QIL(12,8)
      COMMON /B/ LR,DXR(22),KODR(22,8),CKR(22,8),HRP(22,8),ZBR(22,8),
     2QIR(22,8)
C
C     ******************************************************************
C     THIS SUBROUTINE IS CALLED FROM MATSOL TO COMPUTE COEFFICIENTS AND COLUMN
C     VECTOR VALUES FOR GRIDS IN THE THREE-DIMENSIONAL MODEL SEGMENT THAT ARE
C     SURROUNDED LATERALLY BY OTHER THREE-DIMENSIONAL GRIDS.
C     ******************************************************************
C
      PERM(CK1,CK2,SA1,SA2,DIST1,DIST2) = (2.0*CK1*CK2*SA1*SA2)/(DIST2*
     2CK1+DIST1*CK2)
      RPERM(CK1,CK2,SA1,SA2,DIST1,DIST2) = (2.0*CK1*CK2*SA1*SA2)/(DIST2
     2*CK1+2.0*DIST1*CK2)
C     DIST1=TH, CK1=SK
      TPERM(CKB,SA1,SA2,SL)=2.0*CKB*SA1*SA2/SL
      IM=(M-2)*N+1
      IE=IM-1
      IF=IM+1
```

```
      IC=IM-N
      ID=IM+N
      IA=IM-(M-2)*N
      IB=IM+(M-2)*N
      MR=M-1
      LCR=LC-1
      QA=345600.0
      QB=518400.0
      REMA=1.0
      REMB=1.0
      IW=4
      JW=3
      DO 385 K=1,N
      TOP=ZC(IW,JW,K)+0.5*DZ(K)
      IF(HCP(IW,JW,K).GT.TOP) GO TO 385
      HST=HCP(IW,JW,K)
      GO TO 386
  385 CONTINUE
  386 WHTA=HST-(ZC(IW,JW,1)+0.5*DZ(1))
      JW=4
      DO 485 K=1,N
      TOP=ZC(IW,JW,K)+0.5*DZ(K)
      IF(HCP(IW,JW,K).GT.TOP) GO TO 485
      HST=HCP(IW,JW,K)
      GO TO 486
  485 CONTINUE
  486 WHTB=HST-(ZC(IW,JW,1)-0.5*DZ(1))
      DO 8 I=2,LCR
      DO 8 J=2,MR
      DO 7 K=1,N
      IF(KODC(I,J,K).EQ.1.OR.KODC(I,J,K).GE.6) GO TO 90
      IF(CKC(I,J,K).LT.0.005) GO TO 90
C     AAAAAAAAAAAAAAAAAAAAAAAAAAAAAAAAAAAAAAAAAAAAAAAAAAAAAAAAAAAAAAAAAAAAAAA
   10 IF(KODC(I-1,J,K).GE.6.AND.KODC(I,J,K).EQ.2) GO TO 15
      IF(KODC(I-1,J,K).GE.6.AND.KODC(I,J,K).NE.2) GO TO 18
      CM(LB,IA)=PERM(CKC(I,J,K),CKC(I-1,J,K),DY(J),DZ(K),DXC(I),DXC(I-1)
     2)
      IF(KODC(I-1,J,K).NE.1) GO TO 12
      GO TO 11
   18 IF(HCP(I,J,K).GE.HCP(I-1,J,K)) CM(LB,IA)=TPERM(CKC(I,J,K),DY(J),DZ
     2(K),DXC(I))
      IF(HCP(I,J,K).LT.HCP(I-1,J,K)) CM(LB,IA)=RPERM(SK,CKC(I,J,K),DY(J)
     2,DZ(K),TH,DXC(I))
   11 CM(LB,IM)=CM(LB,IM)-CM(LB,IA)
      C(LB)=C(LB)-HCP(I-1,J,K)*CM(LB,IA)
      CM(LB,IA)=0.0
   12 GO TO 20
   15 CM(LB,IA)=0.0
      IJK=KODC(I-1,J,K)
      HT=HCP(I-1,J,K)-(ZC(I-1,J,K)-0.5*DZ(K))
      C(LB)=C(LB)-VMS(IJK)*DY(J)*HT
C     BBBBBBBBBBBBBBBBBBBBBBBBBBBBBBBBBBBBBBBBBBBBBBBBBBBBBBBBBBBBBBBBBBBBBBB
   20 IF(KODC(I+1,J,K).GE.6.AND.KODC(I,J,K).EQ.2) GO TO 25
      IF(KODC(I+1,J,K).GE.6.AND.KODC(I,J,K).NE.2) GO TO 28
      CM(LB,IB)=PERM(CKC(I,J,K),CKC(I+1,J,K),DY(J),DZ(K),DXC(I),DXC(I+1)
     2)
      IF(KODC(I+1,J,K).NE.1) GO TO 22
      GO TO 21
   28 IF(HCP(I,J,K).GE.HCP(I+1,J,K)) CM(LB,IB)=TPERM(CKC(I,J,K),DY(J),DZ
     2(K),DXC(I))
      IF(HCP(I,J,K).LT.HCP(I+1,J,K)) CM(LB,IB)=RPERM(SK,CKC(I,J,K),DY(J)
     2,DZ(K),TH,DXC(I))
   21 CM(LB,IM)=CM(LB,IM)-CM(LB,IB)
      C(LB)=C(LB)-HCP(I+1,J,K)*CM(LB,IB)
      CM(LB,IB)=0.0
   22 GO TO 30
   25 CM(LB,IB)=0.0
      IJK=KODC(I+1,J,K)
      HT=HCP(I+1,J,K)-(ZC(I+1,J,K)-0.5*DZ(K))
      C(LB)=C(LB)-VMS(IJK)*DY(J)*HT
C     CCCCCCCCCCCCCCCCCCCCCCCCCCCCCCCCCCCCCCCCCCCCCCCCCCCCCCCCCCCCCCCCCCCCCCC
   30 IF(KODC(I,J-1,K).GE.6.AND.KODC(I,J,K).EQ.3) GO TO 35
      IF(KODC(I,J-1,K).GE.6.AND.KODC(I,J,K).NE.3) GO TO 38
      CM(LB,IC)=PERM(CKC(I,J,K),CKC(I,J-1,K),DXC(I),DZ(K),DY(J),DY(J-1))
      IF(KODC(I,J-1,K).NE.1) GO TO 32
      GO TO 31
```

```
   38 IF(HCP(I,J,K).GE.HCP(I,J-1,K)) CM(LB,IC)=TPERM(CKC(I,J,K),DXC(I),D
     2Z(K),DY(J))
      IF(HCP(I,J,K).LT.HCP(I,J-1,K)) CM(LB,IC)=RPERM(SK,CKC(I,J,K),DXC(I
     2),DZ(K),TH,DY(J))
   31 CM(LB,IM)=CM(LB,IM)-CM(LB,IC)
      C(LB)=C(LB)-HCP(I,J-1,K)*CM(LB,IC)
      CM(LB,IC)=0.0
   32 GO TO 40
   35 CM(LB,IC)=0.0
      IJK=KODC(I,J-1,K)
      HT=HCP(I,J-1,K)-(ZC(I,J-1,K)-0.5*DZ(K))
      C(LB)=C(LB)-VMS(IJK)*DXC(I)*HT
C     DDDDDDDDDDDDDDDDDDDDDDDDDDDDDDDDDDDDDDDDDDDDDDDDDDDDDDDDDDDDDDDDDD
   40 IF(KODC(I,J+1,K).GE.6.AND.KODC(I,J,K).EQ.3) GO TO 45
      IF(KODC(I,J+1,K).GE.6.AND.KODC(I,J,K).NE.3) GO TO 48
      CM(LB,ID)=PERM(CKC(I,J,K),CKC(I,J+1,K),DXC(I),DZ(K),DY(J),DY(J+1))
      IF(KODC(I,J+1,K).NE.1) GO TO 42
      GO TO 41
   48 IF(HCP(I,J,K).GE.HCP(I,J+1,K)) CM(LB,ID)=TPERM(CKC(I,J,K),DXC(I),D
     2Z(K),DY(J))
      IF(HCP(I,J,K).LT.HCP(I,J+1,K)) CM(LB,ID)=RPERM(SK,CKC(I,J,K),DXC(I
     2),DZ(K),TH,DY(J))
   41 CM(LB,IM)=CM(LB,IM)-CM(LB,ID)
      C(LB)=C(LB)-HCP(I,J+1,K)*CM(LB,ID)
      CM(LB,ID)=0.0
   42 GO TO 50
   45 CM(LB,ID)=0.0
      IJK=KODC(I,J+1,K)
      HT=HCP(I,J+1,K)-(ZC(I,J+1,K)-0.5*DZ(K))
      C(LB)=C(LB)-VMS(IJK)*DXC(I)*HT
C     FFFFFFFFFFFFFFFFFFFFFFFFFFFFFFFFFFFFFFFFFFFFFFFFFFFFFFFFFFFFFFFFFF
   50 IF(K.EQ.N) GO TO 59
      IF(KODC(I,J,K+1).EQ.5) GO TO 59
      IF(CKC(I,J,K+1).LT.0.005) GO TO 59
      IF(KODC(I,J,K+1).GE.6.AND.KODC(I,J,K).EQ.4) GO TO 55
      IF(KODC(I,J,K+1).GE.6.AND.KODC(I,J,K).NE.4) GO TO 58
      CM(LB,IF)=PERM(CKSAT(I,J,K),CKSAT(I,J,K+1),DXC(I),DY(J),DZ(K),
     2DZ(K+1))
      IF(KODC(I,J,K+1).NE.1) GO TO 52
      GO TO 51
   58 IF(HCP(I,J,K).LT.HCP(I,J,K+1)) CM(LB,IF)=TPERM(CKC(I,J,K),DXC(I),D
     2Y(J),DZ(K))
      IF(HCP(I,J,K).LT.HCP(I,J,K+1)) CM(LB,IF)=RPERM(SK,CKC(I,J,K),DXC(I
     2),DY(J),TH,DZ(K))
   51 CM(LB,IM)=CM(LB,IM)-CM(LB,IF)
      C(LB)=C(LB)-HCP(I,J,K+1)*CM(LB,IF)
      CM(LB,IF)=0.0
   52 GO TO 60
   55 CM(LB,IF)=0.0
      IJK=KODC(I,J,K+1)
      C(LB)=C(LB)-VMB(IJK)*DXC(I)*DY(J)
      GO TO 60
   59 CM(LB,IF)=0.0
      C(LB)=C(LB)-QIC(I,J)
C     EEEEEEEEEEEEEEEEEEEEEEEEEEEEEEEEEEEEEEEEEEEEEEEEEEEEEEEEEEEEEEEEEE
   60 IF(K.EQ.1) GO TO 65
      CM(LB,IE)=PERM(CKSAT(I,J,K),CKSAT(I,J,K-1),DXC(I),DY(J),DZ(K),
     2DZ(K-1))
      IF(KODC(I,J,K-1).NE.1) GO TO 62
      CM(LB,IM)=CM(LB,IM)-CM(LB,IE)
      C(LB)=C(LB)-HCP(I,J,K-1)*CM(LB,IE)
      CM(LB,IE)=0.0
   62 GO TO 70
   65 CM(LB,IE)=0.0
C     MMMMMMMMMMMMMMMMMMMMMMMMMMMMMMMMMMMMMMMMMMMMMMMMMMMMMMMMMMMMMMMMMM
   70 CM(LB,IM)=CM(LB,IM)-(CM(LB,IA)+CM(LB,IB)+CM(LB,IC)+CM(LB,ID)+
     2CM(LB,IE)+CM(LB,IF))-POR*DXC(I)*DY(J)*DZ(K)*DSDHP(I,J,K)/DT
   71 C(LB)=C(LB)-HCP(I,J,K)*POR*DXC(I)*DY(J)*DZ(K)*DSDHP(I,J,K)/DT
C   LAMAR WELLS
      QP=0.0
      IF(I.EQ.4.AND.J.EQ.3.AND.K.GT.1) GO TO 601
      IF(I.EQ.4.AND.J.EQ.4) GO TO 602
      GO TO 72
  601 IF(WHTA.LT.0.0) GO TO 72
      IF(WHTA.GT.DZ(K)) QP=REMA*QA*DZ(K)/WHTA
      IF(WHTA.LE.DZ(K)) QP=REMA*QA
```

```
      REMA=REMA-QP/QA
      WHTA=WHTA-DZ(K)
      C(LB)=C(LB)+QP
      WRITE(6,901) QP
  901 FORMAT(5X,*QP=*,F9.2,5X,*CFD*,/)
      GO TO 72
  602 IF(WHTB.LT.0.0) GO TO 72
      IF(WHTB.GT.DZ(K)) QP=REMB*QB*DZ(K)/WHTB
      IF(WHTB.LE.DZ(K)) QP=REMB*QB
      REMB=REMB-QP/QB
      WHTB=WHTB-DZ(K)
      C(LB)=C(LB)+QP
      WRITE(6,901) QP
   72 GO TO 99
   90 CM(LB,IM)=1.0
      C(LB)=HCP(I,J,K)
   99 LB=LB+1
    7 CONTINUE
    8 CONTINUE
      LCK=LB-1
      IF(LCK.NE.LE) WRITE(6,3)
    3 FORMAT(5X,*ERROR IN LOOP INDEX IN SUBROUTINE CENTER*,/)
      RETURN
      END
      SUBROUTINE BSOLVE (C,N,M,V)
      DIMENSION C(N,M),V(N)
C
C  ***************************************************************************
C  THIS SUBROUTINE IS CALLED FROM MATSOL TO SOLVE THE MATRIX FOR NEW VALUES
C  OF HEAD IN EACH GROUNDWATER GRID USING THE GAUSS-ELIMINATION TECHNIQUE.
C  ***************************************************************************
C
      LR=(M-1)/2
      DO 2 L=1,LR
      IM=LR-L+1
      DO 2 I=1,IM
      DO 1 J=2,M
    1 C(L,J-1)=C(L,J)
      KN=N-L
      KM=M-I
      C(L,M)=0.0
    2 C(KN+1,KM+1)=0.0
      LR=LR+1
      IM=N-1
      DO 10 I=1,IM
      NPIV=I
      LS=I+1
      DO 3 L=LS,LR
      IF (ABS(C(L,1)).GT.ABS(C(NPIV,1))) NPIV=L
    3 CONTINUE
      IF (NPIV.LE.I) 6,4
    4 DO 5 J=1,M
      TEMP=C(I,J)
      C(I,J)=C(NPIV,J)
    5 C(NPIV,J)=TEMP
      TEMP=V(I)
      V(I)=V(NPIV)
      V(NPIV)=TEMP
    6 V(I)=V(I)/C(I,1)
      DO 7 J=2,M
    7 C(I,J)=C(I,J)/C(I,1)
      DO 9 L=LS,LR
      TEMP=C(L,1)
      V(L)=V(L)-TEMP*V(I)
      DO 8 J=2,M
    8 C(L,J-1)=C(L,J)-TEMP*C(I,J)
    9 C(L,M)=0.0
      IF (LR.LT.N) LR=LR+1
   10 CONTINUE
      V(N)=V(N)/C(N,1)
      JM=2
      DO 12 I=1,IM
      L=N-I
      DO 11 J=2,JM
      KM=L+J
```

```
   11 V(L)=V(L)-C(L,J)*V(KM-1)
      IF (JM.LT.M) JM=JM+1
   12 CONTINUE
      RETURN
      END
      SUBROUTINE RIVBND
      COMMON LC,M,N,LRL,LRM,LRIV,NADJ,NCAN,HPB,SK,TH,SY,AN,BSC,VT,POR,
     2TIME,TCON,DT,C(384),DXC(8),DY(8),DZ(4),DB(8),IRIV(47),JRIV(47),
     3RBED(47),RWID(47),RSLP(47),QRIV(47),DIV(47),RSO(47),VMS(47),
     4VMB(47),SDRIV(20),FKFAC(20),CDV(9),PCT(9),AREA(9),LCAN(10),
     5QJMD(3),QLAM(3),QKAN(3),CM(384,49),NDL(12,8),NDC(8,8),NDR(22,8),
     6HTEMP(8,8),QIC(8,8),KODC(8,8,4),HCP(8,8,4),ZC(8,8,4),CKC(8,8,4),
     7CKSAT(8,8,4),DSDHP(8,8,4)
      COMMON /A/ LL,DXL(12),KODL(12,8),CKL(12,8),HLP(12,8),ZBL(12,8),
     2QIL(12,8)
      COMMON /B/ LR,DXR(22),KODR(22,8),CKR(22,8),HRP(22,8),ZBR(22,8),
     2QIR(22,8)
C  *****ATTENTION***** RIVER MUST REMAIN IN SAME GRID IN Y DIRECTION
C  (SAME J SUBSCRIPT) CROSSING FROM 2-D TO 3-D OR 3-D TO 2-D REGION
C
C  ************************************************************************
C  THIS SUBROUTINE COMPUTES SEEPAGE RATES TO AND FROM THE AQUIFER FOR EACH
C  RIVER GRID OF THE MODEL.
C  ************************************************************************
C
      TPERM(CK1,CK2,H1,Z1,H2,Z2,XY,DXY1,DXY2)=(2.0*CK1*CK2*(H1-Z1)*(H2-Z
     22)*XY)/(DXY2*CK1*(H1-Z1)+DXY1*CK2*(H2-Z2))
      VT=0.0
      DO 6 I=1,LRIV
      RSO(I)=0.0
    6 CONTINUE
      DO 7 L=6,LRL
      I=IRIV(L)
      J=JRIV(L)
      IF(KODL(I,J-1).GE.6) GO TO 10
      RSO(L)=RSO(L)+TPERM(CKL(I,J),CKL(I,J-1),HLP(I,J),ZBL(I,J),HLP(I,J-
     21),ZBL(I,J-1),DXL(I),DY(J),DY(J-1))*(HLP(I,J)-HLP(I,J-1))
   10 IF(KODL(I,J+1).GE.6) GO TO 11
      RSO(L)=RSO(L)+TPERM(CKL(I,J),CKL(I,J+1),HLP(I,J),ZBL(I,J),HLP(I,J+
     21),ZBL(I,J+1),DXL(I),DY(J),DY(J+1))*(HLP(I,J)-HLP(I,J+1))
   11 IF(I.LE.1) GO TO 12
      IF(KODL(I-1,J).GE.6) GO TO 12
      RSO(L)=RSO(L)+TPERM(CKL(I,J),CKL(I-1,J),HLP(I,J),ZBL(I,J),HLP(I-1,
     2J),ZBL(I-1,J),DY(J),DXC(I),DXC(I-1))*(HLP(I,J)-HLP(I-1,J))
   12 IF(I.GE.LL) GO TO 13
      IF(KODL(I+1,J).GE.6) GO TO 13
      RSO(L)=RSO(L)+TPERM(CKL(I,J),CKL(I+1,J),HLP(I,J),ZBL(I,J),HLP(I+1,
     2J),ZBL(I+1,J),DY(J),DXC(I),DXC(I+1))*(HLP(I,J)-HLP(I+1,J))
   13 VT=VT+RSO(L)*DT
    7 CONTINUE
      LB=LRL+1
      LBCA=LB
      LBCB=LRM
      CALL SPLIT(LBCA,LBCB)
      LB=LRM+1
      DO 9 L=LB,LRIV
      I=IRIV(L)
      J=JRIV(L)
      IF(I.EQ.8) DXR(I)=DB(J)
      IF(KODR(I,J-1).GE.6) GO TO 70
      RSO(L)=RSO(L)+TPERM(CKR(I,J),CKR(I,J-1),HRP(I,J),ZBR(I,J),HRP(I,J-
     21),ZBR(I,J-1),DXR(I),DY(J),DY(J-1))*(HRP(I,J)-HRP(I,J-1))
   70 IF(KODR(I,J+1).GE.6) GO TO 71
      RSO(L)=RSO(L)+TPERM(CKR(I,J),CKR(I,J+1),HRP(I,J),ZBR(I,J),HRP(I,J+
     21),ZBR(I,J+1),DXR(I),DY(J),DY(J+1))*(HRP(I,J)-HRP(I,J+1))
   71 IF(I.LE.1) GO TO 72
      IF(KODR(I-1,J).GE.6) GO TO 72
      RSO(L)=RSO(L)+TPERM(CKR(I,J),CKR(I-1,J),HRP(I,J),ZBR(I,J),HRP(I-1,
     2J),ZBR(I-1,J),DY(J),DXR(I),DXR(I-1))*(HRP(I,J)-HRP(I-1,J))
   72 IF(I.GE.LR) GO TO 73
      IF(KODR(I+1,J).GE.6) GO TO 73
      RSO(L)=RSO(L)+TPERM(CKR(I,J),CKR(I+1,J),HRP(I,J),ZBR(I,J),HRP(I+1,
     2J),ZBR(I+1,J),DY(J),DXR(I),DXR(I+1))*(HRP(I,J)-HRP(I+1,J))
   73 VT=VT+RSO(L)*DT
    9 CONTINUE
```

```
   80 RETURN
      END
      SUBROUTINE SPLIT(LAC,LBC)
      COMMON LC,M,N,LRL,LRM,LRIV,NADJ,NCAN,HPB,SK,TH,SY,AN,BSC,VT,POR,
     2TIME,TCON,DT,C(384),DXC(8),DY(8),DZ(4),DB(8),IRIV(47),JRIV(47),
     3RBED(47),RWID(47),RSLP(47),QRIV(47),DIV(47),RSO(47),VMS(47),
     4VMB(47),SDRIV(20),FKFAC(20),CDV(9),PCT(9),AREA(9),LCAN(10),
     5QJMD(3),QLAM(3),QKAN(3),CM(384,49),NDL(12,8),NDC(8,8),NDR(22,8),
     6HTEMP(8,8),QIC(8,8),KODC(8,8,4),HCP(8,8,4),ZC(8,8,4),CKC(8,8,4),
     7CKSAT(8,8,4),DSDHP(8,8,4)
      COMMON /A/ LL,DXL(12),KODL(12,8),CKL(12,8),HLP(12,8),ZBL(12,8),
     2QIL(12,8)
      COMMON /B/ LR,DXR(22),KODR(22,8),CKR(22,8),HRP(22,8),ZBR(22,8),
     2QIR(22,8)
C  *****ATTENTION***** RIVER MUST REMAIN IN SAME GRID IN Y DIRECTION
C  (SAME J SUBSCRIPT) CROSSING FROM 2-D TO 3-D OR 3-D TO 2-D REGION
C
C  ************************************************************************
C  THIS SUBROUTINE IS CALLED FROM RIVBND TO COMPUTE SEEPAGE RATES IN THE
C  RIVER GRIDS LOCATED IN THE THREE-DIMENSIONAL MODEL SEGMENT.
C  ************************************************************************
C
      APERM(CK1,SKA,DXA1,DXA2,THA,DS)=(2.0*CK1*SKA*DXA1*DXA2)/(2.0*THA*C
     2K1+DS*SKA)
      BPERM(CK1,DXA1,DXA2,DS)=(2.0*CK1*DXA1*DXA2/DS)
      DO 8 L=LAC,LBC
      I=IRIV(L)
      J=JRIV(L)
      VMB(L)=SK*(((HCP(I,J,N)-RBED(L))-HPB)+TH)/TH
      VMS(L)=SK*((HCP(I,J,N)-RBED(L))-HPB)*0.5/TH
      IF(KODC(I,J-1,N).GE.6) GO TO 20
      IF(HCP(I,J,N).LT.HCP(I,J-1,N)) GO TO 112
      QS=APERM(CKSAT(I,J-1,N),SK,DXC(I),DZ(N),TH,DY(J-1))*(HCP(I,J,N)-
     2HCP(I,J-1,N))
      GO TO 114
  112 QS=BPERM(CKC(I,J-1,N),DXC(I),DZ(N),DY(J-1))*(HCP(I,J,N)-HCP(I,J-1,
     2N))
  114 QU=VMS(L)*DXC(I)*DZ(N)
      IF(QU.GT.QS) GO TO 15
      KODC(I,J-1,N)=3
      RSO(L)=RSO(L)+QU
      GO TO 20
   15 KODC(I,J-1,N)=0
      RSO(L)=RSO(L)+QS
   20 IF(KODC(I,J+1,N).GE.6) GO TO 30
      IF(HCP(I,J,N).LT.HCP(I,J+1,N)) GO TO 122
      QS=APERM(CKSAT(I,J+1,N),SK,DXC(I),DZ(N),TH,DY(J+1))*(HCP(I,J,N)-
     2HCP(I,J+1,N))
      GO TO 124
  122 QS=BPERM(CKC(I,J+1,N),DXC(I),DZ(N),DY(J+1))*(HCP(I,J,N)-HCP(I,J+1,
     2N))
  124 QU=VMS(L)*DXC(I)*DZ(N)
      IF(QU.GT.QS) GO TO 25
      KODC(I,J+1,N)=3
      RSO(L)=RSO(L)+QU
      GO TO 30
   25 KODC(I,J+1,N)=0
      RSO(L)=RSO(L)+QS
   30 IF(I.LE.1) GO TO 40
      IF(KODC(I-1,J,N).GE.6) GO TO 40
      IF(HCP(I,J,N).LT.HCP(I-1,J,N)) GO TO 32
      QS=APERM(CKSAT(I-1,J,N),SK,DY(J),DZ(N),TH,DXC(I-1))*(HCP(I,J,N)-
     2HCP(I-1,J,N))
      GO TO 34
   32 QS=BPERM(CKC(I-1,J,N),DY(J),DZ(N),DXC(I-1))*(HCP(I,J,N)-HCP(I-1,J,
     2N))
   34 QU=VMS(L)*DY(J)*DZ(N)
      IF(QU.GT.QS) GO TO 35
      KODC(I-1,J,N)=2
      RSO(L)=RSO(L)+QU
      GO TO 40
   35 KODC(I-1,J,N)=0
      RSO(L)=RSO(L)+QS
   40 IF(I.GE.LC) GO TO 50
      IF(KODC(I+1,J,N).GE.6) GO TO 50
      IF(HCP(I,J,N).LT.HCP(I+1,J,N)) GO TO 42
```

```
      QS=APERM(CKSAT(I+1,J,N),SK,DY(J),DZ(N),TH,DXC(I+1))*(HCP(I,J,N)-
     2HCP(I+1,J,N))
      GO TO 44
   42 QS=BPERM(CKC(I+1,J,N),DY(J),DZ(N),DXC(I+1))*(HCP(I,J,N)-HCP(I+1,J,
     2N))
   44 QU=VMS(L)*DY(J)*DZ(N)
      IF(QU.GT.QS) GO TO 45
      KODC(I+1,J,N)=2
      RSO(L)=RSO(L)+QU
      GO TO 50
   45 KODC(I+1,J,N)=0
      RSO(L)=RSO(L)+QS
   50 IF(HCP(I,J,N).LT.HCP(I,J,N-1)) GO TO 52
      QS=APERM(CKSAT(I,J,N-1),SK,DXC(I),DY(J),TH,DZ(N-1))*(HCP(I,J,N)-
     2HCP(I,J,N-1))
      GO TO 54
   52 QS=BPERM(CKC(I,J,N-1),DXC(I),DY(J),DZ(N-1))*(HCP(I,J,N)-HCP(I,J,N-
     21))
   54 QU=VMB(L)*DXC(I)*DY(J)
      IF(QU.GT.QS) GO TO 55
      KODC(I,J,N-1) =4
      RSO(L)=RSO(L)+QU
      GO TO 60
   55 KODC(I,J,N-1)=0
      RSO(L)=RSO(L)+QS
   60 VT=VT+RSO(L)*DT
    8 CONTINUE
      RETURN
      END
      SUBROUTINE STORE
      COMMON LC,M,N,LRL,LRM,LRIV,NADJ,NCAN,HPB,SK,TH,SY,AN,BSC,VT,POR,
     2TIME,TCON,DT,C(384),DXC(8),DY(8),DZ(4),DB(8),IRIV(47),JRIV(47),
     3RBED(47),RWID(47),RSLP(47),QRIV(47),DIV(47),RSO(47),VMS(47),
     4VMB(47),SDRIV(20),FKFAC(20),CDV(9),PCT(9),AREA(9),LCAN(10),
     5QJMD(3),QLAM(3),QKAN(3),CM(384,49),NDL(12,8),NDC(8,8),NDR(22,8),
     6HTEMP(8,8),QIC(8,8),KODC(8,8,4),HCP(8,8,4),ZC(8,8,4),CKC(8,8,4),
     7CKSAT(8,8,4),DSDHP(8,8,4)
      COMMON /A/ LL,DXL(12),KODL(12,8),CKL(12,8),HLP(12,8),ZBL(12,8),
     2QIL(12,8)
      COMMON /B/ LR,DXR(22),KODR(22,8),CKR(22,8),HRP(22,8),ZBR(22,8),
     2QIR(22,8)
C
C  ***********************************************************************
C  THIS SUBROUTINE COMPUTES THE MASS BALANCE FOR THE AQUIFER IN ALL INTERIOR
C  GRIDS OF THE MODEL AT THE END OF EACH TIME INCREMENT.  BECAUSE STORAGE ABOVE
C  THE WATER TABLE IS NOT INCLUDED IN THESE CALCULATIONS, THIS MASS BALANCE
C  IS NOT EXACT.
C  ***********************************************************************
C
      MR=M-1
      LRR=LR-1
      STORP=STOR
      IF(TIME.LE.DT) STORP=0.0
      STOR=0.0
      SURF=0.0
      SEEP=0.0
      UFL=0.0
      PUMP=0.0
C  $$$$$$$$$$$$$$$$$$$$$$$$$$$$$$$$$$$$$$$$$$$$$$$$$$$$$$$$$$$$$$$$$$$$$$$$$$$
C   SATURATED STORAGE
      DO 7 I=2,LL
      DO 7 J=2,MR
      STOR=STOR+DXL(I)*DY(J)*(HLP(I,J)-ZBL(I,J))
    7 CONTINUE
      DO 8 I=1,LC
      DO 8 J=2,MR
      DO 8 K=1,N
      GTOP=ZC(I,J,K)+0.5*DZ(K)
      IF(HCP(I,J,K).LT.GTOP) GO TO 15
      STOR=STOR+DXC(I)*DY(J)*DZ(K)
      GO TO 8
   15 GBOT=ZC(I,J,K)-0.5*DZ(K)
      IF(HCP(I,J,K).LT.GBOT) GO TO 8
      STOR=STOR+DXC(I)*DY(J)*(HCP(I,J,K)-GBOT)
```

```
    8 CONTINUE
      DO 9 I=1,LRR
      DO 9 J=2,MR
      IF(I.EQ.8) DXR(I)=DB(J)
      STOR=STOR+DXR(I)*DY(J)*(HRP(I,J)-ZBR(I,J))
    9 CONTINUE
      STOR=STOR*POR/43560.0
      WRITE(6,11)
   11 FORMAT(5X,*STORAGE AT PREVIOUS TIME INCREMENT, AF*,7X,*STORAGE AT
     2PRESENT TIME INCREMENT, AF*,/)
      WRITE(6,12) STORP,STOR
   12 FORMAT(15X,F9.2,27X,F9.2)
   20 CONTINUE
C  $$$$$$$$$$$$$$$$$$$$$$$$$$$$$$$$$$$$$$$$$$$$$$$$$$$$$$$$$$$$$$$$$$$$$$$$
C  SURFACE FLUX
      DO 27 I=2,LL
      DO 27 J=2,MR
      SURF=SURF+QIL(I,J)
   27 CONTINUE
      DO 28 I=1,LC
      DO 28 J=2,MR
      SURF=SURF+QIC(I,J)
   28 CONTINUE
      DO 29 I=1,LRR
      DO 29 J=2,MR
      SURF=SURF+QIR(I,J)
   29 CONTINUE
      SURF=SURF*DT/43560.0
C  $$$$$$$$$$$$$$$$$$$$$$$$$$$$$$$$$$$$$$$$$$$$$$$$$$$$$$$$$$$$$$$$$$$$$$$$
C  SEEPAGE FROM RIVER
      DO 30 L=6,LRIV
      SEEP=SEEP+RSO(L)
   30 CONTINUE
      SEEP=SEEP*DT/43560.0
C  $$$$$$$$$$$$$$$$$$$$$$$$$$$$$$$$$$$$$$$$$$$$$$$$$$$$$$$$$$$$$$$$$$$$$$$$
C  UNDERFLOW
      DO 37 J=2,MR
      IF(CKL(1,J).LE.1.0.OR.CKL(2,J).LE.1.0) GO TO 38
      UFL=UFL+((2.0*CKL(1,J)*CKL(2,J)*(HLP(1,J)-ZBL(1,J))*(HLP(2,J)-ZBL(
     22,J))*DY(J))/(DXL(2)*CKL(1,J)*(HLP(1,J)-ZBL(1,J))+DXL(1)*CKL(2,J)*
     3(HLP(2,J)-ZBL(2,J))))*(HLP(1,J)-HLP(2,J))
   38 IF(CKR(21,J).LE.1.0.OR.CKR(22,J).LT.1.0) GO TO 37
      UFL=UFL+((2.0*CKR(21,J)*CKR(22,J)*(HRP(21,J)-ZBR(21,J))*(HRP(22,J)
     2-ZBR(22,J))*DY(J))/(DXR(22)*CKR(21,J)*(HRP(21,J)-ZBR(21,J))+DXR(21
     3)*CKR(22,J)*(HRP(22,J)-ZBR(22,J))))*(HRP(22,J)-HRP(21,J))
   37 CONTINUE
      DO 47 I=4,LL
      IF(CKL(I,1).LE.1.0.OR.CKL(I,2).LE.1.0) GO TO 48
      UFL=UFL+((2.0*CKL(I,1)*CKL(I,2)*(HLP(I,1)-ZBL(I,1))*(HLP(I,2)-ZBL(
     2I,2))*DXL(I))/(DY(2)*CKL(I,1)*(HLP(I,1)-ZBL(I,1))+DY(1)*CKL(I,2)*(
     3HLP(I,2)-ZBL(I,2))))*(HLP(I,1)-HLP(I,2))
   48 IF(CKL(I,8).LT.1.0.OR.CKL(I,7).LT.1.0) GO TO 47
      UFL=UFL+((2.0*CKL(I,8)*CKL(I,7)*(HLP(I,8)-ZBL(I,8))*(HLP(I,7)-ZBL(
     2I,7))*DXL(I))/(DY(7)*CKL(I,8)*(HLP(I,8)-ZBL(I,8))+DY(8)*CKL(I,7)*(
     3HLP(I,7)-ZBL(I,7))))*(HLP(I,8)-ZBL(I,8))
   47 CONTINUE
      DO 57 I=1,LRR
      IF(CKR(I,1).LT.1.0.OR.CKR(I,2).LT.1.0) GO TO 58
      UFL=UFL+((2.0*CKR(I,1)*(HRP(I,1)-ZBR(I,1))*(HRP(I,2)-ZBR(I,2))*DXR
     2(I))/(DY(2)*CKR(I,1)*(HRP(I,1)-ZBR(I,1))+DY(1)*CKR(I,2)*(HRP(I,2)-
     3ZBR(I,2))))*(HRP(I,1)-HRP(I,2))
   58 IF(CKR(I,8).LT.1.0.OR.CKR(I,7).LT.1.0) GO TO 57
      UFL=UFL+((2.0*CKR(I,8)*CKR(I,7)*(HRP(I,8)-ZBR(I,8))*(HRP(I,7)-ZBR(
     2I,7))*DXR(I))/(DY(7)*CKR(I,8)*(HRP(I,8)-ZBR(I,8))+DY(8)*CKR(I,7)*(
     3HRP(I,7)-ZBR(I,7))))*(HRP(I,8)-HRP(I,7))
   57 CONTINUE
      DO 67 I=1,LC
      DO 67 K=1,N
      IF(CKC(I,1,K).LT.1.0.OR.CKC(I,2,K).LT.1.0) GO TO 68
      UFL=UFL+((2.0*CKC(I,1,K)*CKC(I,2,K)*DXC(I)*DZ(K))/(DY(2)*CKC(I,1,K
     2)+DY(1)*CKC(I,2,K)))*(HCP(I,1,K)-HCP(I,2,K))
   68 IF(CKC(I,8,K).LE.1.0.OR.CKC(I,7,K).LT.1.0) GO TO 67
      UFL=UFL+((2.0*CKC(I,8,K)*CKC(I,7,K)*DXC(I)*DZ(K))/(DY(7)*CKC(I,8,K
     2)+DY(8)*CKC(I,7,K)))*(HCP(I,8,K)-HCP(I,7,K))
   67 CONTINUE
      UFL=UFL*DT/43560.0
```

```
C  $$$$$$$$$$$$$$$$$$$$$$$$$$$$$$$$$$$$$$$$$$$$$$$$$$$$$$$$$$$$$$$$$$$$$$$$$$$
C  PUMPING
       PUMP=864000.0*30.0/43560.0
C  $$$$$$$$$$$$$$$$$$$$$$$$$$$$$$$$$$$$$$$$$$$$$$$$$$$$$$$$$$$$$$$$$$$$$$$$$$$
C  MASS BALANCE
       ADD=SURF+SEEP+UFL-PUMP
       ERR=STOR-ADD-STORP
       WRITE(6,13)
   13 FORMAT(5X,*ADDITION TO STORAGE, AF*,7X,*ERROR IN STORAGE COMPUTATI
     2ON, AF*,/)
       WRITE(6,14) ADD,ERR
   14 FORMAT(12X,F9.2,25X,F9.2)
       RETURN
       END
       SUBROUTINE ADJUST
       COMMON LC,M,N,LRL,LRM,LRIV,NADJ,NCAN,HPB,SK,TH,SY,AN,BSC,VT,POR,
     2TIME,TCON,DT,C(384),DXC(8),DY(8),DZ(4),DB(8),IRIV(47),JRIV(47),
     3RBED(47),RWID(47),RSLP(47),QRIV(47),DIV(47),RSO(47),VMS(47),
     4VMB(47),SDRIV(20),FKFAC(20),CDV(9),PCT(9),AREA(9),LCAN(10),
     5QJMD(3),QLAM(3),QKAN(3),CM(384,49),NDL(12,8),NDC(8,8),NDR(22,8),
     6HTEMP(8,8),QIC(8,8),KODC(8,8,4),HCP(8,8,4),ZC(8,8,4),CKC(8,8,4),
     7CKSAT(8,8,4),DSDHP(8,8,4)
       COMMON /A/ LL,DXL(12),KODL(12,8),CKL(12,8),HLP(12,8),ZBL(12,8),
     2QIL(12,8)
       COMMON /B/ LR,DXR(22),KODR(22,8),CKR(22,8),HRP(22,8),ZBR(22,8),
     2QIR(22,8)
C
C  ***************************************************************************
C  THIS SUBROUTINE COMPUTES VALUES FOR UNSATURATED HYDRAULIC CONDUCTIVITY AND
C  DERIVATIVE OF SATURATION WITH RESPECT TO HEAD FOR EVERY GRID IN THE
C  THREE-DIMENSIONAL MODEL SEGMENT AT THE BEGINNING OF EACH TIME INCREMENT.
C  ***************************************************************************
C
C  ALL DZ MUST BE EVENLY DIVISIBLE BY HSTEP
       HSTEP=0.5
       DO 7 I=1,LC
       DO 7 J=1,M
       DO 7 K=1,N
       ADDS=0.0
       ADDK=0.0
       TOP=ZC(I,J,K)+0.5*DZ(K)
       BOT=ZC(I,J,K)-0.5*DZ(K)
       IF(TOP.LE.HCP(I,J,K))GO TO 5
       IF(BOT.LT.HCP(I,J,K)) GO TO 104
       IF(K.LE.1) GO TO 104
       HCP(I,J,K)=HCP(I,J,K-1)
       IF(KODC(I,J,K).EQ.0) KODC(I,J,K)=5
       GO TO 105
  104 IF(KODC(I,J,K).EQ.5) KODC(I,J,K)=0
  105 CONTINUE
       ZIP=BOT+0.5*HSTEP
       ANZ=DZ(K)/HSTEP
       NZ=IFIX(ANZ)
       DO 6 NN=1,NZ
       HP=ZIP-HCP(I,J,K)
       IF(HP.LT.0.0) GO TO 12
       AINC=ABS(HP/HSTEP)+1.0
       INC=IFIX(AINC)
       IF(INC.LT.1) INC=1
       IF(INC.GT.NADJ) INC=NADJ
       IF(INC.LT.1.OR.INC.GT.NADJ) WRITE(6,8) INC
    8 FORMAT(5X,*ERROR IN ADJUST*,5X,*INC=*,I5)
       GO TO 13
   12 INC=1
   13 ADDS=ADDS+SDRIV(INC)
       ADDK=ADDK+FKFAC(INC)
       ZIP=ZIP+HSTEP
    6 CONTINUE
       DSDHP(I,J,K)=ADDS/ANZ
       CKC(I,J,K)=CKSAT(I,J,K)*ADDK/ANZ
       GO TO 7
    5 DSDHP(I,J,K)=0.0
       CKC(I,J,K)=CKSAT(I,J,K)
```

```
    7 CONTINUE
      RETURN
      END
      SUBROUTINE KFNP(HELEV,HHYD,CFK,TOP,BOT)
      COMMON LC,M,N,LPL,LRM,LRIV,NADJ,NCAN,HPB,SK,TH,SY,AN,BSC,VT,POR,
     2TIME,TCON,DT,C(384),DXC(8),DY(8),DZ(4),DB(8),IRIV(47),JRIV(47),
     3RBED(47),RWID(47),RSLP(47),QRIV(47),DIV(47),RSO(47),VMS(47),
     4VMB(47),SDRIV(20),FKFAC(20),CDV(9),PCT(9),AREA(9),LCAN(10),
     5QJMD(3),QLAM(3),QKAN(3),CM(384,49),NDL(12,8),NDC(8,8),NDR(22,8),
     6HTEMP(8,8),QIC(8,8),KODC(8,8,4),HCP(8,8,4),ZC(8,8,4),CKC(8,8,4),
     7CKSAT(8,8,4),DSDHP(8,8,4)
C
C   ***************************************************************************
C   THIS SUBROUTINE IS CALLED FROM CTRAN TO COMPUTE VALUES OF UNSATURATED
C   HYDRAULIC CONDUCTIVITY ABOVE THE WATER TABLE FOR TWO-DIMENSIONAL GRIDS.
C   ***************************************************************************
C
C   ALL DZ MUST BE EVENLY DIVISIBLE BY STEP
      STEP=0.5
      ADDK=0.0
      ZIP=BOT+0.5*STEP
      ANZ=(TOP-BOT)/STEP
      NZ=IFIX(ANZ)
      DO 6 NN=1,NZ
      HP=ZIP-HHYD
      IF(HP.LT.0.0) GO TO 12
      AINC=HP/STEP+1.0
      INC=IFIX(AINC)
      IF(INC.LT.1) INC=1
      IF(INC.GT.NADJ) INC=NADJ
      IF(INC.LT.1.OR.INC.GT.NADJ) WRITE(6,8) INC
    8 FORMAT(5X,*ERROR IN KFNP*,5X,*INC=*,I5)
      GO TO 13
   12 INC=1
   13 ADDK=ADDK+FKFAC(INC)
      ZIP=ZIP+STEP
    6 CONTINUE
      CFK=ADDK/ANZ
      RETURN
      END
```

Key Words: Stream-adquifer system, numerical modeling, steady flow, unsteady flow, saturated flow, unsaturated flow, three-dimensional finite difference modeling.

Abstract: A three-dimensional, finite difference model was developed for simulating steady and unsteady, saturated and unsaturated flow in a stream-aquifer system. The basis of the model is the finite difference form of Richard's equation for unsaturated and saturated subsurface flow. Effects of streamflow on groundwater movement are treated by applying the appropriate boundary conditions to Richard's equation. Contributions of groundwater to river flow are quantified by including seepage rates in the computation of river discharge. The three-dimensional model was developed for use in this study to interact with two-dimensional model segments, which were interfaced with the three-dimensional model on its upstream and downstream ends.

Key Words: Stream-adquifer system, numerical modeling, steady flow, unsteady flow, saturated flow, unsaturated flow, three-dimensional finite difference modeling.

Abstract: A three-dimensional, finite difference model was developed for simulating steady and unsteady, saturated and unsaturated flow in a stream-aquifer system. The basis of the model is the finite difference form of Richard's equation for unsaturated and saturated subsurface flow. Effects of streamflow on groundwater movement are treated by applying the appropriate boundary conditions to Richard's equation. Contributions of groundwater to river flow are quantified by including seepage rates in the computation of river discharge. The three-dimensional model was developed for use in this study to interact with two-dimensional model segments, which were interfaced with the three-dimensional model on its upstream and downstream ends.

Key Words: Stream-adquifer system, numerical modeling, steady flow, unsteady flow, saturated flow, unsaturated flow, three-dimensional finite difference modeling.

Abstract: A three-dimensional, finite difference model was developed for simulating steady and unsteady, saturated and unsaturated flow in a stream-aquifer system. The basis of the model is the finite difference form of Richard's equation for unsaturated and saturated subsurface flow. Effects of streamflow on groundwater movement are treated by applying the appropriate boundary conditions to Richard's equation. Contributions of groundwater to river flow are quantified by including seepage rates in the computation of river discharge. The three-dimensional model was developed for use in this study to interact with two-dimensional model segments, which were interfaced with the three-dimensional model on its upstream and downstream ends.

Key Words: Stream-adquifer system, numerical modeling, steady flow, unsteady flow, saturated flow, unsaturated flow, three-dimensional finite difference modeling.

Abstract: A three-dimensional, finite difference model was developed for simulating steady and unsteady, saturated and unsaturated flow in a stream-aquifer system. The basis of the model is the finite difference form of Richard's equation for unsaturated and saturated subsurface flow. Effects of streamflow on groundwater movement are treated by applying the appropriate boundary conditions to Richard's equation. Contributions of groundwater to river flow are quantified by including seepage rates in the computation of river discharge. The three-dimensional model was developed for use in this study to interact with two-dimensional model segments, which were interfaced with the three-dimensional model on its upstream and downstream ends.

The model produced results which match observed data for the study area, which consisted of a 40 mile reach of the Arkansas Valley of Southeastern Colorado. Computed estimates of river discharge at each end of the study area and water table elevations throughout the region agreed reasonably well with observed data. An analysis of the sensitivity of results produced by the model to variation in the values of several input parameters was included as part of the study.

Reference: Rovey, Catherine E. Kraeger, Colorado State University, Hydrology Paper No. 74 (July 1975), Numerical Model of Flow in a Stream-Aquifer System.

The model produced results which match observed data for the study area, which consisted of a 40 mile reach of the Arkansas Valley of Southeastern Colorado. Computed estimates of river discharge at each end of the study area and water table elevations throughout the region agreed reasonably well with observed data. An analysis of the sensitivity of results produced by the model to variation in the values of several input parameters was included as part of the study.

Reference: Rovey, Catherine E. Kraeger, Colorado State University, Hydrology Paper No. 74 (July 1975), Numerical Model of Flow in a Stream-Aquifer System.

The model produced results which match observed data for the study area, which consisted of a 40 mile reach of the Arkansas Valley of Southeastern Colorado. Computed estimates of river discharge at each end of the study area and water table elevations throughout the region agreed reasonably well with observed data. An analysis of the sensitivity of results produced by the model to variation in the values of several input parameters was included as part of the study.

Reference: Rovey, Catherine E. Kraeger, Colorado State University, Hydrology Paper No. 74 (July 1975), Numerical Model of Flow in a Stream-Aquifer System.

The model produced results which match observed data for the study area, which consisted of a 40 mile reach of the Arkansas Valley of Southeastern Colorado. Computed estimates of river discharge at each end of the study area and water table elevations throughout the region agreed reasonably well with observed data. An analysis of the sensitivity of results produced by the model to variation in the values of several input parameters was included as part of the study.

Reference: Rovey, Catherine E. Kraeger, Colorado State University, Hydrology Paper No. 74 (July 1975), Numerical Model of Flow in a Stream-Aquifer System.

LIST OF PREVIOUS 25 PAPERS

No. 49 Infiltration Affected by Flow of Air, by David B. McWhorter, May 1971.

No. 50 Probabilities of Observed Droughts, by Jaime Millan and Vujica Yevjevich, June 1971.

No. 51 Amplification Criterion of Gradually Varied, Single Peaked Waves, by John Peter Jolly and Vujica Yevjevich, December 1971.

No. 52 Stochastic Structure of Water Use Time Series, by Jose D. Salas-La Cruz and Vujica Yevjevich, June 1972.

No. 53 Agricultural Response to Hydrologic Drought, by V. J. Bidwell, July 1972.

No. 54 Loss of Information by Discretizing Hydrologic Series, by Mogens Dyhr-Nielsen, October 1972.

No. 55 Drought Impact on Regional Economy, by Jaime Millan, October 1972.

No. 56 Structural Analysis of Hydrologic Time Series, by Vujica Yevjevich, November 1972.

No. 57 Range Analysis for Storage Problems of Periodic-Stochastic Processes, by Jose Salas-La Cruz, November 1972.

No. 58 Applicability of Canonical Correlation in Hydrology, by Padoong Torranin, December 1972.

No. 59 Transposition of Storms, by Vijay Kumar Gupta, December 1972.

No. 60 Response of Karst Aquifers to Recharge, by Walter G. Knisel, December 1972.

No. 61 Drainage Design Based Upon Aeration by Harold R. Duke, June 1973.

No. 62 Techniques for Modeling Reservoir Salinity by John Hendrick, August 1973.

No. 63 Mechanics of Soil Erosion From Overland Flow Generated by Simulated Rainfall by Mustafa Kilinc and Everett V. Richardson, September 1973.

No. 64 Area-Time Structure of the Monthly Precipitation Process by V. Yevjevich and Alan K. Karplus, August 1973.

No. 65 Almost-Periodic, Stochastic Process of Long-Term Climatic Changes, by William Q. Chin and Vujica Yevjevich, March 1974.

No. 66 Hydrologic Effects of Patch Cutting of Lodgepole Pine, by Thomas L. Dietrich and James R. Meiman, April 1974.

No. 67 Economic Value of Sediment Discharge Data, by Sven Jacobi and Everett V. Richardson, April 1974.

No. 68 Stochastic Analysis of Groundwater Level Time Series in the Western United States, by Albert G. Law, May 1974.

No. 69 Efficient Sequential Optimization in Water Resources, by Thomas E. Croley II, September 1974.

No. 70 Regional Water Exchange for Drought Alleviation, by Kuniyoshi Takeuchi, November 1974.

No. 71 Determination of Urban Watershed Response Time, by E. F. Schulz, December, 1974.

No. 72 Generation of Hydrologic Samples, Case Study of the Great Lakes, by V. Yevjevich May, 1975.

No. 73 Extraction of Information on Inorganic Water Quality, by William L. Lane, August, 1975.